Title

The biosynthesis and structure of lipooligosaccharide from gut microbe Bacteroides thetaiotaomicron

Author

Jacobson, Amy Nicole

Publication Date

2017

Peer reviewed|Thesis/dissertation

The biosynthesis and structure of lipooligosaccharide from gut microbe *Bacteroides thetaiotaomicron*

by

Amy Nicole Jacobson

DISSERTATION

Submitted in partial satisfaction of the requirements for the degree of

DOCTOR OF PHILOSOPHY

in

Chemistry and Chemical Biology

in the

GRADUATE DIVISION

of the

UNIVERSITY OF CALIFORNIA, SAN FRANCISCO

[redacted]

Acknowledgements

There are moments when graduate school can feel like a lonely endeavor, but in reality that sentiment could not be further from the truth. When I think back over the last six years, the number of people who have helped me to succeed along the way is astounding.

To my advisor, Michael Fischbach—thank you for giving me the opportunity to study a fascinating topic in such a supportive environment. Your optimism and imagination have allowed me take risks and persevere, and I am deeply grateful to you for trusting me to do my best work and guiding me along the way.

To my thesis committee members Zev Gartner and Anita Sil—thank you for your advice and feedback. You always have a way of getting right to the heart of a problem and helping me see my way through it.

To Nancy Phillips and Constance John—thank you for being so generous with your time and expertise. I cannot imagine how many years would have been added on to my graduate school career if I had not had the good fortune to meet you both.

To the Fischbach lab—thank you for making our lab feel like a home. I am indebted to every single lab member, past and present. Jan Claesen, Sloan Devlin, Colleen O'Loughlin, Mao Taketani, and Brianna Williams, thank you for countless discussions, endless support, and most of all your friendship.

To the CCB program—thank you to program coordinators Julia Molla and Nicole Flowers and director Charly Craik for fostering creativity at the interface of chemistry and biology in this unique graduate program.

To my fellow CCB graduate students Jordan Carelli, Christina Fitzsimmons, Louise Goupil, Charlie Morgan, and Ben Spangler—thank you for coffee breaks, Sunday brunches, and game nights, for practice talks, proposal editing, and experimental advice. You have become excellent scientists, but you have always been wonderful people.

To my friends Arpana Arjun, Ed Burke, Sam Creely, Nathan Hobbs, Michael Rooney, and Carl Sverre—thank you for being my safety net. I am unbelievably lucky to have each of you in my life.

To my Stanford undergraduate mentors Lynette Cegelski and Joshua Landy—thank you for helping me to find my way to graduate school in the first place. Lynette, your attention and mentorship throughout my time in your lab let me see myself as a scientist for the first time. Josh, working with you showed me that I could pursue a career in research without sacrificing the many other facets that make me who I am.

Finally, to my family—thank you for being my fiercest supporters and my strongest champions. You have helped me find my voice, and now I am ready to use it.

Portions of Chapters 1, 2, and 3 of this dissertation contain material submitted for publication:

Jacobson AN, Fischbach MA. The biosynthesis of lipooligosaccharide from gut microbe *Bacteroides thetaiotaomicron*. mBio, under review.

The biosynthesis and structure of lipooligosaccharide from gut microbe *Bacteroides thetaiotaomicron*

by

Amy Nicole Jacobson

Abstract

Lipopolysaccharide (LPS), a cell-associated glycolipid that makes up the outer leaflet of the outer membrane of Gram-negative bacteria, is a canonical mediator of microbe-host interactions. It is sensed by the immune system through Toll-like receptor 4 on innate immune cells, typically indicating to the host that an outside invader is present that needs to be cleared, prompting an inflammatory response. LPS is a potent immunostimulatory molecule, and when this process goes unchecked the consequences can be severe: just nanograms of LPS from a pathogenic bacterium injected into the bloodstream of a mouse will cause the mouse to die of septic shock. Puzzlingly, the human microbiota seems to avoid this response altogether and can be tolerated by the immune system despite producing the same classes of molecules that, when made by pathogens, prompt inflammation. The most prevalent Gram-negative gut bacterial taxon, *Bacteroides*, makes up ~50% of the cells in a typical Western gut; these cells harbor ~300 mg of LPS, making it one of the highest-abundance molecules in the intestine. However, remarkably little is known about the molecular details of microbiota-immune interactions mediated by *Bacteroides* LPS. As a starting point for understanding the biological function of *Bacteroides* LPS, we sought to characterize the biosynthesis and structure of the three classical components of LPS: lipid A, the core

oligosaccharide, and the O-antigen repeating unit. We identified genes in *Bacteroides thetaiotaomicron* involved in the biosynthesis of its lipid A core and glycan, generated mutants that elaborate altered forms of LPS, and used mass spectrometry to interrogate the molecular features of these variants. We demonstrate that the glycan does not appear to have a repeating unit and is therefore better categorized as lipooligosaccharide (LOS) rather than LPS. Our work lays the foundation for developing a structure-function relationship for *Bacteroides* LPS in the context of host colonization.

Table of Contents

List of Figures

List of Tables

Chapter 1

Lipopolysaccharide in microbe-host interactions

1.1 The human microbiota and innate immunity

The human body hosts trillions of microbes—the gut alone contains more bacteria than human cells—yet how these bacteria manage to be tolerated by the immune system is not well understood (1). The purpose of the innate immune system is to detect organisms that are 'non-self' like bacterial pathogens and trigger a response resulting in the elimination of the unwanted agent. It does so by monitoring the body with cells expressing pattern recognition receptors (PRRs) on their surface (2). These receptors are typically specific for a particular class of molecule that is made by microbes but not by humans. The presence of such a molecule tells the immune cell that an organism is present that should not be there, and signaling cascades in response to the molecule liganding a PRR produce an inflammatory response and clearance of the pathogen. However, the task of the innate immune system is not as simple as telling 'self' from 'non-self.' Bacteria from the human microbiota produce the same classes of molecules that ligand PRRs, yet the body does not respond to these mutualistic human-associated bacteria with inflammation under normal circumstances (3). This work focuses on understanding microbiota-host interactions mediated by one particular group of PRR ligands: the cell surface glycolipids.

1.2 Cell surface glycolipids as immune signaling molecules

High-abundance cell-associated molecules are of great interest to understanding microbiota-host interactions at the level of molecular mechanism. Unlike high-abundance diffusible molecules, which are the characteristic products of amino acid and sugar metabolism, high-abundance cell-associated molecules are often lipids and

glycolipids (4). These molecules tend to be structural components of the cell membrane or cell wall that are architecturally similar although chemically different among bacterial taxa—lipopolysaccharides, lipoteichoic and wall teichoic acids, mycolic acids, and muramyl dipeptides are key examples (2). Their ubiquity on the cell surface makes them excellent targets for bacterial detection by innate immune PRRs, including Toll-like receptors and NOD proteins (5). However, a long-standing question remains: How do innate immune cells 'know' whether the bacterial cell they encounter is a mutualist or a pathogen and 'decide' how to respond appropriately? Part of the answer likely involves unique strain-specific chemical signatures within these cell-associated molecules.

1.3 Lipopolysaccharide structure and function

1.3.1 Lipopolysaccharide structure: lipid A, core oligosaccharide, and O-antigen

Lipopolysaccharide (LPS) is a canonical cell-associated glycolipid. LPS is generally composed of a lipid anchor called lipid A, a core oligosaccharide region, and a polysaccharide repeating unit called the O-antigen (Figure 1.1). While lipid A structure is somewhat conserved among bacteria with only small differences in the overall structure between Gram-negative genera, the saccharide regions vary considerably more (6). For example, within *Escherichia coli* five different classes of core oligosaccharide are represented even though under normal growth circumstances all would produce the same lipid A structure (7). Even greater diversity is found at the level of the O-antigen. Additionally, the core oligosaccharide and O-antigen are typically biosynthesized by separate gene clusters, while lipid A biosynthesis genes are distributed throughout the genome (6).

1.3.2 Lipopolysaccharide signaling: Toll-like receptor 4 complex

The interaction between LPS and host Toll-like receptor 4 (TLR4) is a paradigm for immunologic sensing of Gram-negative bacteria. TLR4 is a transmembrane receptor that requires interaction with helper protein MD-2 in order to bind LPS. Lipid A is the only portion of the LPS molecule known to make direct contact with the TLR4/MD-2 complex, and additional proteins CD14 and LPS binding protein are involved in shuttling the glycolipid to the receptor on the immune cell surface (8). Once LPS binds to the TLR4/MD-2 complex, signaling cascades occur through MyD88- or TRIF-dependent mechanisms via activation of the transcription factor NF-κB, resulting in cytokine production and a typically proinflammatory response (9).

1.3.3 Lipid A biosynthesis

Lipid A biosynthesis has been well studied in *E. coli* and the nine enzymes that build lipid A from its starting materials in the cell are known as the Raetz pathway (Figure 1.2). When lipid A structures do differ between bacteria, they commonly have different acylation or phosphorylation patterns (Figure 1.3). Modulation of the late acyltransferases LpxL and LpxM, responsible for the attachment of the lipid A secondary acyl chains, can be beneficial for a bacterium. For example, *Yersinia pestis* down regulates *lpxL* and *lpxM*, thereby removing two acyl chains from its lipid A, when infecting humans, thus avoiding detection by TLR4 (10, 11). The crystal structure of the TLR4/MD-2 complex with *E. coli* lipid A suggests that the number of acyl chains and the number and position of phosphate groups on the molecule may affect binding affinity to the receptor and possibly receptor dimerization (12).

1.3.4 Lipid A mimics as TLR4 antagonists

Lipid A acylation and phosphorylation are important both for bacterial membrane physiology and for the interaction between LPS and host TLR4. *E. coli* lipid IV_A is capable of inhibiting TLR4 activation by wild-type *E. coli* lipid A (13). This tetra-acylated di-phosphorylated scaffold has been used in the design of Eritoran, a lipid A mimic developed as a TLR4 antagonist and as a potential treatment for sepsis (Figure 1.3) (14). Additionally, lipid A mutants in *E. coli* differentially stimulate NF-κB production in a THP-1 reporter cell line (15).

1.3.5 Variety in LPS core oligosaccharide and O-antigen

More drastic changes in overall structure of LPS have also been observed. Rather than differing in core oligosaccharide or O-antigen composition, species of *Neisseria* produce an LPS variant known as lipooligosaccharide (LOS), which has a more elaborate core oligosaccharide in place of the conventional O-antigen (16-17). Additionally, *Helicobacter pylori* elaborates its O-antigen with Lewis antigens to mimic host glycans (18-19). Notably, almost everything known about the biosynthesis, structure, and function of LPS comes from studies of 'conventional' pathogens. Remarkably little is known about LPS from commensal organisms and its importance to host innate immunity.

1.3.6 Relevance of LPS saccharides to the host

As demonstrated above, the chemical structure of LPS varies considerably among species, and these differences in structure are relevant to function. In addition to the

examples already provided, recent work on the human-associated bacteria *H. pylori* and *Hafnia alvei* indicate that the glycan portion of LPS from these strains can interact with C-type lectin receptors DC-SIGN and Dectin-2, respectively, to influence a dendritic cell's cytokine output (20-21). C-type lectin receptors are yet another type of PRR that are typically liganded by carbohydrate groups (22). Engagement of this class of receptors by a human-associated bacterium lacking an O-antigen has not been investigated.

1.4 *Bacteroides* LPS in the human gut

Among the glycolipids found in the gut microbiome, *Bacteroides* LPS is of particular interest. *Bacteroides*, and, in ~10% of humans, its relative *Prevotella*, are the only high-abundance Gram-negative bacterial genera in the gut. *Bacteroides* as a genus makes up ~50% of the typical Western gut community. Notably, the species distribution within that 50% is highly variable between individuals (23). *Bacteroides* LPS is already known to have a different lipid A structure than 'pathogenic' LPS: *B. thetaiotaomicron*, *B. fragilis*, and *B. dorei* produce penta-acylated, mono-phosphorylated lipid A, in contrast to the hexa-acylated, di-phosphorylated lipid A from *Escherichia coli* (24-27). With a recent exception reporting a *Bt* lipid A phosphatase, very little is known about the biosynthetic genes involved in *Bacteroides* LPS biogenesis (28). Different *Bacteroides* species have been reported to produce LPS molecules with distinct architectures based on their banding pattern on an SDS-PAGE gel, suggesting that each *Bacteroides* species has the potential to influence innate immunity in its own way (29-30).

1.5 Project goal

It takes as little as 50 ng of *E. coli* LPS injected intravenously into a mouse to cause septic shock (30). By contrast, given our laboratory purification yield of approximately 10 mg *B. thetaiotaomicron* LPS per 1L confluent culture, and assuming 20 trillion *Bacteroides* per individual, we estimate that a typical western human gut contains ~300 mg of *Bacteroides* LPS, likely making it one of the highest-abundance bacterially derived molecules present (1). However, because so little is known about the specific details of LPS from *Bacteroides*, it is challenging to predict what kind of an effect these molecules might have on host biology. We hypothesized that we would be able to identify lipid A biosynthesis genes in *Bacteroides* by sequence homology to the known genes from *E. coli.* Additionally, we predicted that the carbohydrate region of *B. thetaiotaomicron* LPS would be biosynthesized from a single gene cluster. We set out to better define the biosynthesis and structure of *Bacteroides* LPS as a starting point for understanding and manipulating the interaction between *Bacteroides* and the human immune system.

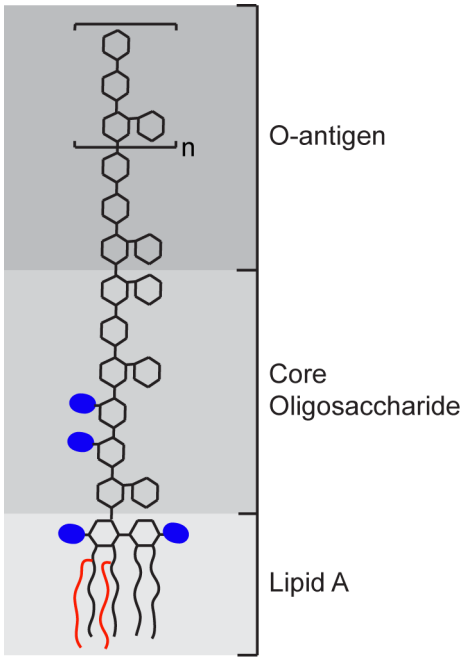

Figure 1.1. Cartoon representation of *E. coli* LPS structure. Black curved lines represent primary acyl chains, red curved lines represent secondary acyl chains, blue ovals represent phosphate groups, and black hexagons represent individual saccharides. This drawing is an approximation of *E. coli* LPS structure and does not depict a specific core oligosaccharide or O-antigen.

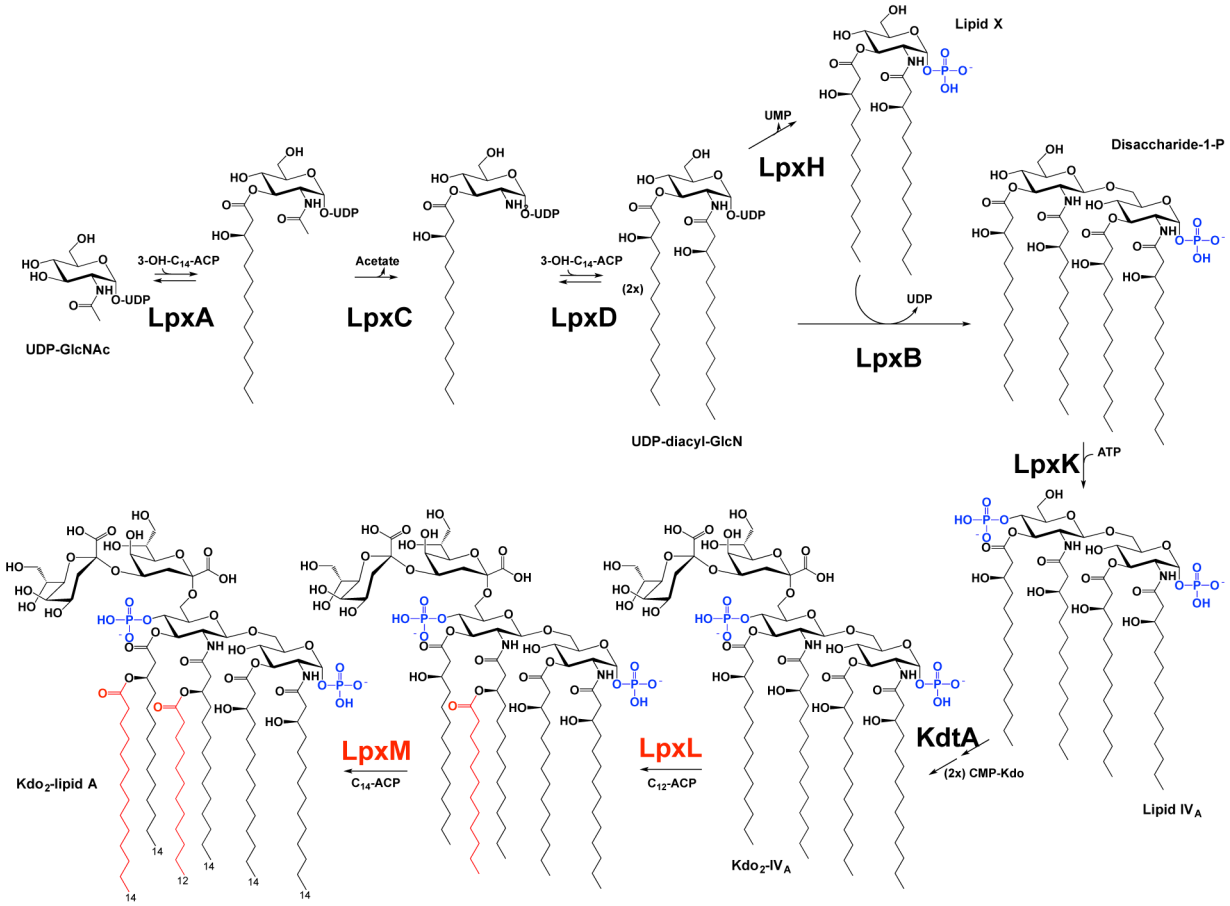

Figure 1.2. The Raetz pathway for *E. coli* lipid A biosynthesis. The Raetz pathway contains the nine enzymes involved in the biosynthesis of lipid A (32). Secondary acyl chains and the enzymes responsible for their addition are colored red, and phosphate groups are colored blue.

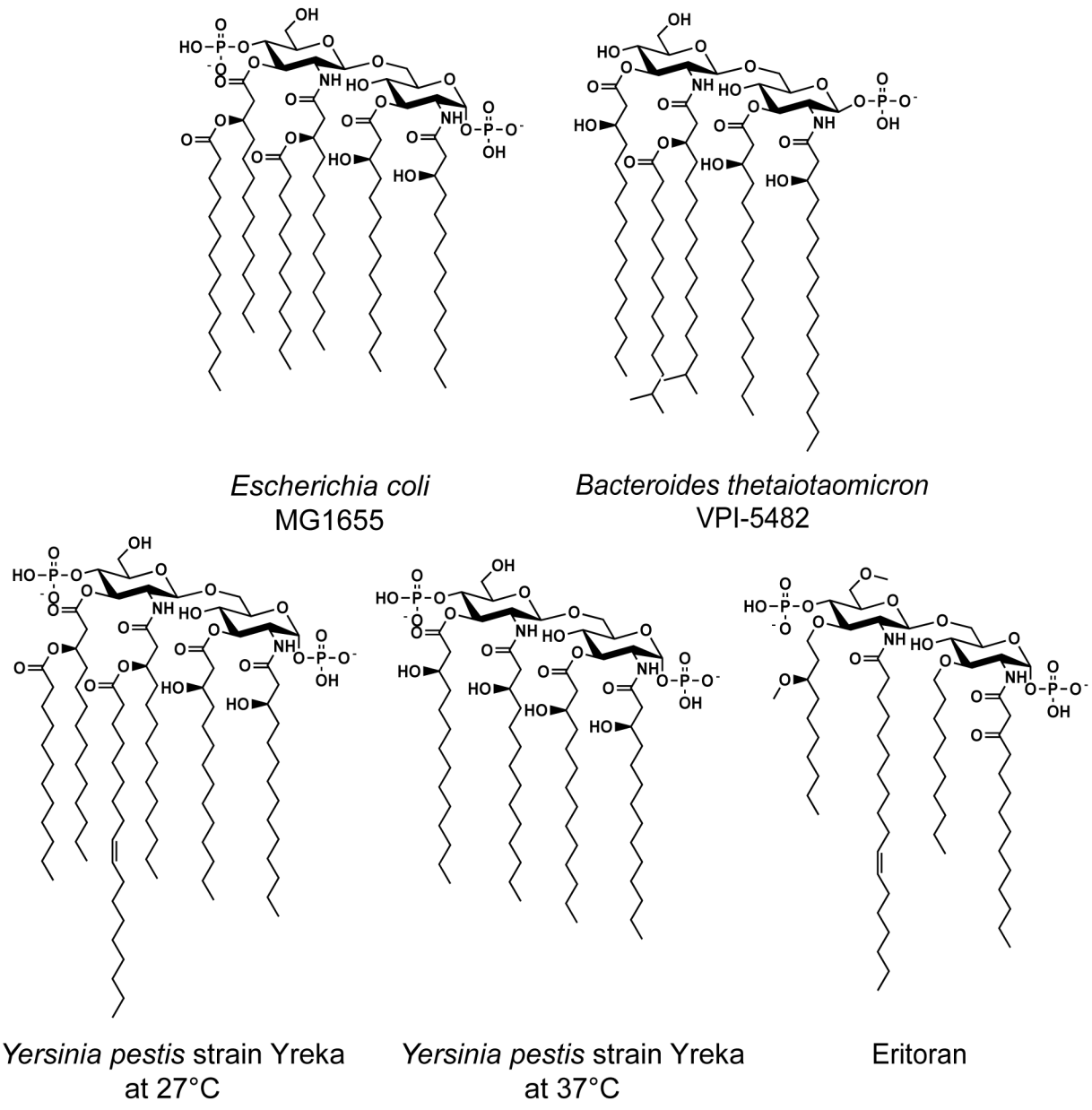

Figure 1.3. Chemical structures of lipid A from a selection of bacteria and Eritoran.

References

1. **Sender R**, **Fuchs S**, **Milo R**. 2016. Are We Really Vastly Outnumbered? Revisiting the Ratio of Bacterial to Host Cells in Humans. Cell **164**:337–340.

2. **Akira S**, **Uematsu S**, **Takeuchi O**. 2006. Pattern Recognition in Innate Immunity. Cell **124**:783-801.

3. **Belkaid Y**, **Harrison OJ**. 2017. Homeostatic Immunity and the Microbiota. Immunity **46**:562-576.

4. **Donia MS**, **Fischbach MA**. 2015. Small molecules from the human microbiota. Science **349**:1254766–1254766.

5. **Medzhitov R**. 2007. Recognition of microorganisms and activation of the immune response. Nature **449**:819–826.

6. **Raetz CRH**, **Whitfield C**. 2002. Lipopolysaccharide Endotoxins. Annu Rev Biochem **71**:635–700.

7. **Amor K, Heinrichs DE, Frirdich E, Ziebell K, Johnson RP, Whitfield C.** 2000. Distribution of Core Oligosaccharide Types in Lipopolysaccharides from *Escherichia coli*. Infect Immun 1116-1124.

8. **Park BS**, **Lee J**. 2013. Recognition of lipopolysaccharide pattern by TLR4 complexes. Exp Mol Med **45**:e66.

9. **Lu Y**, **Yeh W**, **Ohashi P**. 2008. LPS/TLR4 signal transduction pathway. Cytokine **42**:145-151.

10. **Montminy SW**, **Khan N**, **McGrath S**, **Walkowicz MJ**, **Sharp F**, **Conlon JE**, **Fukase K**, **Kusumoto S**, **Sweet C**, **Miyake K**, **Akira S**, **Cotter RJ**, **Goguen JD**, **Lien E**. 2006. Virulence factors of Yersinia pestis are overcome by a strong lipopolysaccharide response. Nat Immunol **7**:1066–1073.

11. **Kawahara K**, **Tsukano H**, **Watanabe H**, **Lindner B**, **Matsuura M**. 2002. Modification of the Structure and Activity of Lipid A in Yersinia pestis Lipopolysaccharide by Growth Temperature. **70**:4092-4098.

12. **Park BS**, **Song DH**, **Kim HM**, **Choi B**, **Lee H**, **Lee J**. 2009. The structural basis of lipopolysaccharide recognition by the TLR4-MD-2 complex. Nature **458**:1191–1195.

13. **Golenbock DT, Hampton RY, Qureshi N, Takayama K, Raetz CRH.** 1991. Lipid A-like Molecules That Antagonize the Effects of Endotoxins on Human Monocytes. J Biol Chem **266**:19490-19498.

14. **Mullarkey M**. 2002. Inhibition of Endotoxin Response by E5564, a Novel Toll-Like

Receptor 4-Directed Endotoxin Antagonist. Journal of Pharmacology and Experimental Therapeutics **304**:1093–1102.

15. **Needham BD, Carroll SM, Giles DK, Georgiou G, Whiteley M, Trent MS.** 2013. Modulating the innate immune response by combinatorial engineering of endotoxin. PNAS **110**:1464-1469.

16. **Kahler CM**, **Datta A**, **Tzeng Y-L**, **Carlson RW**, **Stephens DS**. 2004. Inner core assembly and structure of the lipooligosaccharide of Neisseria meningitidis: capacity of strain NMB to express all known immunotype epitopes. Glycobiology **15**:409–419.

17. **John CM**, **Liu M**, **Jarvis GA**. 2009. Profiles of structural heterogeneity in native lipooligosaccharides of Neisseria and cytokine induction. J Lipid Res **50**:424–438.

18. **Wirth HP**. 2006. Host Lewis phenotype-dependent Helicobacter pylori Lewis antigen expression in rhesus monkeys. The FASEB Journal **20**:1534–1536.

19. **Lozniewski A**, **Haristoy X**, **Rasko DA**, **Hatier R**, **Plenat F**, **Taylor DE**, **Angioi-Duprez K**. 2003. Influence of Lewis Antigen Expression by Helicobacter pylori on Bacterial Internalization by Gastric Epithelial Cells. Infection and Immunity **71**:2902–2906.

20. **Gringhuis SI**, **Dunnen den J**, **Litjens M**, **van der Vlist M**, **Geijtenbeek TBH**. 2009. Carbohydrate-specific signaling through the DC-SIGN signalosome tailors immunity to Mycobacterium tuberculosis, HIV-1 and Helicobacter pylori. Nat Immunol **10**:1081–1088.

21. **Wittmann A**, **Lamprinaki D**, **Bowles KM**, **Katzenellenbogen E**, **Knirel YA**, **Whitfield C**, **Nishimura T**, **Matsumoto N**, **Yamamoto K**, **Iwakura Y**, **Saijo S**, **Kawasaki N**. 2016. Dectin-2 Recognizes Mannosylated O-antigens of Human Opportunistic Pathogens and Augments Lipopolysaccharide Activation of Myeloid Cells. Journal of Biological Chemistry **291**:17629–17638.

22. **Geijtenbeek TBH**, **Gringuis SI**. 2009. Signalling through C-type lectin receptors: shaping immune responses. Nat Rev Immunol **9**:465-479.

23. **Kraal L**, **Abubucker S**, **Kota K**, **Fischbach MA**, **Mitreva M**. 2014. The Prevalence of Species and Strains in the Human Microbiome: A Resource for Experimental Efforts. PLoS ONE **9**:e97279–11.

24. **Berezow AB**, **Ernst RK**, **Coats SR**, **Braham PH**, **Karimi-Naser LM**, **Darveau RP**. 2009. The structurally similar, penta-acylated lipopolysaccharides of Porphyromonas gingivalis and Bacteroides elicit strikingly different innate immune responses. Microbial Pathogenesis **47**:68–77.

25. **Weintraub A, Zähringer U, Wollenweber H-W, Seydel U, Rietschel ET.** 1989. Structural characterization of the lipid A component of Bacteroides fragilis strain

NCTC 9343 lipopolysaccharide. Eur J Biochem **183**:425-431.

26. **Vatanen T**, **Kostic AD**, **d'Hennezel E**, **Siljander H**, **Franzosa EA**, **Yassour M**, **Kolde R**, **Vlamakis H**, **Arthur TD**, **Hämäläinen A-M**, **Peet A**, **Tillmann V**, **Uibo R**, **Mokurov S**, **Dorshakova N**, **Ilonen J**, **Virtanen SM**, **Szabo SJ**, **Porter JA**, **Lähdesmäki H**, **Huttenhower C**, **Gevers D**, **Cullen TW**, **Knip M**, **Xavier RJ**, **Group DS**. 2016. Variation in Microbiome LPS Immunogenicity Contributes to Autoimmunity in Humans. Cell **165**:842–853.

27. **Brozek KA, Raetz CRH.** 1990. Biosynthesis of Lipid A in Escherichia coli. J Biol Chem **265**:15410-15417.

28. **Cullen TW**, **Schofield WB**, **Barry NA**, **Putnam EE**, **Rundell EA**, **Trent MS**, **Degnan PH**, **Booth CJ**, **Yu H**, **Goodman AL**. 2015. Antimicrobial peptide resistance mediates resilience of prominent gut commensals during inflammation. Science **347**:170–175.

29. **Maskell JP**. 1991. The resolution of bacteroides lipopolysaccharides by polyacrylamide gel electrophoresis. J Med Microbiol **34**:253-257.

30. **Maskell JP**. 1994. Electrophoretic analysis of the lipopolysaccharides of Bacteroides spp. Antonie Leeuwenhoek **65**:155-161.

31. **Roger T, Froidevaux C, Le Roy D, Reymond MK, Chanson A-L, Mauri D, Burns K, Riederer BM, Akira S, Calandra T.** 2009. Protection from lethal Gram-negative bacterial sepsis by targeting Toll-like receptor 4. PNAS **7**: 2348-2352.

32. **Raetz CRH, Reynolds CM, Trent MS, Bishop RE**. 2007. Lipid A Modification Systems in Gram-Negative Bacteria. Annu Rev Biochem **76**:295-329.

Chapter 2

Characterization of *B. thetaiotaomicron* lipid A

2.1 Identification of candidate *Bacteroides* lipid A biosynthesis genes

In order to identify candidate biosynthetic genes for *Bacteroides* lipid A, we performed BLAST searches against *Bacteroides* genomes using, as queries, the *E. coli* MG1655 lipid A biosynthesis genes (1). As expected, orthologs of each Raetz pathway enzyme were identified, except the *Bacteroides* species had only one ortholog of the acyltransferases LpxL and LpxM; we refer to this ortholog as LpxL for simplicity (Table 2.1). This finding is consistent with the *B. thetaiotaomicron, B. fragilis,* and *Bacteroides dorei* lipid A structure being penta-acylated rather than hexa-acylated (2-4). *B. vulgatus* was the only surveyed species to have a second LpxL/LpxM homolog, BVU_1014. Previous work indicates that this gene is part of an aryl polyene gene cluster, indicating that it likely transfers an acyl chain to a non-LPS substrate (5). We next used BLAST to predict lipid A phosphorylation by sequence homology to the lipid A 1- and 4'-phosphatases discovered in *Porphyromonas gingivalis* (Figure 2.1, Table S1) (6-7). While this search resulted in only one candidate for some species like *B. thetaiotaomicron*, for others there were multiple candidates, and experimental validation will be necessary to conclude which, if any, perform the predicted function.

2.2 Chemical structure of *Bacteroides* lipid A

In order to determine the lipid A profile of each species, we isolated lipid A from five common *Bacteroides* species using the Tri-Reagent method and characterized their lipid A profile by MALDI-TOF mass spectrometry (8). Consistent with previous reports, the structures of *B. thetaiotaomicron* VPI-5482 and *B. fragilis* NCTC 9343 lipid A are penta-acylated and mono-phosphorylated, with their MALDI spectra showing a cluster

of peaks around 1688 m/z (2-3). Moreover, *B. uniformis* ATCC 8492, *B. vulgatus* ATCC 8482, and *B. ovatus* ATCC 8483 produce lipid A with virtually identical mass spectra (Figure 2.2). A contaminating cluster of peaks appears in all spectra around 1250 m/z, but we do not believe this species to be relevant to lipid A. Additionally, some spectra, for example the *B. vulgatus* spectrum, present peaks that are about 224 m/z higher mass than the 1688 m/z cluster. This result suggests that certain *Bacteroides* species may be able to add another acyl chain to their lipid A. Such a modification would require a lipid A secondary acyltransferase with little to no homology to the known enzymes, since we have reported all the homologs identified by our BLAST search. Because the bacteria were grown in rich media under normal anaerobic growth conditions, we cannot be certain that the structure of their lipid A is the same under conditions of host colonization, nor do we know whether it can change in response to stresses encountered in the host.

2.3 Targeting late biosynthesis genes for modification

Because lipid A is typically an essential component of the outer membrane of Gram-negative bacteria, deletion of genes in the lipid A biosynthetic pathway is frequently lethal to bacteria (9-14). Interestingly, the later biosynthetic genes such as the acyltransferases and phosphatases can often be deleted (15). Working in *B. thetaiotaomicron* VPI-5482 *Δtdk*, our background strain for genetic knockouts lacking the thymidine kinase gene *tdk*, we made scarless single deletions of the putative *lpxL* and *lpxF* orthologs we had identified by BLAST search (BT2152 and BT1854, respectively) and isolated lipid A from the resulting mutants.

2.3.1 *B. thetaiotaomicron* lipid A biosynthesis: *lpxL*

MALDI-TOF analysis showed a loss of 224 m/z in the Δ*lpxL* mutant, consistent with the loss of a 15-carbon acyl chain from the wild-type structure of lipid A at 1688 m/z (Figure 2.3). The characteristic cluster of peaks each separated by 14 m/z is still present as expected. Notably, the contaminating peak cluster at around 1250 m/z does not change mass when the mass of lipid A changes, which has led us to determine that the contaminant molecule is unrelated to lipid A (Appendix 3).

2.3.2 *B. thetaiotaomicron* lipid A biosynthesis: *lpxF*

MALDI-TOF analysis of the Δ*lpxF* mutant showed a gain of 80 m/z over the wild-type molecule at 1688 m/z, indicating the addition of a phosphate group (Figure 2.4). The assignment of BT1854 as the *B. thetaiotaomicron* lipid A 4'-phosphatase represents independent confirmation of a result first reported by Goodman and coworkers (16). The addition of a phosphate group on *B. thetaiotaomicron* lipid A appears to make the molecule more susceptible to being sodiated, because a similar cluster of peaks to the 1755 m/z cluster is visible on the mass spectrum, with each peak separated from its corresponding 1755m/z cluster peak by 22 m/z.

2.3.3 Further structural modification of *B. thetaiotaomicron* lipid A

From previous work in *E. coli* testing the ability of a wide variety of lipid A structural variants to stimulate the human monocytic cell line THP-1, we hypothesize that identifying lipid A biosynthesis genes in *Bacteroides* will allow us to make mutants that may have different immunostimulatory abilities and could be used to control innate

immune responses in a host (17). Towards this goal, we generated a *B. thetaiotaomicron* Δ*lpxL* Δ*lpxF* double mutant that elaborates tetra-acylated, di-phosphorylated lipid A, which we anticipate will be a TLR4 antagonist due to its structural similarity to Eritoran (Figure 2.5). After MALDI-TOF analysis of the purified lipid A, the mass of the resulting cluster of peaks is around 1544 m/z, which is 144 m/z less than wild-type *Bt* lipid A at 1688 m/z. That 144 m/z decrease is equivalent to the loss of 224 m/z observed in the *B. thetaiotaomicron ΔlpxL* mutant plus the addition of 80 m/z as observed in the *B. thetaiotaomicron ΔlpxF* mutant, indicating that we have made a tetra-acylated di-phosphorylated lipid A molecule in *B. thetaiotaomicron.* Consistent with the result from the diphosphorylated Δ*lpxF* single mutant, this diphosphorylated molecule also appears to be sodiated with a similar +22 m/z cluster apparent.

2.4 Discussion

An mutant of *E. coli* which lacks secondary acyl chains on lipid A—yielding a tetra-acylated, di-phosphorylated molecule referred to as lipid IV_A—cannot grow above 32°C (18). Due to this finding, we were surprised at how well *B. thetaiotaomicron* was able to tolerate these alterations to its outer membrane. In order for *E. coli* to tolerate making tetra-acylated lipid A, either it must be grown at a cooler temperature or its inner membrane lipid A flippase MsbA must be overexpressed (19). This finding suggests that the problem for *E. coli* is not that the outer membrane cannot function properly with tetra-acylated lipid A but that MsbA does not transport a tetra-acylated lipid A molecule as efficiently as a hexa-acylated molecule. Deletion of an acyl chain makes lipid A a smaller, less hydrophobic molecule, and addition of a phosphate group adds more

negative charge to the molecule, alterations which both could be significant in the recognition of *B. thetaiotaomicron* lipid A by its MsbA homolog (BT3386). We were prepared for the these mutants to be temperature sensitive or not viable, even going as far as to perform the *lpxL* knockout at 37°C and 30°C in parallel and exploring the idea of attempting to overexpress BT3386 as, at the time, gene overexpression in *B. thetaiotaomicron* was not trivial. Ultimately, the single and double mutants in *B. thetaiotaomicron* could be performed under normal conditions, and they all grow in rich media at 37°C. The Δ*lpxL* Δ*lpxF* double mutant does appear to have a slight growth defect—it takes about 40 hours for colonies to appear compared to 24-30 hours for wild-type *B. thetaiotaomicron* and the single mutants. However, if colonies of *B. thetaiotaomicron* Δ*lpxL* Δ*lpxF* and wild-type *B. thetaiotaomicron* are picked and used to inoculate liquid media at the same time, both strains will reach mid-log phase in 16-20 hours. The ability of these lipid A mutants to grow under normal conditions was encouraging because we expect these molecules have the ability to interact differently with the TLR4/MD-2 complex, especially the tetra-acylated mono-phosphorylated double mutant as it mimics the general structure of the TLR4/MD-2 antagonist Eritoran. In future work, we plan to test the ability of this mutant to colonize mice and would like to profile the innate immune response to a gut colonized by a normally mutualistic bacterium now harboring an antagonist of TLR4. We initially hypothesized this would be a beneficial change, with a TLR4 antagonist blocking signals from any potentially inflammatory ligands present in the gut. However, *Yersinia pestis* purposefully tetra-acylates its lipid A so that it can persist in humans without being detected by the innate immune system, so it is possible that colonizing a mouse with our tetra-acylated

diphosphorylated strain could result in an animal that is more susceptible to bacterial infection (20).

2.5 Materials and methods

2.5.1 Bacterial strains, growth conditions, and reagents

See Appendix 1 for a full list of bacterial strains and plasmids used in this study. All *Bacteroides* strains were cultured anaerobically at 37°C in peptone-yeast extract-glucose (PYG) liquid medium or brain heart infusion (BHI) agar (BD Biosciences) at 10% defibrinated horse blood (Hardy Diagnostics). The gas mix for the anaerobic chamber (Coy Laboratory Products) was 5% hydrogen and 20% carbon dioxide, balanced with nitrogen (Airgas). The *E. coli* strains used for cloning the pExchange-*tdk* knockout constructs were cultured in Luria broth (LB) or agar supplemented with carbenicillin.

2.5.2 Construction of *B. thetaiotaomicron* clean deletion mutants

See Appendix 2 for a list of all primers used for making scarless gene deletions in *B. thetaiotaomicron*. To make clean deletions via conjugation and homologous recombination as described by Koropatkin and coworkers, approximately 1000bp upstream and downstream of the desired gene to be deleted, including the start and stop codons, respectively, were amplified by PCR (Figures 2.6 and 2.7) (21). For BT2152 and BT1854, the two fragments were stitched together by PCR taking advantage of the overlapping regions in the original primers. For BT2152, the pExchange-*tdk* vector (gift from Justin Sonnenburg, Stanford University) and the fused

insert were digested with SalI and NotI and ligated together. For BT1854, only the pExchange-*tdk* vector was digested with SalI and XbaI, and the insert was assembled with the vector by circular polymerase extension cloning (CPEC). Ligation and CPEC products were transformed into electrocompetent *E. coli* S17-1 *λ pir* (Bio-Rad *MicroPulser*™, 18 kV in 0.1 cm cuvettes), selected for on LB agar plus carbenicillin, and conjugated into *B. thetaiotaomicron* VPI-5482 *Δtdk*, which serves as the background strain for all the clean deletions. Single recombinants were selected for on BHI-blood agar supplemented with 200 μg/mL gentamicin and 25 μg/mL erythromycin, picked, cultured overnight in PYG medium, and plated on BHI-blood agar supplemented with 200 μg/mL 5-fluoro-2'-deoxyuridine. Colonies were screened for success of the gene deletion by PCR, and deletion was confirmed by DNA sequencing.

2.5.2 The Tri-Reagent method for lipid A extraction

To purify lipid A from *Bacteroides* species, we used the Tri-Reagent method (22). Briefly, bacterial cells were grown in 10 mL liquid cultures to mid-log phase, harvested by centrifugation at 3270 xg for 10 minutes, resuspended in 1 mL Tri-Reagent (Molecular Research Center), vortexed vigorously, and left at room temperature for 10 minutes. 1 mL chloroform was added and the mixture was vortexed and left at room temperature for another 10 minutes. The mixture was centrifuged at 15,000 xg for 10 minutes and the aqueous layer was removed to a clean tube. The sample was extracted again with 200 μL deionized water, and the resulting aqueous layer was removed to the same tube as above. The aqueous extraction was repeated two more times, and the collected aqueous material was pooled and lyophilized (Labconco FreeZone). A mild

acid hydrolysis was used to separate the lipid A from its poly- or oligosaccharide chain. The lyophilized material was resuspended in 1 mL 10 mM sodium acetate pH 4.5 and 1% sodium dodecyl sulfate (SDS). Samples were boiled at 100°C for one hour and then lyophilized again. To remove SDS from the lipid A, the lyophilized material was washed with 1 mL ice cold acidified ethanol (20 mM hydrochloric acid in 95% ethanol) once followed by three washes each with 500 µL ice cold 95% ethanol, centrifuging at 3270 xg at 4°C for five minutes each time. A Bligh-Dyer extraction was used to separate the hydrolyzed lipid A from the saccharides, and the organic and interface layers were removed to a small glass vial. Solvent was removed by rotary evaporator and the material was stored at -20°C.

2.5.3 MALDI-TOF MS analysis of lipid A: sample and matrix preparation

Three to five drops of 3:1 chloroform/methanol was added to a thawed vial of dried lipid A, with gentle rocking to help the lipid A dissolve. The matrix was a saturated solution of 5-chloro-2-mercaptobenzothiazole (CMBT) in 3:1 chloroform/methanol. To spot the sample on the target, 3 µL dissolved sample was mixed with 3 µL matrix, and 1 µL of the resulting mixture was spotted within an inscribed circle on the MALDI target (Waters Corporation) and allowed to dry (23).

2.5.4 MALDI-TOF MS analysis of lipid A: Negative-ion MALDI-TOF MS

Lipid A mass spectrometry analysis on the Waters Synapt G2 HDMS 32k instrument was performed at the University of California, San Francisco Sandler-Moore Mass Spectrometry Core Facility. MALDI-TOF MS analysis was carried out on a Waters

Corporation Synapt G2 high definition mass spectrometer with a 355 nm Nd:YAG laser in reflectron negative-ion mode. The instrument was calibrated using a mixture of angiotensin II, renin substrate, insulin chain B, and bovine insulin (Sigma-Aldrich), with monoisotopic $[M-H]^-$ ion masses of 1044.5267, 1756.9175, 3492.6357, and 5728.5931 *m/z*, respectively (24). The standards were dissolved together in a solution 0.1% trifluoroacetic acid in water. Because the standard mixture was not in the same solvent as the CMBT matrix mentioned above, 1µL of CMBT matrix was spotted on the target and allowed to dry before 1 µL of the standard mixture was spotted on top of the matrix. MS data were collected between 400-5000 *m/z*, and the resulting spectra were smoothed and baseline-corrected using MassLynx software.

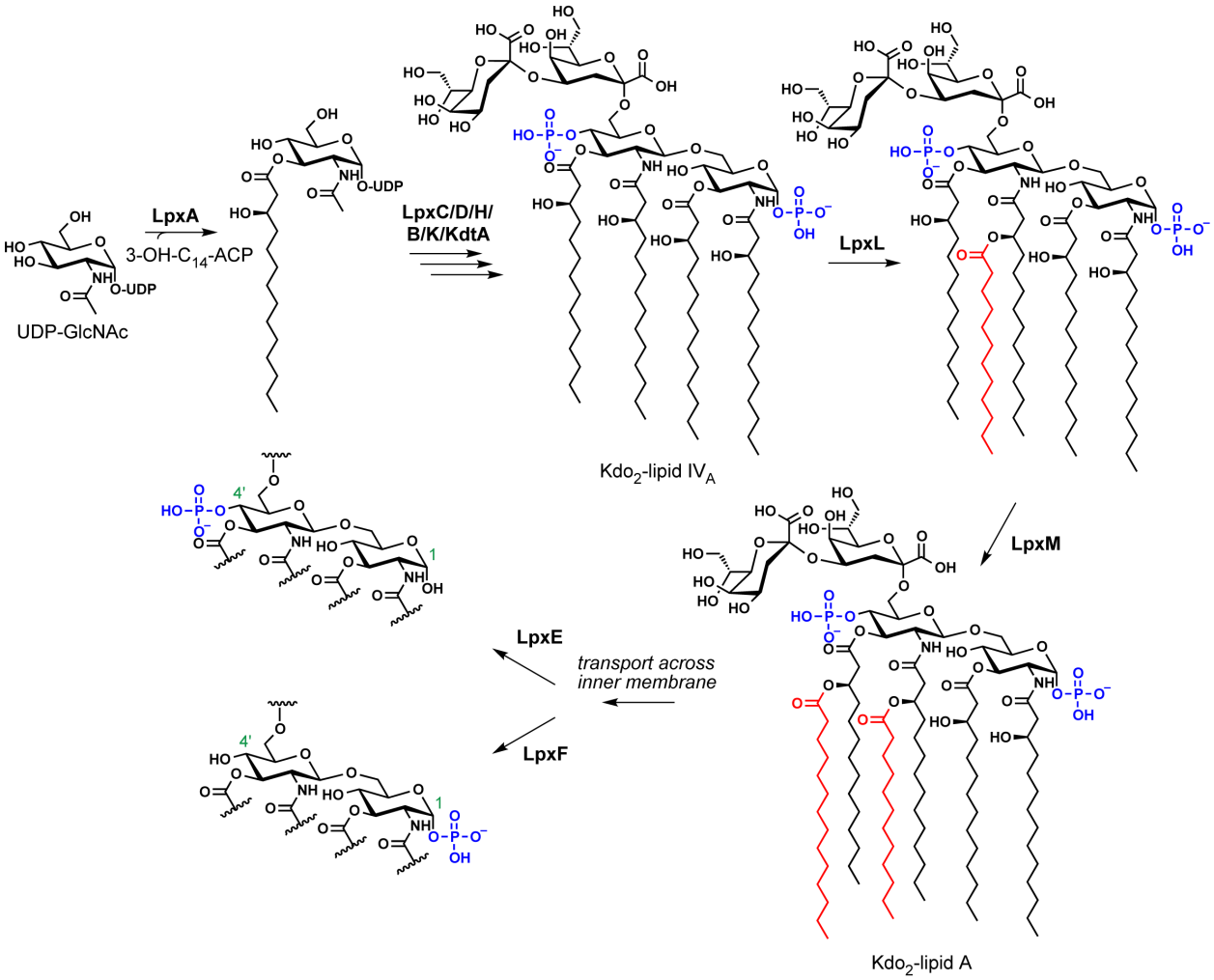

Figure 2.1. Modifications to lipid A by 1- and 4' phosphatases. After the enzymes in the Raetz pathway act and lipid A is diphosphorylated, bacteria possessing the required genes can use lipid A 1- and 4'-phosphatases to remove either or both phosphate groups.

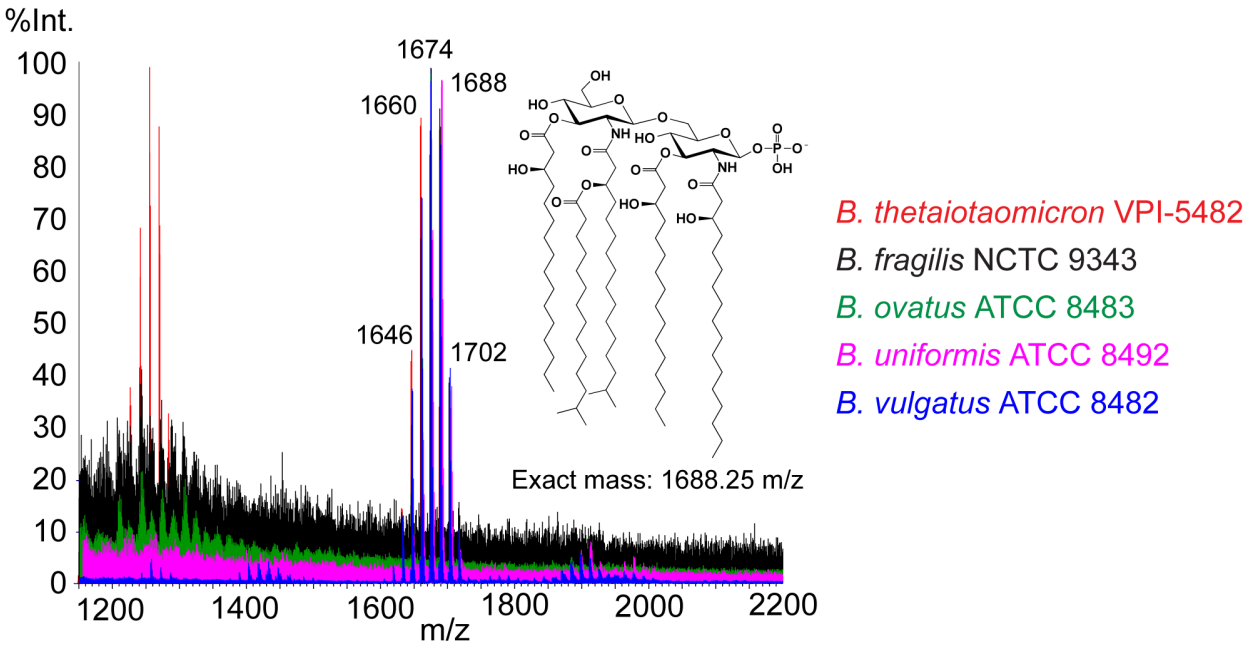

Figure 2.2. Mass spectra of purified lipid A from five *Bacteroides* species. Lipid A was purified from *B. thetaiotaomicron* VPI-5482, *B. fragilis* NCTC 9343, *B. ovatus* ATCC 8343, *B. uniformis* ATCC 8492, and *B. vulgatus* ATCC 8482 by the Tri-Reagent method, dissolved in 3:1 chloroform/methanol and spotted on a 5-chloro-2-mercaptobenzothiazole (CMBT) matrix, and analyzed on a Waters Corporation Synapt G2 HDMS 32k MALDI-TOF instrument in reflectron negative-ion mode. All five have as their dominant lipid A species a cluster of peaks around 1688 m/z corresponding to the published structure of *B. thetaiotaomicron* lipid A. The peaks in the cluster are separated by 14 m/z (methylene group, CH_2) likely caused by heterogeneity in the number of carbons in each acyl chain of lipid A.

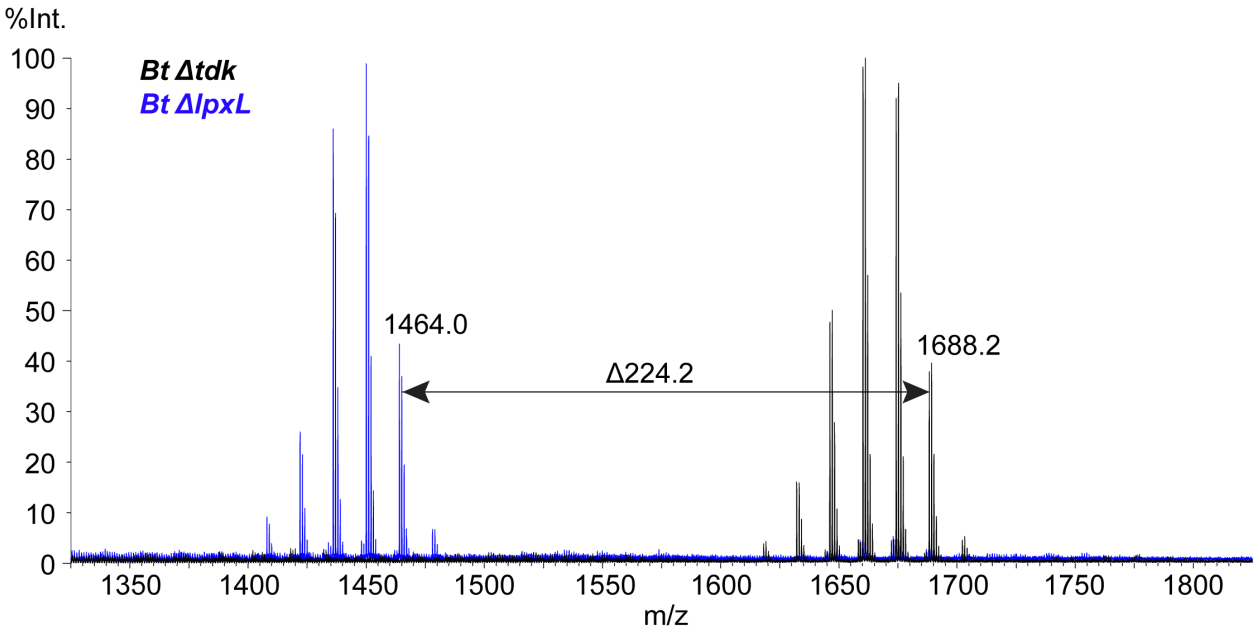

Figure 2.3. Mass spectrum of *B. thetaiotaomicron* Δ*lpxL* lipid A compared to wild-type. Lipid A was isolated from *B. thetaiotaomicron* Δ*lpxL* and by the Tri-Reagent method, dissolved in 3:1 chloroform/methanol and spotted on a CMBT matrix, and analyzed on a Waters Corporation Synapt G2 HDMS 32k MALDI-TOF instrument in reflectron negative-ion mode. *B. thetaiotaomicron* Δ*lpxL* produced a spectrum where the cluster of peaks characteristic of lipid A has decreased in mass by 224 m/z, the same mass as the 15-carbon secondary acyl chain from the published *B. thetaiotaomicron* structure.

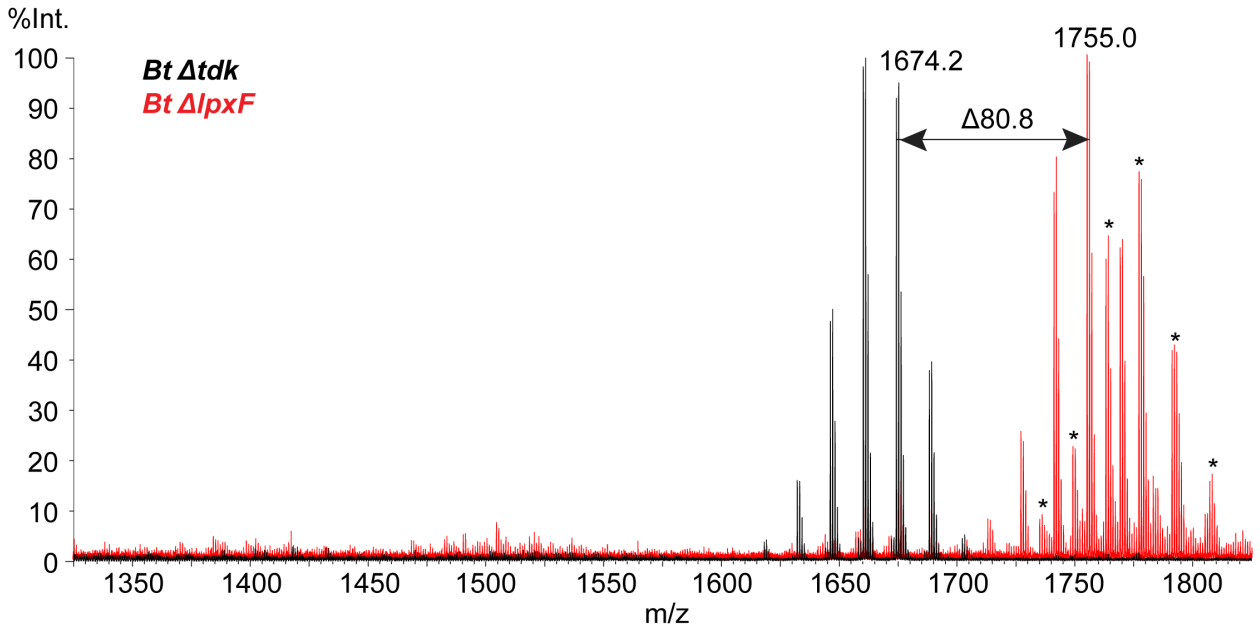

Figure 2.4. Mass spectrum of *B. thetaiotaomicron* Δ*lpxF* lipid A compared to wild-type. Lipid A was isolated from *B. thetaiotaomicron* Δ*lpxF* by the Tri-Reagent method, dissolved in 3:1 chloroform/methanol and spotted on a CMBT matrix, and analyzed on a Waters Corporation Synapt G2 HDMS 32k MALDI-TOF instrument in reflectron negative-ion mode. *B. thetaiotaomicron* Δ*lpxF* lipid A increased by 80 m/z over wild-type *B. thetaiotaomicron* indicating the presence of a phosphate group as expected. Sodiated peaks are marked with an asterisk.

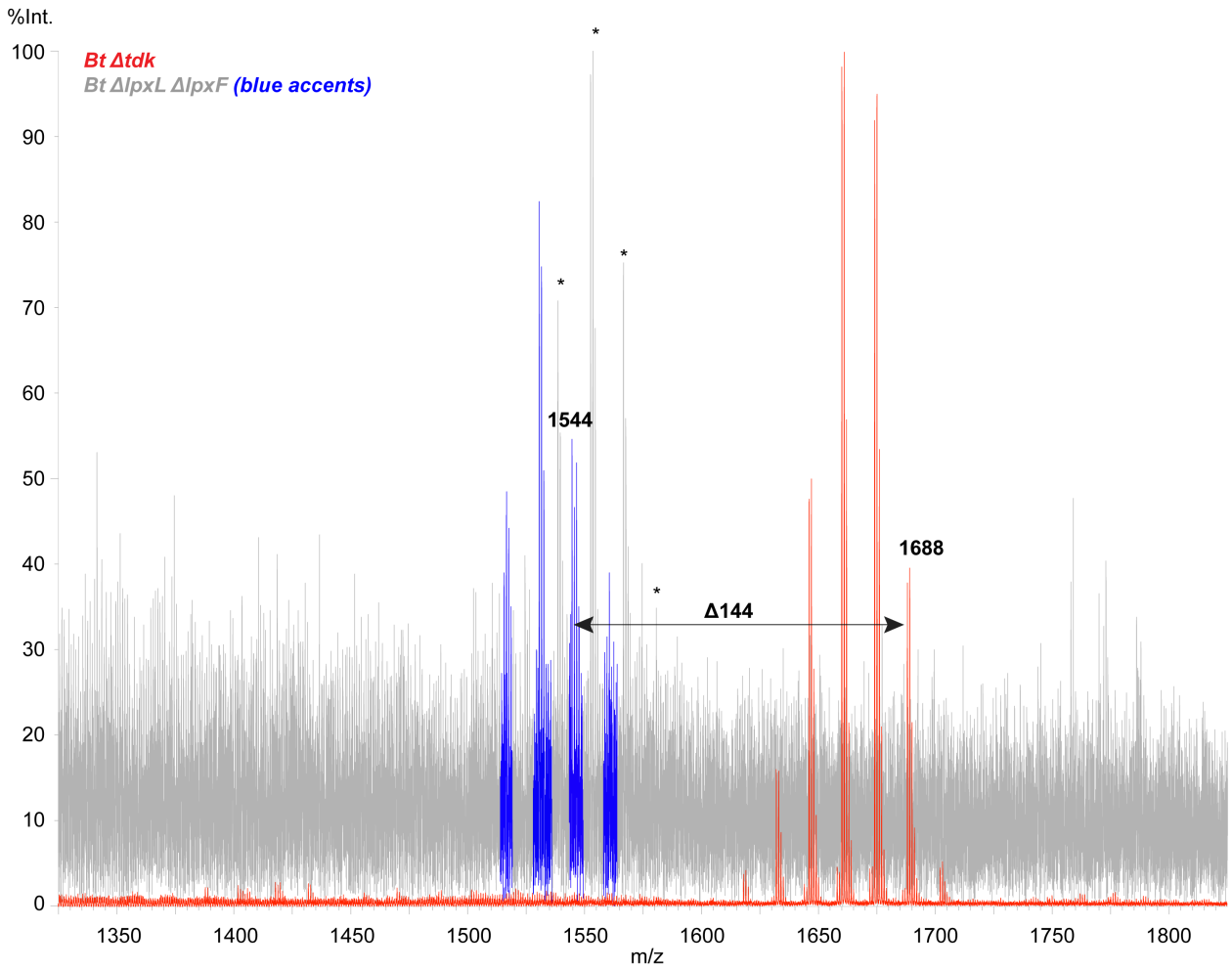

Figure 2.5. Mass spectrum of *B. thetaiotaomicron* Δ*lpxL* Δ*lpxF* lipid A compared to wild-type. Lipid A was isolated from *B. thetaiotaomicron ΔlpxL ΔlpxF* using the Tri-Reagent method. The resulting material was dissolved in 3:1 chloroform/methanol, mixed in a 1:1 ratio with saturated 5-chloro-2-mercaptobenzothiazole in 3:1 chloroform/methanol, and spotted on a Waters Corporation MALDI target. The sample was analyzed on a Waters Synapt G2 MALDI-TOF mass spectrometer in reflectron negative-ion mode. *B. thetaiotaomicron ΔlpxL ΔlpxF* peaks are accented in blue for clarity and sodiated *B. thetaiotaomicron ΔlpxL ΔlpxF* peaks are in grey and marked with an asterisk. The mutant lipid A decreased by 144 m/z over wild-type *B. thetaiotaomicron.*

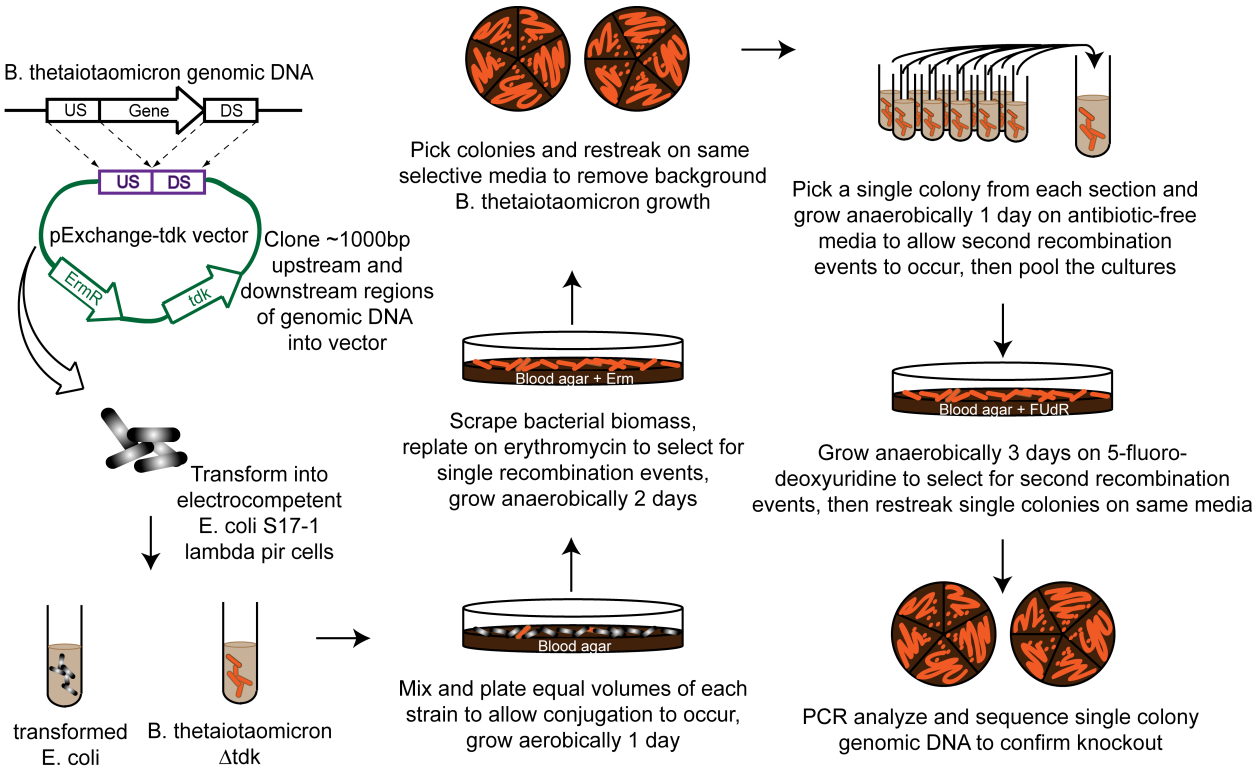

Figure 2.6. Cartoon representation of the steps required for generating clean deletion mutants in *B. thetaiotaomicron.*

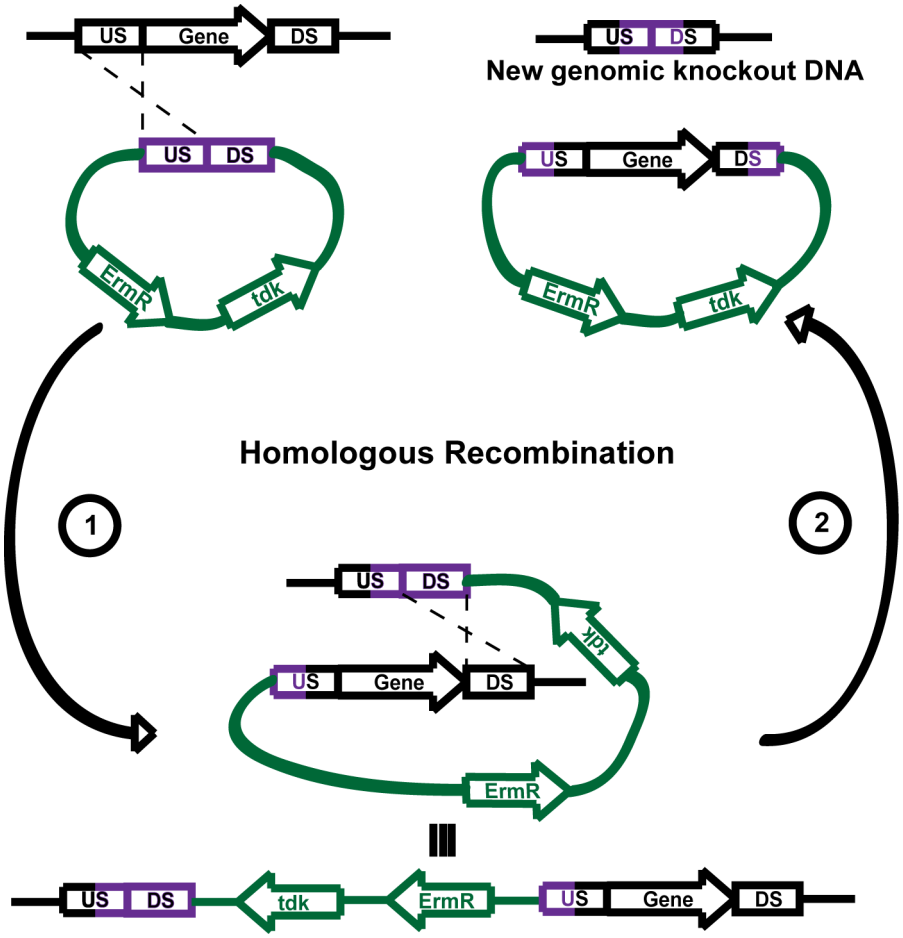

Figure 2.7. Depiction of the double recombination steps in the deletion protocol. After the first recombination step, either the second recombination occurs thereby deleting the gene, or the first recombination reverses, reverting to the wild-type sequence.

Table 2.1. Raetz pathway and lipid A phosphatase homologs in *Bacteroides*. Locus tags of homologs of the Raetz pathway genes in *E. coli* MG1655, and *lpxE* and *lpxF* in *Porphyromonas gingivalis* W83 from a selection of *Bacteroides* species. *Bacteroides* have homologs for every gene in the pathway except they have only one secondary acyltransferase, suggesting that their lipid A is predominantly penta-acylated. The species vary more in their putative homologs of the *P. gingivalis* phosphatases.

	E.coli MG1655	*P. gingivalis* W83	*B. thetaiotaomicron* VPI-5482	*B. fragilis* NCTC 9343	*B. ovatus* ATCC 8483	*B. uniformis* ATCC 8492	*B. vulgatus* ATCC 8482
lpxA	b0181		BT4205	BF0827	BACOVA_05052	BACUNI_03478	BVU_0099
lpxC	b0096		BT4206	BF0828	BACOVA_05053	BACUNI_03477	BVU_0098
lpxD	b0179		BT4207	BF0829	BACOVA_05054	BACUNI_03476	BVU_0097
lpxH	b0524		BT3697	BF0427	BACOVA_03513	BACUNI_00210	BVU_0525
lpxB	b0182		BT4004	BF0699	BACOVA_04823	BACUNI_03661	BVU_1917
lpxK	b0915		BT1880	BF3273	BACOVA_02939	BACUNI_02480	BVU_1603
kdtA	b3633		BT2747	BF4029	BACOVA_01057	BACUNI_00837	BVU_1476
lpxL	b1054		BT2152	BF3626	BACOVA_03194	BACUNI_03369	BVU_1062
lpxM	b1855						
lpxE		PG_1773		BF2346 BF4336		BACUNI_04140	BVU_3834 BVU_1238
lpxF		PG_1587	BT1854	BF3253	BACOVA_04598 BACOVA_04257	BACUNI_01242	BVU_3293

References

1. **Raetz CRH, Reynolds CM, Trent MS, Bishop RE**. 2007. Lipid A Modification Systems in Gram-Negative Bacteria. Annu Rev Biochem **76**:295-329.

2. **Berezow AB**, **Ernst RK**, **Coats SR**, **Braham PH**, **Karimi-Naser LM**, **Darveau RP**. 2009. The structurally similar, penta-acylated lipopolysaccharides of Porphyromonas gingivalis and Bacteroides elicit strikingly different innate immune responses. Microbial Pathogenesis **47**:68–77.

3. **Weintraub A, Zähringer U, Wollenweber H-W, Seydel U, Rietschel ET.** 1989. Structural characterization of the lipid A component of Bacteroides fragilis strain NCTC 9343 lipopolysaccharide. Eur J Biochem **183**:425-431.

4. **Vatanen T**, **Kostic AD**, **d'Hennezel E**, **Siljander H**, **Franzosa EA**, **Yassour M**, **Kolde R**, **Vlamakis H**, **Arthur TD**, **Hämäläinen A-M**, **Peet A**, **Tillmann V**, **Uibo R**, **Mokurov S**, **Dorshakova N**, **Ilonen J**, **Virtanen SM**, **Szabo SJ**, **Porter JA**, **Lähdesmäki H**, **Huttenhower C**, **Gevers D**, **Cullen TW**, **Knip M**, **Xavier RJ**, **Group DS**. 2016. Variation in Microbiome LPS Immunogenicity Contributes to Autoimmunity in Humans. Cell **165**:842–853.

5. **Cimermancic P**, **Medema MH**, **Claesen J**, **Kurita K**, **Brown LCW**, **Mavrommatis K**, **Pati A**, **Godfrey PA**, **Koehrsen M**, **Clardy J**, **Birren BW**, **Takano E**, **Sali A**, **Linington RG**, **Fischbach MA**. 2014. Insights into Secondary Metabolism from a Global Analysis of Prokaryotic Biosynthetic Gene Clusters. Cell **158**:412–421.

6. **Coats SR**, **Jones JW**, **Do CT**, **Braham PH**, **Bainbridge BW**, **To TT**, **Goodlett DR**, **Ernst RK**, **Darveau RP**. 2009. Human Toll-like receptor 4 responses to P. gingivalis are regulated by lipid A 1- and 4′-phosphatase activities. Cell Microbiol **11**:1587–1599.

7. **Coats SR**, **Berezow AB**, **To TT**, **Jain S**, **Bainbridge BW**, **Banani KP**, **Darveau RP**. 2010. The Lipid A Phosphate Position Determines Differential Host Toll-Like Receptor 4 Responses to Phylogenetically Related Symbiotic and Pathogenic Bacteria. Infection and Immunity **79**:203–210.

8. **Yi EC**, **Hackett M**. 2000. Rapid isolation method for lipopolysaccharide and lipid A from Gram-negative bacteria. Analyst **125**:651–656.

9. **Nishijima M, Bulawa CE, Raetz CRH.** 1981. Two Interacting Mutations Causing Temperature-Sensitive Phosphatidylglycerol Synthesis in Escherichia coli membranes. J Bacteriol 113-121.

10. **Crowell DN, Anderson MS, Raetz CRH.** 1986. Molecular Cloning of the Genes for Lipid A Disaccharide Synthase and UDP-N-Acetylglucosamine Acyltransferase in Escherichia coli. J Bacteriol 152-159.

11. **Galloway SM, Raetz CRH.** 1990. A Mutant of Escherichia coli Defective in the First Step of Endotoxin Biosynthesis. J Biol Chem **265**:6394-6402.

12. **Meredith TC**, **Aggarwal P**, **Mamat U**, **Lindner B**, **Woodard RW**. 2006. Redefining the Requisite Lipopolysaccharide Structure in Escherichia coli. ACS Chem Biol **1**:33–42.

13. **Reynolds CM**, **Raetz CRH**. 2009. Replacement of Lipopolysaccharide with Free Lipid A Molecules in Escherichia coli Mutants Lacking All Core Sugars. Biochemistry **48**:9627–9640.

14. **Tomaras AP**, **McPherson CJ**, **Kuhn M**, **Carifa A**, **Mullins L**, **George D**, **Desbonnet C**, **Eidem TM**, **Montgomery JI**, **Brown MF**, **Reilly U**, **Miller AA**, **O'Donnell JP**. 2014. LpxC Inhibitors as New Antibacterial Agents and Tools for Studying Regulation of Lipid A Biosynthesis in Gram-Negative Pathogens. MBio **5**:e01551–14–e01551–14.

15. **Klein G, Lindner B, Brabetz W, Brade H, Raina S.** 2009. Escherichia coli K-12 Suppressor-free Mutants Lacking Early Glycosyltransferases and Late Acyltransferases. J Biol Chem **284**:15369-15389.

16. **Cullen TW**, **Schofield WB**, **Barry NA**, **Putnam EE**, **Rundell EA**, **Trent MS**, **Degnan PH**, **Booth CJ**, **Yu H**, **Goodman AL**. 2015. Antimicrobial peptide resistance mediates resilience of prominent gut commensals during inflammation. Science **347**:170–175.

17. **Needham BD, Carroll SM, Giles DK, Georgiou G, Whiteley M, Trent MS.** 2013. Modulating the innate immune response by combinatorial engineering of endotoxin. PNAS **110**:1464-1469.

18. **Vorachek-Warren MK**, **Ramirez S**, **Cotter RJ**, **Raetz CRH**. 2002. A Triple Mutant of Escherichia coli Lacking Secondary Acyl Chains on Lipid A. Journal of Biological Chemistry **277**:14194–14205.

19. **Zhou Z**, **White KA**, **Polissi A**, **Georgopoulos C**, **Raetz CRH**. 1998. Function of Escherichia coli MsbA, an Essential ABC Family Transporter, in Lipid A and Phospholipid Biosynthesis. J Biol Chem **273**:12466-12475.

20. **Montminy SW**, **Khan N**, **McGrath S**, **Walkowicz MJ**, **Sharp F**, **Conlon JE**, **Fukase K**, **Kusumoto S**, **Sweet C**, **Miyake K**, **Akira S**, **Cotter RJ**, **Goguen JD**, **Lien E**. 2006. Virulence factors of Yersinia pestis are overcome by a strong lipopolysaccharide response. Nat Immunol **7**:1066–1073.

21. **Koropatkin NM**, **Martens EC**, **Gordon JI**, **Smith TJ**. 2008. Starch Catabolism by a Prominent Human Gut Symbiont Is Directed by the Recognition of Amylose Helices. Structure **16**:1105–1115.

22. **Yi EC**, **Hackett M**. 2000. Rapid isolation method for lipopolysaccharide and lipid A

from Gram-negative bacteria. Analyst **125**:651–656.

23. **Schilling B**, **McLendon MK**, **Phillips NJ**, **Apicella MA**, **Gibson BW**. 2007. Characterization of Lipid A Acylation Patterns in Francisella tularensis, Francisella novicida, and Francisella philomiragia Using Multiple-Stage Mass Spectrometry and Matrix-Assisted Laser Desorption/Ionization on an Intermediate Vacuum Source Linear Ion Trap. Anal Chem **79**:1034–1042.

24. **Phillips NJ**, **Schilling B**, **McLendon MK**, **Apicella MA**, **Gibson BW**. 2004. Novel Modification of Lipid A of Francisella tularensis. Infection and Immunity **72**:5340–5348.

Chapter 3

Discovery of the *B. thetaiotaomicron* LOS oligosaccharide biosynthesis gene cluster

3.1 Initial characterization of *Bacteroides* LPS/LOS architecture

In contrast to the level of structural detail already available about *B. thetaiotaomicron* lipid A, relatively little is known about the oligosaccharide component of the *Bacteroides* LPS molecule (1-2). About 15 years ago, two studies were conducted isolating LPS from a variety of *Bacteroides* species and analyzed by SDS-PAGE (3-4). Purified LPS molecules can be visualized by SDS-PAGE to gain a general idea of the number of molecules present in the preparation and their relative sizes (Figure 3-1). The data from the study indicated that each *Bacteroides* species elaborated LPS structures that were different from each other, to greater or lesser degrees depending on the species in question. Most species, including *B. thetaiotaomicron*, showed three to five bands on the gel at a relatively low molecular weight, and *B. vulgatus* was the only *Bacteroides* species to make LPS that had the hallmark 'laddering' pattern on the gel associated with the presence of an O-antigen repeating unit. We hypothesized after studying the results that *B. thetaiotaomicron* likely does not make 'traditional' LPS with a repeating unit but rather a set of smaller oligosaccharide attachments to lipid A, and thus is likely to be assembled by one biosynthetic gene cluster. We set out to investigate the structure and biosynthetic route for *B. thetaiotaomicron* LPS to explore its apparent lack of an O-antigen and provide tools for manipulating the glycan structure.

3.1.1 Purification of *Bacteroides* LOS

The hot-phenol water method for purifying LPS from bacteria was developed on bacterial strains producing LPS with an O-antigen, but we found that this method still worked well for our purposes despite our hypothesis that *B. thetaiotaomicron* LPS is

smaller than O-antigen containing LPS (5). We discovered in our purification attempts, however, that the hot-phenol water extraction is more of a glycolipid preparation than an LPS-specific extraction method. When we analyzed our 'pure' samples by SDS-PAGE as described below, we observed a high molecular weight band that we determined corresponds to capsular polysaccharides (CPS), which are a separate class of glycolipid produced by *Bacteroides* and others. This contamination made certain types of analysis more difficult, but we were still able to conduct our experiments as planned. However, it is useful when considering future *in vitro* and *in vivo* studies to examine the biological effects of these molecules or critically analyzing the work of others to keep in mind that attaining truly 'pure' preparations of LPS may not be possible.

3.1.2 SDS-PAGE analysis of *Bacteroides* LOS

We purified LPS from *B. thetaiotaomicron and B. vulgatus* ATCC 8482 and compared them to commercially available *E. coli* O55:B5 and *E. coli* MG1655 LPS to confirm the previous observation that *B. vulgatus* produces LPS exhibiting a laddered pattern on a gel like *E. coli* O55:B5, whereas *B. thetaiotaomicron* LPS does not (3-4). The laddering pattern is of note because it indicates the presence of an O-antigen; the number of repeating units added to the core oligosaccharide is variable, so the result is a population of LPS molecules of different sizes. As shown in Figure 3.2, *B. vulgatus* LPS appears to have an O-antigen based on the laddered pattern of its LPS as expected, but *B. thetaiotaomicron* instead appears to synthesize a small number of structures that we propose are more likely to be lipooligosaccharides (LOSs) due to their apparent lack

of an O-antigen. Hereafter, we will refer to the *B. thetaiotaomicron* outer membrane glycolipid as a LOS rather than LPS.

3.2 Identification of the *B. thetaiotaomicron* gene cluster for LOS oligosaccharide biosynthesis

3.2.1 Investigating capsular polysaccharide gene clusters

Previous work analyzing biosynthetic gene clusters from the NIH Human Microbiome Project data indicated that the phylum Bacteroidetes contains the largest number of predicted saccharide-producing gene clusters (6). *B. thetaiotaomicron* alone is known to harbor eight gene clusters responsible for making different capsular polysaccharides (39-40). We first wanted to determine whether any of these CPS gene clusters influenced the assembly of LOS. We isolated LOS from a *B. thetaiotaomicron* mutant constructed by Martens and coworkers in which all eight of its CPS clusters have been deleted (labeled here as ΔCPS), as well as eight additional strains that each possess only one CPS cluster (labeled here as CPS1-only, CPS2-only, and so on) (7). By SDS-PAGE gel we determined that neither deletion nor expression of CPS clusters affect the banding pattern of *Bt* LOS, indicating that these gene clusters do not encode the biosynthetic machinery for synthesis of *Bt* LOS (Figure 3.3). As visualized on the gel, no change in the CPS gene environment changed the pattern of the LOS bands.

3.2.2 BT3362-BT3380 as a candidate gene cluster

An independent lead came from a recently published report: By screening a *B. thetaiotaomicron* transposon library using an antibody that binds the bacterial cell

surface of *B. thetaiotaomicron*, Peterson et al. identified a gene cluster that they predicted would produce an extracellular polysaccharide structure, due to a lack of antibody binding when the cluster was mutated (8). Interestingly, nine out of the thirteen transposon mutants that did not bind the antibody had insertions in genes in the same gene cluster: BT3362-BT3380 (Figure 3.4). No transposon insertions were obtained in the first three genes of the cluster, indicating that these genes might be essential, or their disruption might lead to the accumulation of a toxic intermediate. This cluster caught our attention because it bears some resemblance to the *waa* core oligosaccharide gene clusters characterized in *E. coli*, with the first gene BT3362 sharing homology with the heptosyltransferases WaaC and WaaQ (9). Overall, the cluster possesses thirteen predicted glycosyltransferases (BT3362-BT3363, BT3365-BT3372, BT3377, BT3379-BT3380), a putative LPS kinase (BT3363), four tailoring enzymes (BT3373-BT3376), and a GtrA-like protein (BT3378). It is unclear what specific structural modifications BT3373-BT3376 might make based solely on sequence homology. Proteins in the GtrA-like family are typically integral membrane proteins that are thought to play a role in the transport of cell-surface polysaccharides (10-11).

3.2.3 Confirmation of BT3362-BT3380 as the *B. thetaiotaomicron* LOS oligosaccharide biosynthesis gene cluster

Intrigued, we obtained a subset of these transposon mutants and analyzed LOS isolated from each mutant by SDS-PAGE (Figure 3.4). Each mutant produced LOS with a banding pattern that appeared different from wild-type, except for the mutant with an insertion in the final gene in the cluster, BT3380. These data suggest that BT3362-

BT3380 encodes the biosynthesis of the *B. thetaiotaomicron* LOS oligosaccharide. Additionally, this striking result supports our hypothesis that bands observed on the SDS-PAGE gel are glycans that do not have a single polymerized repeating unit, but rather are variants of a heterogeneous oligosaccharide.

3.3 Intact LOS MALDI-TOF MS as a diagnostic tool for LOS mutants

While the SDS-PAGE analysis of LOS from the transposon mutants strongly implicates BT3362-BT3380 in *Bt* LOS oligosaccharide biosynthesis, we wanted to learn more about the specific profile of LOS molecules present on the gel using mass spectrometry. The LPS/LOS bands on an SDS-PAGE gel are approximations of the sizes of molecules in a sample, and using mass spectrometry would allow us to gain a clearer picture of the molecules made by the transposon mutants. Although it is easier to analyze LPS/LOS by MALDI-TOF after removing the O- and/or N-linked acyl chains via hydrazine or hydrogen fluoride treatment, we chose to analyze intact LOS molecules that were not subjected to chemical degradation or derivatization. We reasoned that LOS from *B. thetaiotaomicron* may contain important functional groups in the oligosaccharide chain that could be removed by these treatments, further complicating our efforts to elucidate detailed structural information about *B. thetaiotaomicron* LOS.

3.3.1 Limitations of the intact LOS MALDI-TOF MS technique

We adapted a previously published strategy for analyzing intact LPS/LOS by MALDI-TOF (12-13). LPS/LOS analysis by MALDI-TOF is typically challenging due to difficulties inducing the glycolipid to ionize because of its size and polarity. Although

instrument-specific limitations prevented us from obtaining resolution as high as others have observed, the degree of resolution we achieved was sufficient for confirming the approximate masses of LOS molecules in the sample and comparing them to those of the truncated mutants (13-14).

3.3.2 MALDI-TOF MS analysis of wild-type and ΔCPS LOS

We analyzed wild-type LOS along with LOS isolated from the *B. thetaiotaomicron* ΔCPS strain on a Shimadzu AXIMA Performance MALDI-TOF instrument in linear negative-ion mode using a unique THAP/nitrocellulose matrix as described below that is the critical step in helping these molecules to fly during analysis (Figure 3.5). The ΔCPS strain has wild-type LOS biosynthetic genes, and its lack of CPS yielded a mass spectrum with a cleaner background than our typical wild-type strain (Figure 3.6). In LOS from the ΔCPS strain, we observed a cluster of peaks around 5209 m/z, the largest mass detected for any of the samples. To the best of our knowledge, this is also ~1000 m/z larger than any LOS molecule previously analyzed using this technique. In addition to the peak we propose corresponds to full-length LOS at 5209 m/z, the ΔCPS sample has additional peaks at 3284 m/z and 3017 m/z, which are likely intermediate (truncated) LOS structures. Additionally, the sample (and all that follow) has a cluster of peaks around 1688 m/z representing lipid A, which likely derives from in-source fragmentation (13).

3.3.3 MALDI-TOF MS analysis of LOS from transposon mutants

We chose three transposon mutants that appeared by SDS-PAGE analysis to be truncated to varying degrees (*Bt* tn3365, *Bt* tn3368, and *Bt* tn3376). The transposon

mutants were created in the background of wild-type *B. thetaiotaomicron*, so CPS is present in those preparations. LOS from the least truncated transposon mutant we assayed, *Bt* tn3376, has its largest peaks around 4497 m/z and 4295 m/z, as well as the 3284 m/z peak common to the ΔCPS sample (Figure 3.7). LOS from *Bt* tn3368 has its largest peaks at 3608 m/z, as well as the 3284 m/z peak from the tn3376 and ΔCPS samples. Finally, the most truncated mutant in the set, *Bt* tn3365, has a single predominant peak at 2961 m/z. All of the transposon mutants have additional peaks between 1500 m/z to 3000 m/z that presumably derive from CPS, since by comparing Figure 3.5 and Figure 3.6 it is clear that these peaks are absent in the ΔCPS sample but present in LOS isolated from *B. thetaiotaomicron Δtdk* (see also Appendix 4).

3.4 Clean deletions of individual LOS cluster genes

In the above analysis, we felt capable choosing peaks to assign as representing of LOS molecules in our MALDI-TOF mass spectra of the transposon mutants, but to collect the cleanest mass spectrometry data we wanted to have truncated LOS mutants in the background of the ΔCPS strain. We also wanted to push the boundary of how much molecular control we could exert over the LOS molecule, so we decided to attempt to make single gene clean deletions of each of the nineteen genes in the LOS biosynthesis cluster. Having this collection of nineteen mutants that we expected would all produce differently truncated species of LOS would give us a set of tools to both determine the chemical structure of the LOS molecules and assess their biological function.

3.4.1 Construction of clean deletion mutants

In our attempt to individually delete every gene in the LOS oligosaccharide biosynthesis gene cluster, we found that clean deletions of BT3362 and BT3364, the first and third genes in the cluster, could not be generated. We expected this result because no transposon insertions were found in the BT3362-BT3364 region of the gene cluster, encoding two putative glycosyltransferases and a putative LPS kinase (8). Interestingly, it was possible to make a clean deletion of BT3363, the second glycosyltransferase, which is found in between the two potentially essential genes. No transposon insertions were found in BT3363 either, but based on our findings it would appear that perhaps a transposon insertion in BT3363 also disrupts BT3364. See Appendix 1 for a complete list of LOS oligosaccharide cluster single gene deletions that were generated.

3.4.2 SDS-PAGE and intact LOS MALDI-TOF analysis of clean deletion mutants

We purified LOS from a small subset of our single clean deletions in the ΔCPS background and analyzed the material by SDS-PAGE gel (Figure 3.8). We were surprised to find that at least in the case of the early genes in the biosynthetic cluster, the clean deletion mutant LOS did not appear to contain the same profile of LOS structures as the transposon mutant. In fact, the clean deletion mutants ΔCPS ΔBT3363 and ΔCPS ΔBT3365 displayed a banding pattern on the gel that looked unmistakable from the wild type banding pattern. This result highlights the need for caution when working with transposon mutants—it suggest that when an in-frame gene deletion is made at least some of the remaining genes downstream in the cluster are still active and can perform their function without their preferred precursor, or that there is a

separate compensatory mechanism that can glycosylate truncated LOS that is not able to function in the transposon mutants.

3.5 Bulk deletion of the LOS gene cluster

To investigate this discrepancy further and still attempt to generate truncated LOS structures in the ΔCPS background, we decided to delete as much of the cluster as possible, which we hypothesized would better represent the genomic state of the transposon mutants.

3.5.1 Construction of the cluster deletion mutant

Because we already had generated a ΔCPS ΔBT3363 strain and BT3362 and BT3364 cannot be deleted, we could essentially delete the cluster in one additional step. We created a vector that would result in the elimination of the entire BT3365-BT3380 block of genes as an in-frame scarless deletion and used it in the background of the ΔCPS ΔBT3363 strain to make a new ΔCPS ΔBT3363 ΔBT3365-BT3380 strain. An analogous set of gene deletions was made in the Δ*tdk* background simultaneously.

3.5.2 SDS-PAGE and intact LOS MALDI-TOF analysis of cluster deletion mutant

We were once again surprised to find that when we compared LOS purified from the ΔCPS ΔBT3363 ΔBT3365-BT3380 strain (and the Δ*tdk* ΔBT3363 ΔBT3365-BT3380 strain) and the wild-type LOS on an SDS-PAGE gel, the banding pattern of the ΔBT3363 ΔBT3365-BT3380 LOS appeared to resemble wild-type LOS (Figure 3.9). However, when we subjected the ΔBT3363 ΔBT3365-BT3380 LOS from either

background to MALDI-TOF analysis, the mass of the intact glycolipid was around 4870 m/z, smaller than the 5209 m/z seen in wild-type LOS (Figure 3.10). These data give some weight to our idea that there may be a compensatory mechanism in which the bacterium is able to glycosylate truncated forms of the LOS molecule in the absence of a functional LOS oligosaccharide gene cluster. Furthermore, this result highlights the limitations of SDS-PAGE analysis in determining structural differences between LOS samples. If we had not started by analyzing the transposon mutants and simply deleted the cluster and analyzed its LOS compared to wild-type by SDS-PAGE, we would have thought that the cluster was not relevant to LOS oligosaccharide biosynthesis. Additional studies are needed to understand whether *B. thetaiotaomicron* has an alternative lipid A glycosylation route in place of the LOS oligosaccharide gene cluster.

3.6 Predicting other *Bacteroides* LOS oligosaccharide gene clusters

Having identified the probable *B. thetaiotaomicron* LOS biosynthetic gene cluster, we hypothesized that it could be used to identify candidate LOS and LPS gene clusters in other *Bacteroides* species. We used the two essential genes in the cluster, BT3362 (a putative heptosyltransferase) and BT3364 (a putative LPS kinase), as queries in BLAST searches against other *Bacteroides* genomes and were able to identify similar clusters in many *Bacteroides* species (Figure 3.11). Given that a homologous cluster is found in *B. vulgatus*, which elaborates a laddered LPS, we expect that *B. vulgatus* harbors an additional cluster encoding the biosynthesis of the O-antigen repeating unit. This would likely be attached to the product of the *B. thetaiotaomicron*-like core oligosaccharide.

3.7 Discussion

Our results are a first step in characterizing what we expect will be a large amount of biosynthetic and structural heterogeneity among *Bacteroides* LPS or LOS molecules, the biological significance of which is yet undiscovered. Future studies will include investigating the mechanism by which LOS is glycosylated when its biosynthetic gene cluster is deleted by RNA-Seq analysis and searching for a mammalian innate immune receptor that is responsive to different *Bacteroides* LOS structures by genome-wide CRISPRi/a screens in an LPS-responsive cell line. Additionally, we plan to characterize a selection of the predicted LOS oligosaccharide biosynthesis gene clusters listed above. In *B. vulgatus*, we will also search for the presence of an O-antigen biosynthesis gene cluster or genes responsible for polymerizing and/or transferring the O-antigen onto the core oligosaccharide. The ability to block O-antigen biosynthesis in *B. vulgatus* by either method would give us the tools that would allow us to explore the function of an O-antigen in a commensal gut microbe in addition to our work determining the role of *Bacteroides* lipooligosaccharide in microbe-host interactions. Combined with our CPS mutants, we will have a set of strains that give us unprecedented control over bacterial glycolipids. Given our understanding of the privileged role glycolipids play in communicating with the mammalian immune system and the sheer quantity of LPS in the gut, *Bacteroides* LPS/LOS molecules are likely to be critical mediators in the interaction between commensal microbes and the host. Through careful characterization of the biosynthesis and structure of these molecules, we gain the possibility of manipulating their structure and by extension the host's immune response.

3.8 Materials and methods

3.8.1 Bacterial strains, growth conditions, and reagents

See Appendix 1 for a full list of bacterial strains and plasmids used in this study. All *Bacteroides* strains were cultured anaerobically at 37°C in peptone-yeast extract-glucose (PYG) liquid medium or brain heart infusion (BHI) agar (BD Biosciences) at 10% defibrinated horse blood (Hardy Diagnostics). The *B. thetaiotaomicron* transposon mutants were grown in liquid and agar media supplemented with 25 μg/mL erythromycin. *B. thetaiotaomicron* strains needed for large-scale LPS extraction were grown in BHI broth (BD Biosciences) supplemented with 5 μg/mL hemin and 500 μg/mL L-cysteine hydrochloride (Sigma-Aldrich). The gas mix for the anaerobic chamber (Coy Laboratory Products) was 5% hydrogen and 20% carbon dioxide, balanced with nitrogen (Airgas). The *E. coli* strains used for cloning the pExchange-*tdk* knockout constructs were cultured in Luria broth (LB) or agar supplemented with carbenicillin.

3.8.2 Construction of *B. thetaiotaomicron* clean deletion mutants

See Appendix 2 for a list of all primers used for making scarless gene deletions in *B. thetaiotaomicron*. To make clean deletions via conjugation and homologous recombination as described by Koropatkin and coworkers (and in Chapter 2 of this work), approximately 1000bp upstream and downstream of the desired gene to be deleted, including the start and stop codons, respectively, were amplified by PCR (15). For all the single gene deletions and the BT3365-BT3380 cluster deletion, Gibson assembly was used to combine the upstream and downstream fragments with SpeI/NotI digested pExchange-*tdk*. Gibson assembly products were transformed into

electrocompetent *E. coli* S17-1 *λ pir* (Bio-Rad *MicroPulser*^{TM}, 18 kV in 0.1 cm cuvettes), selected for on LB agar plus carbenicillin, and conjugated into *B. thetaiotaomicron* VPI-5482 *Δtdk*, which serves as the background strain for all the clean deletions. Single recombinants were selected for on BHI-blood agar supplemented with 200 µg/mL gentamicin and 25 µg/mL erythromycin, picked, cultured overnight in PYG medium, and plated on BHI-blood agar supplemented with 200 µg/mL 5-fluoro-2'-deoxyuridine. Colonies were screened for success of the gene deletion by PCR, and deletion was confirmed by DNA sequencing.

3.8.3 Large-scale LPS/LOS extraction

LPS or LOS was isolated from whole bacteria using the hot phenol-water method (5). Briefly, bacteria were grown overnight in a 10mL culture and then expanded to 2L. Cells were harvested once cultures reached an OD of at least 0.7 and pelleted by centrifugation at 6,000 xg for 30 minutes at 4°C. The entire wet cell pellet from the 2L culture was suspended in 20 mL water. Separately, the cell suspension and 20 mL 90% phenol solution in water were each brought up to 68°C with stirring and held at that temperature for 10 minutes. Once at temperature, the phenol solution was slowly added to the cell suspension using a 9-inch glass Pasteur pipet. The mixture was stirred vigorously for 30 minutes at 68°C and then cooled rapidly in an ice water bath with stirring for 10 minutes. The sample was centrifuged at 15,000 xg for 45 minutes and the upper aqueous layer was transferred into 1,000 MWCO dialysis tubing. The sample was dialyzed against 4L of water for four days, changing the water twice per day. LPS/LOS was pelleted out of the dialysate by ultracentrifugation at 105,000 xg for 4 hours. The

pellet was resuspended in water and treated with RNase A (Thermo Fisher), DNase I (New England Biolabs), and proteinase K (Thermo Fisher) before repeating the ultracentrifugation step. The pellet was resuspended in water, lyophilized, and stored at -20°C. Due to the difficulty and time-intensive nature of this purification, we ultimately decided to partner with Dr. Biswa Choudhury, a scientist at the University of California, San Diego Glycotechnology Core Facility, to have our LPS purifications performed by an expert.

3.8.4 Micro-scale LPS/LOS extraction

The micro-scale LPS/LOS extraction was used when a large number of samples was needed for SDS-PAGE analysis. Adapted from Marolda and coworkers, bacteria were grown to mid-log phase in 5 mL of media and pelleted (16). Cell pellets were resuspended in 150 µL lysis buffer (0.5 M Tris-hydrochloride pH 6.8, 2% SDS, 4% β-mercaptoethanol) and boiled at 100°C for 10 minutes. Proteinase K was added to each sample before incubating at 60°C for one hour. The sample temperature was raised to 70°C and 150 µL pre-warmed 90% phenol in water was added. Samples were vortexed three times at five-minute intervals during a 15-minute incubation. The samples were immediately cooled on ice for 10 minutes and centrifuged at 10,000 xg for 1 minute. The aqueous layer (~100 µL) was pipetted into a clean tube and five volumes of ethyl ether saturated with 10 mM Tris-hydrochloride pH 8.0 and 1 mM EDTA was added. The samples were vortexed and centrifuged, and the aqueous layer was removed to a clean tube. An appropriate amount of 3x loading dye (0.187 M Tris-hydrochloride pH 6.8, 6%

SDS, 30% glycerol, 0.03% bromophenol blue, 15% β-mercaptoethanol) was added and the samples were stored at -20°C.

3.8.5 SDS-PAGE analysis of LPS/LOS

To visualize LPS/LOS on an SDS-PAGE gel, we used Novex™ 16% tricine protein gels, 1.0 mm, 12 wells and 10x Novex™ tricine SDS running buffer (Thermo Fisher) (4). For samples prepared by the LPS/LOS micro-scale extraction, 15 µL of the resulting aqueous layer mixed with 3x loading dye were added to each lane. For samples prepared by the LPS/LOS large-scale extraction or purchased from Invivogen, 2.5 µg of material was resuspended in 15 µL 1x loading dye and the whole volume was added to a lane. Gels were run at 125 V for 90 minutes at room temperature, stained with Pro-Q™ Emerald 300 Lipopolysaccharide Gel Stain (Thermo Fisher) per manufacturer's instructions, and imaged on a Bio-Rad Gel Doc™ EZ Imager using the SYBR green filter.

3.8.6 MALDI-TOF MS analysis of intact LOS: sample and matrix preparation

To detect intact LPS by MALDI-TOF MS, we closely followed the technique developed by Phillips and coworkers adapted from Sturiale and coworkers to study *Neisseria* lipooligosaccharides (12-13). 1 mg of lyophilized LOS was dissolved in 100 µL 1:3 methanol/water with 5mM EDTA. Cation exchange beads (Dowex 50WX8, 200-400 mesh) were converted to the ammonium form by resuspending them in a 10% solution ammonium hydroxide in water (Sigma-Aldrich), briefly centrifuging them to pellet the beads, and carefully aspirating the supernatant. To desalt the LOS samples, each

sample suspension was added to the beads, vortexed, and centrifuged briefly to pellet the beads. The sample was removed to a clean tube and mixed 9:1 with 100 mM dibasic ammonium citrate before spotting on the target. The matrix was made by mixing a 15 mg/mL solution of nitrocellulose membrane in 1:1 isopropanol/acetone with a 200 mg/mL solution of 2'-4'-6'-trihydroxyacetophenone in methanol in a 1:3 ratio. The matrix was deposited by pipetting 1 µL within an inscribed circle on the target (Shimadzu) and allowed to dry. Once the matrix had dried completely, 1 µL of the sample preparation was added on top of the matrix and allowed to dry.

3.8.7 MALDI-TOF MS analysis of intact LOS: Negative-ion MALDI-TOF MS

Intact LOS mass spectrometry analysis was completed using the Shimadzu AXIMA Performance MALDI-TOF instrument in the laboratory of William DeGrado at the University of California, San Francisco. MALDI-TOF MS analysis was performed on a Shimadzu AXIMA Performance mass spectrometer with an N2 laser in linear negative-ion mode. It was calibrated using the same solution of four standards that was used to calibrate the Waters Synapt G2 for lipid A analysis: angiotensin II, renin substrate, insulin chain B, and bovine insulin in 0.1% trifluoroacetic acid, and the standards were spotted as described in the previous section except on the THAP/nitrocellulose matrix (17). MS data were collected between 700-7000 *m/z*, and the resulting spectra were smoothed and baseline-corrected using Shimadzu Biotech Launchpad software.

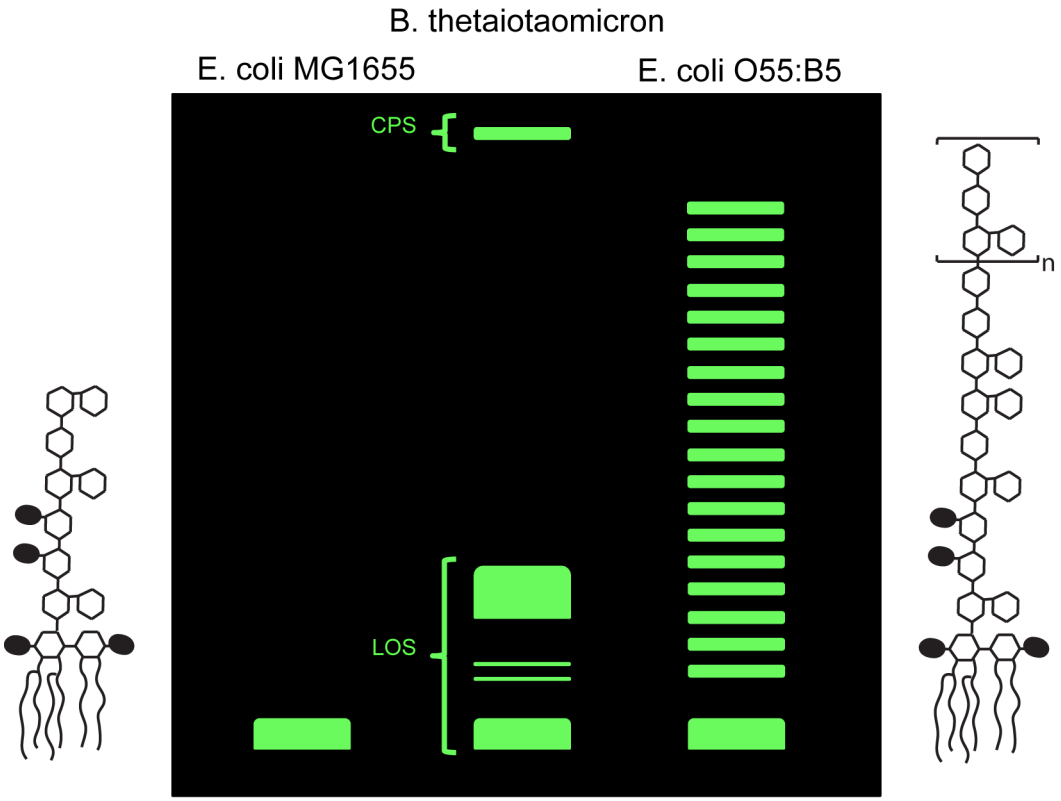

Figure 3.1. Cartoon representation of SDS-PAGE migration patterns of LPS/LOS.

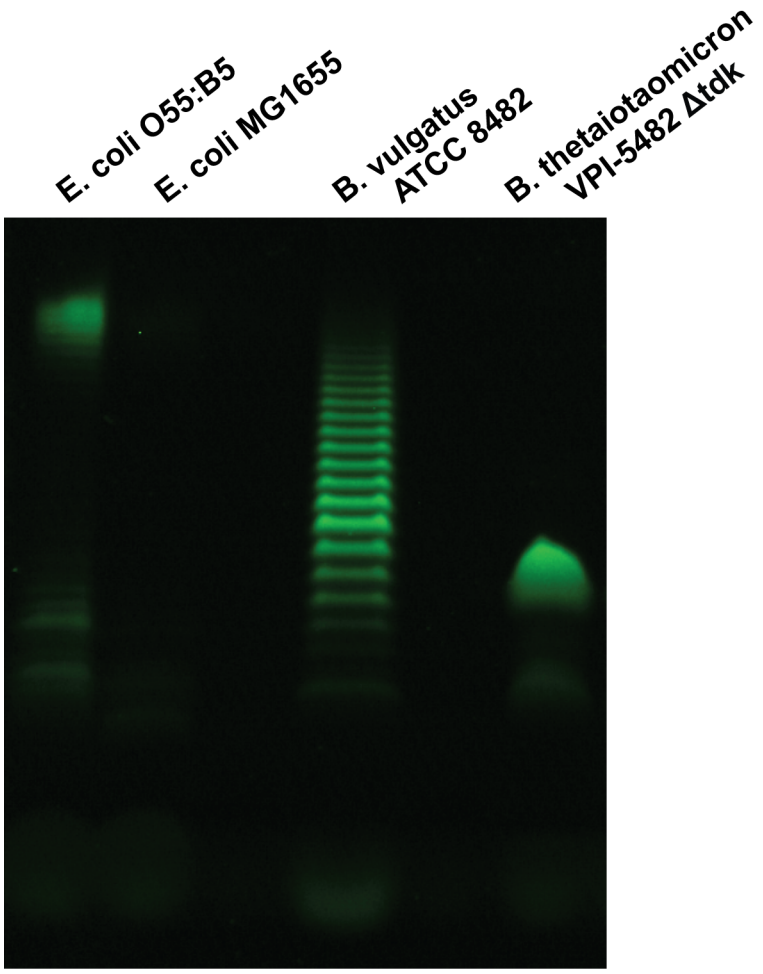

Figure 3.2. Comparison of *Bacteroides* LPS/LOS by SDS-PAGE. Purified LPS from *E. coli* O55:B5, *E. coli* MG1655, *B. vulgatus* ATCC 8482, and *B. thetaiotaomicron* Δ*tdk* were run on a 16% tricine SDS-PAGE gel. *B. vulgatus* LPS has a laddered pattern similar to LPS from *E. coli* O55:B5 suggesting the presence of an O-antigen repeating unit, but *B. thetaiotaomicron* LPS appears to lack a repeating unit and is therefore better characterized as lipooligosaccharide (LOS). *B. vulgatus* LPS was isolated using the microscale LPS extraction, and *B. thetaiotaomicron* LOS was isolated using the large-scale LPS extraction. LPS from *E. coli* O55:B5 and *E. coli* MG1655 was purchased from Invivogen.

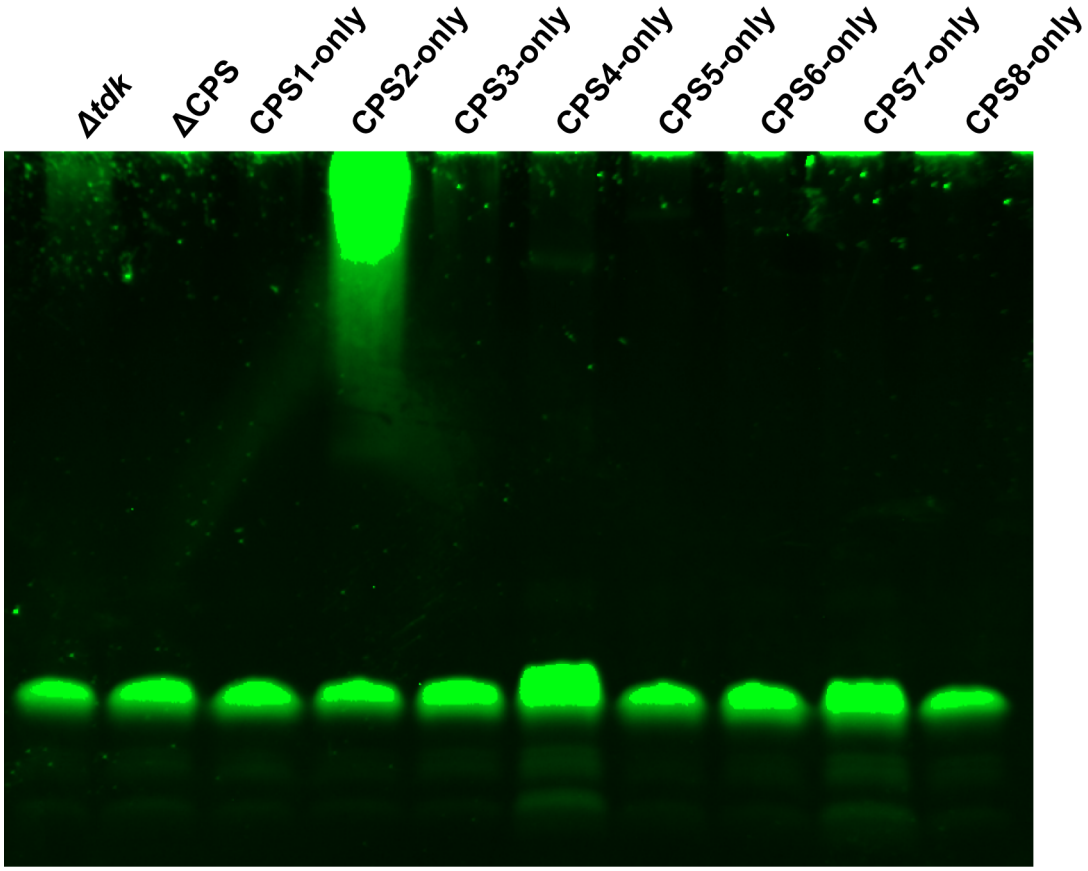

Figure 3.3. SDS-PAGE analysis of capsular polysaccharide mutants. LOS was isolated from all ten of these strains using the microscale extraction method and analyzed by SDS-PAGE, staining with the Pro-Q Emerald 300 Lipopolysaccharide Gel Stain Kit (Thermo Fisher). CPS bands can be seen for certain samples like CPS2-only and CPS4-only near the top of the gel. Whether the strains contain the gene clusters for all the CPSs (Δ*tdk*), none of the CPSs (ΔCPS), or one CPS at a time (CPS1-only, CPS2-only, and so on), the LOS bands appear unchanged, suggesting that the CPS gene clusters do not contribute to LOS biosynthesis.

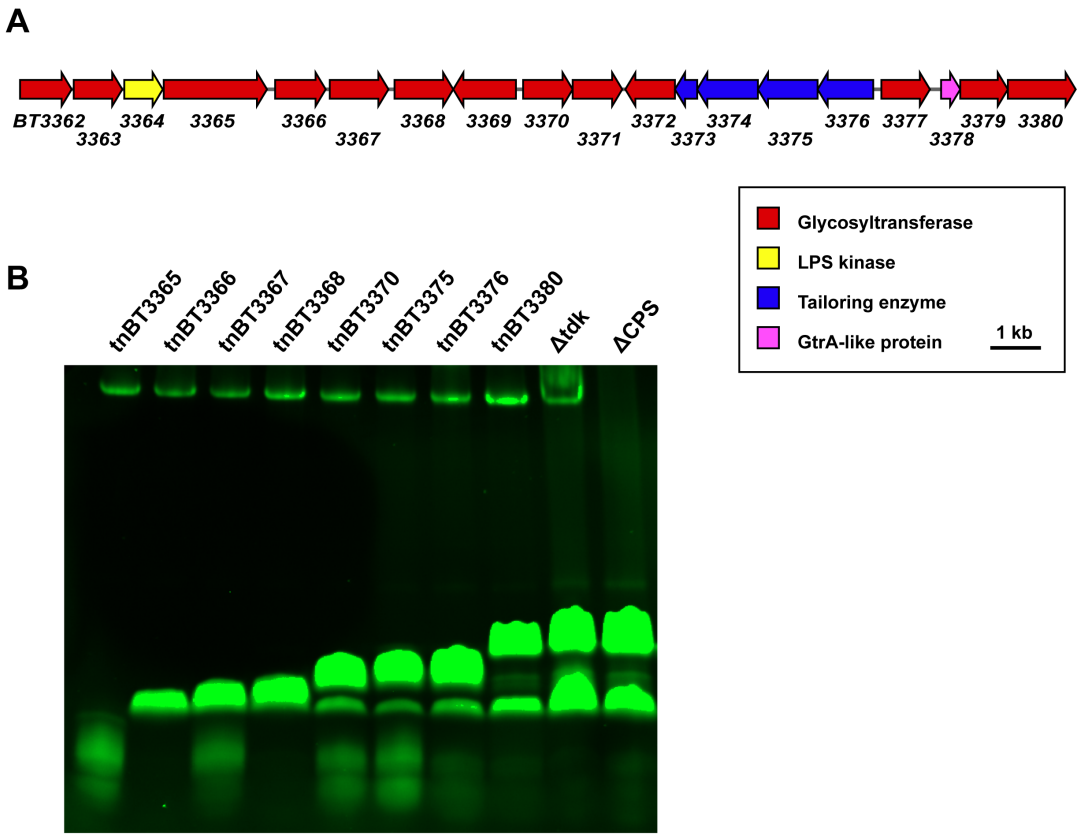

Figure 3.4. Analysis of BT3362-BT3380 cluster transposon mutants by SDS-PAGE. (A) Schematic of the gene cluster BT3362-BT3380, which includes genes predicted to encode 13 glycosyltransferases shown in red, an LPS kinase shown in yellow, four tailoring enzymes shown in blue, and a putative GtrA-like protein shown in magenta. (B) LOS was isolated from all ten strains by the microscale extraction method and the resulting material was run on a 16% tricine SDS-PAGE gel. The transposon mutants are labeled 'tn' followed by the locus tag of the gene in which the transposon has inserted. For example, 'tnBT3365' indicates a *Bt* strain with a transposon inserted in BT3365. All transposon mutants are in the wild type *Bacteroides thetaiotaomicron* VPI-5482 background with the *tdk* gene present and are erythromycin-resistant. The band at the top of the gel is CPS, which is present in all of the transposon mutants and *Bt* Δ*tdk* but not *Bt* ΔCPS.

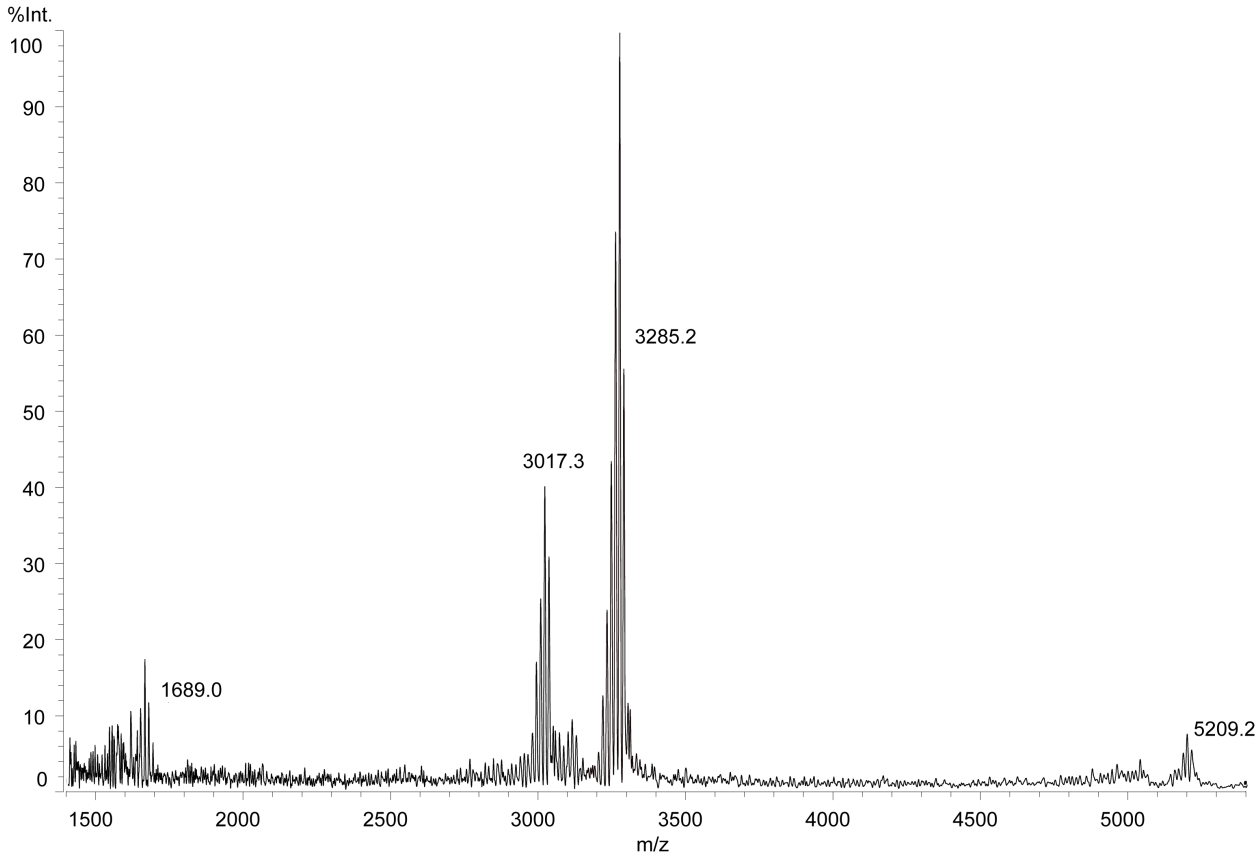

Figure 3.5. MALDI-TOF mass spectrum of *B. thetaiotaomicron* ΔCPS LOS. LOS was isolated using the large-scale extraction method and the resulting material was analyzed on a Shimadzu AXIMA Performance MALDI-TOF mass spectrometer in linear negative-ion mode. The peak at 5209 m/z represents the largest LOS molecule in the sample with two intermediate structures between 3000-3500 m/z. The cluster of peaks at 1689 m/z represents lipid A.

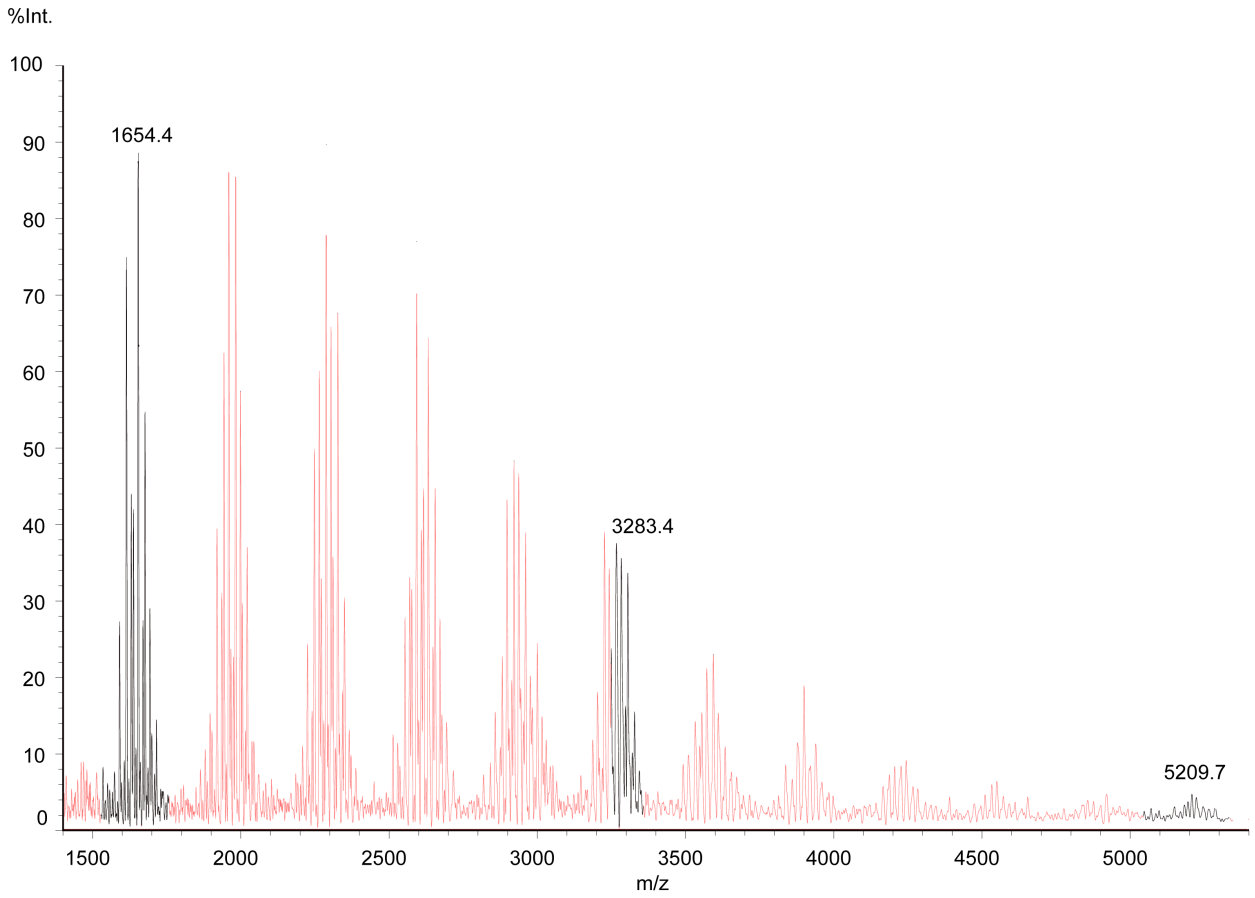

Figure 3.6. MALDI-TOF mass spectrum of *B. thetaiotaomicron* Δ*tdk* LOS. LOS from *B. thetaiotaomicron Δtdk* was purified by the large scale extraction method and the intact molecule was analyzed on a Shimadzu AXIMA Performance MALDI-TOF MS instrument in linear negative-ion mode. The peaks in black are those species that are also present in the ΔCPS intact LOS sample, but the rest of the peaks in red are unique to the *Δtdk* sample despite differing from ΔCPS only in that it contains capsule. Because similar peaks are noted in the intact LOS MALDI-TOF spectra of the transposon mutants, which also contain capsule, we conclude that the peaks in red are due to the presence of CPS in the LOS preparation.

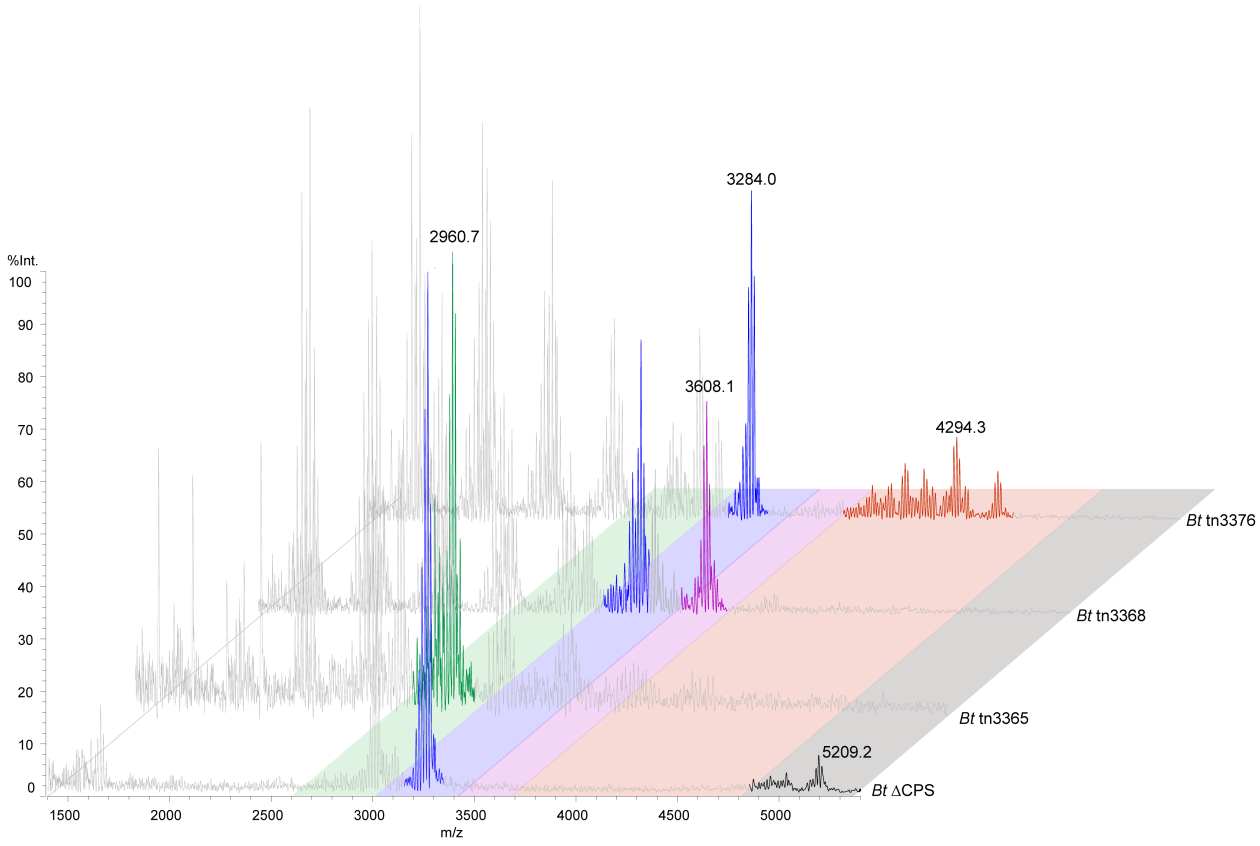

Figure 3.7. MALDI-TOF MS analysis of intact LOS from transposon mutants. LOS from *B. thetaiotaomicron* ΔCPS, *B. thetaiotaomicron* tnBT3365, *B. thetaiotaomicron* tnBT3368, and *B. thetaiotaomicron* tnBT3376 were isolated using the large-scale LPS/LOS extraction method. The resulting material was desalted and spotted on a THAP/nitrocellulose matrix for analysis on a Shimadzu AXIMA Performance MALDI-TOF mass spectrometer in linear negative-ion mode. LOS peaks of interest have been colored, with each color representing a different LOS species present in the different strains. Peaks colored gray are likely derived from capsular polysaccharide (those that do not appear in the *Bt* ΔCPS spectrum) or lipid A in the case of the peak clusters around 1650-1700 m/z.

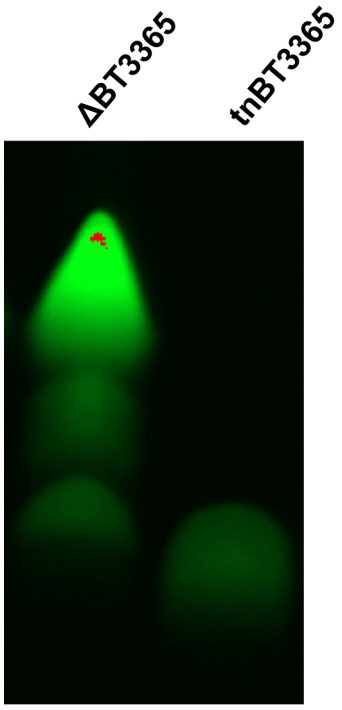

Figure 3.8. SDS-PAGE analysis of LOS from a clean deletion mutant compared to a transposon mutant. LOS was isolated from *B. thetaiotaomicron* ΔBT3365 and *B. thetaiotaomicron* tnBT3365 by the large-scale LPS/LOS extraction method. The resulting material was analyzed by SDS-PAGE and stained using the Pro-Q Emerald 300 Lipopolysaccharide Gel Stain Kit (Thermo Fisher). While a transposon insertion in BT3365 results in what appears to be a truncated LOS structure, a clean deletion of the same gene looks like it has a wild-type banding pattern.

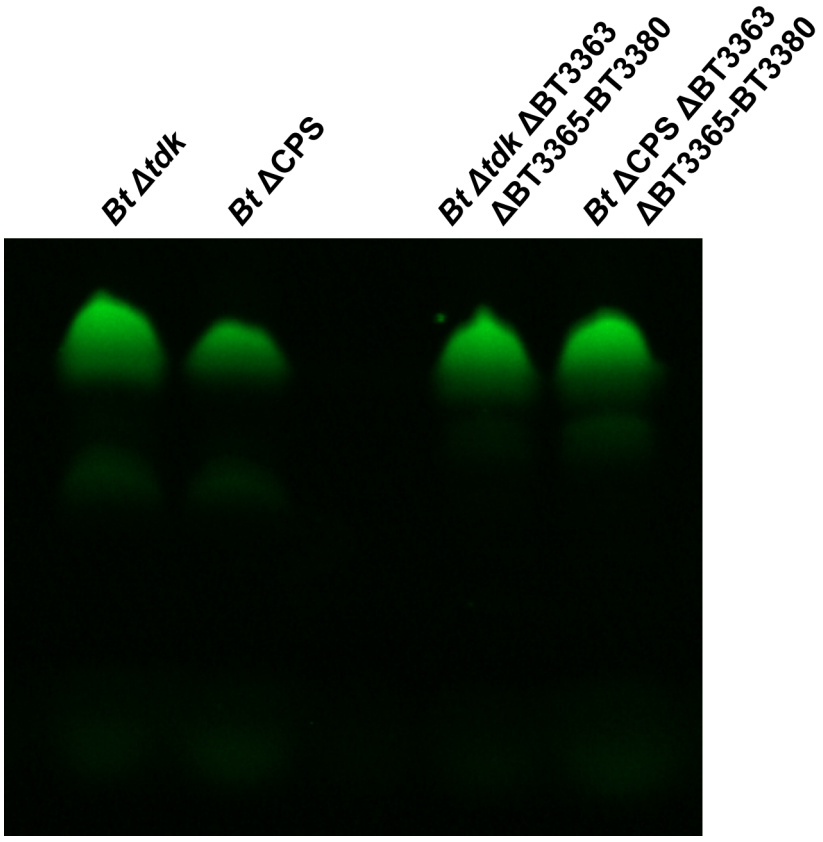

Figure 3.9. Analysis of LOS oligosaccharide cluster deletion mutants compared to wild-type by SDS-PAGE. LOS was isolated using the large-scale extraction method and analyzed by SDS-PAGE. Just by viewing the banding pattern on the gel, it is difficult to see any difference between the cluster deletion mutants in either the *B. thetaiotaomicron* Δ*tdk* and *B. thetaiotaomicron* ΔCPS background compared to their wild-type counterparts.

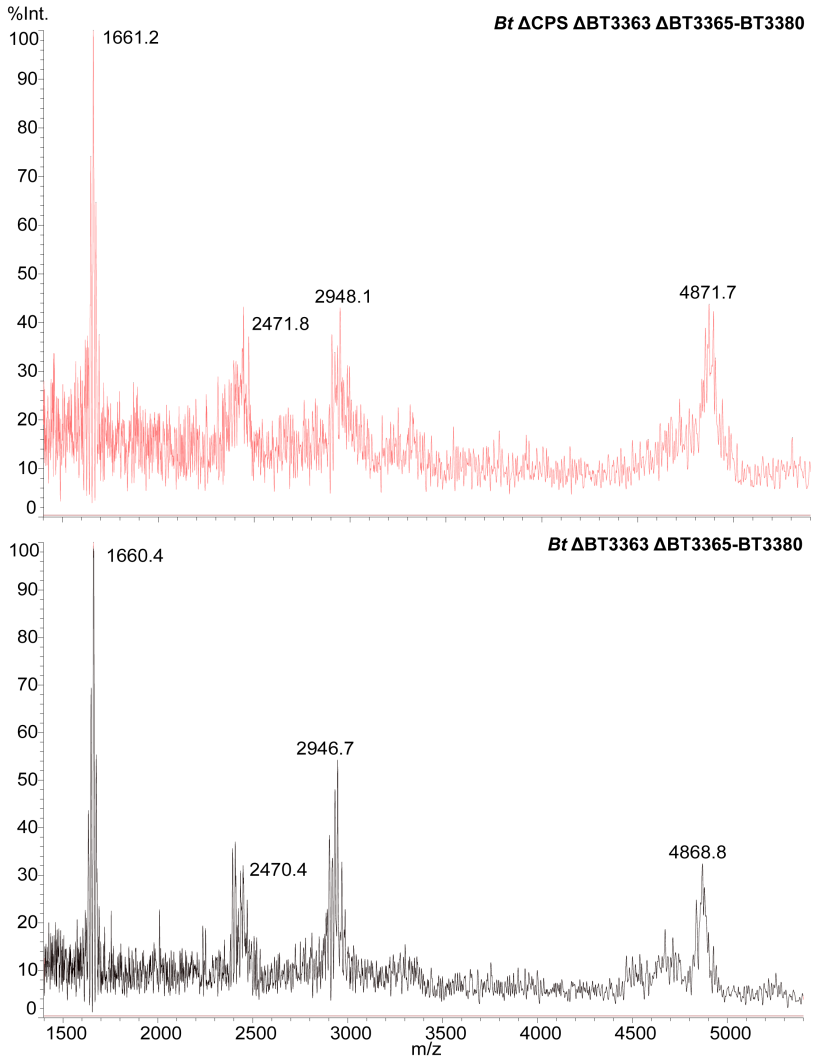

Figure 3.10. Intact LOS MALDI-TOF MS analysis of LOS cluster deletion mutants. LOS was isolated from *B. thetaiotaomicron* ΔCPS ΔBT3363 ΔBT3365-BT3380 (red) and *B. thetaiotaomicron* ΔBT3363 ΔBT3365-BT3380 (black) by the large-scale extraction method and analyzed on a Shimadzu AXIMA Performance MALDI-TOF MS instrument in linear negative-ion mode. These mutants have as much of the LOS oligosaccharide biosynthesis cluster deleted as possible and should not be able to make glycosylated LOS, yet they appear to make new molecules in its stead. Lipid A is still present in both samples, suggesting that a new oligosaccharide may be getting attached to the truncated LOS left over after the cluster deletion.

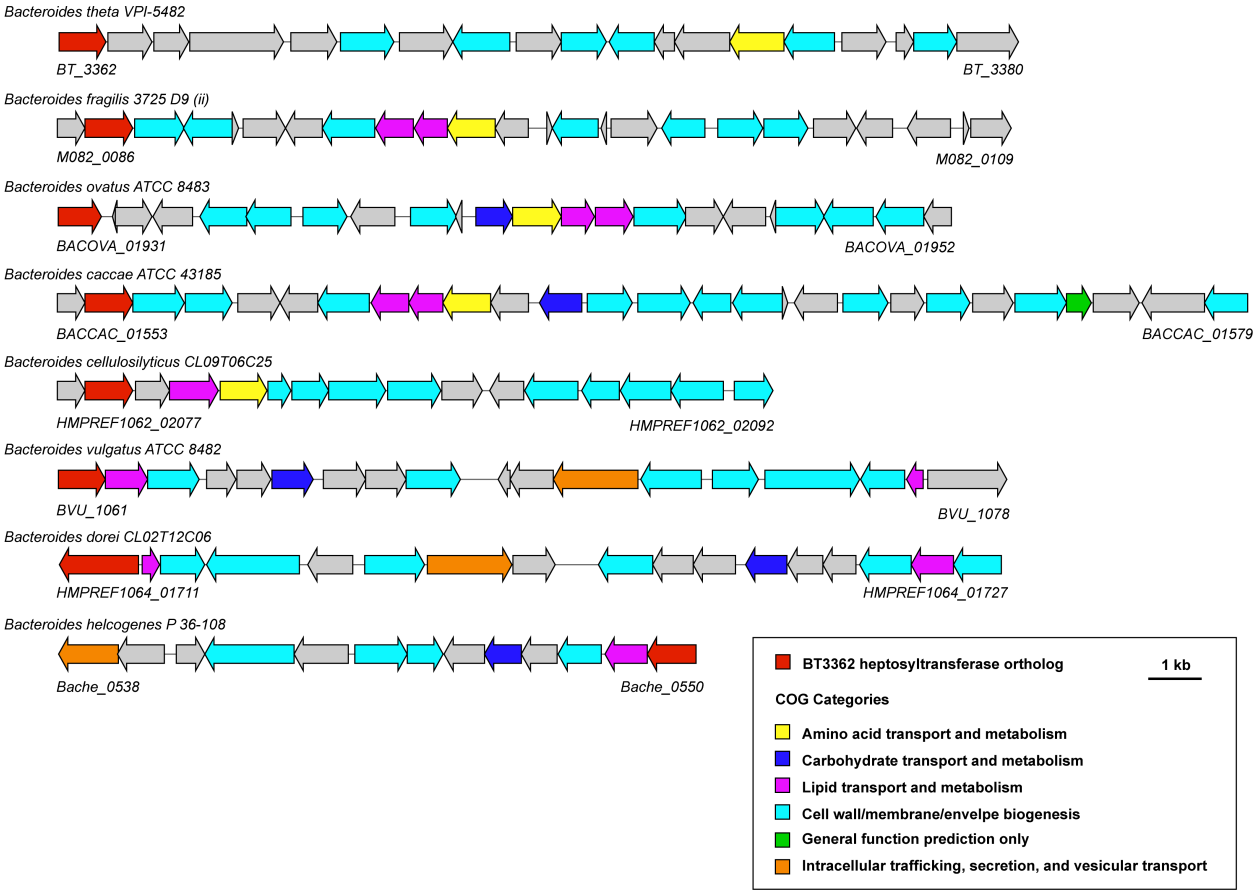

Figure 3.11. Orthologous clusters to the *B. thetaiotaomicron* LOS oligosaccharide gene cluster in additional *Bacteroides* species. Orthologs of the BT3362-BT3380 cluster in *B. thetaiotaomicron* were identified using the 'Show neighborhood ortholog regions with the same top COG hit' function within the DOE Joint Genome Institute's IMG portal, using BT3362, the putative *B. thetaiotaomicron* LOS heptosyltransferase, as the query gene. We have estimated the start and end of each gene cluster by inspecting the surrounding genomic area of each ortholog and comparing it to the *B. thetaiotaomicron* cluster. Our list shows a representative sample of the clusters resulting from this search.

References

1. **Cullen TW**, **Schofield WB**, **Barry NA**, **Putnam EE**, **Rundell EA**, **Trent MS**, **Degnan PH**, **Booth CJ**, **Yu H**, **Goodman AL**. 2015. Antimicrobial peptide resistance mediates resilience of prominent gut commensals during inflammation. Science **347**:170–175.

2. **Coats SR**, **Berezow AB**, **To TT**, **Jain S**, **Bainbridge BW**, **Banani KP**, **Darveau RP**. 2010. The Lipid A Phosphate Position Determines Differential Host Toll-Like Receptor 4 Responses to Phylogenetically Related Symbiotic and Pathogenic Bacteria. Infection and Immunity **79**:203–210.

3. **Maskell JP**. 1991. The resolution of bacteroides lipopolysaccharides by polyacrylamide gel electrophoresis. J Med Microbiol **34**:253-257.

4. **Maskell JP**. 1994. Electrophoretic analysis of the lipopolysaccharides of Bacteroides spp. Antonie Leeuwenhoek **65**:155-161.

5. **Westphal O, Jann K.** 1965. Bacterial Lipopolysaccharides Extraction with Phenol-Water and Further Applications of the Procedure. Methods Carbohydr Chem **5**:83-91.

6. **Donia MS**, **Cimermancic P**, **Schulze CJ**, **Brown LCW**, **Martin J**, **Mitreva M**, **Clardy J**, **Linington RG**, **Fischbach MA**. 2014. A Systematic Analysis of Biosynthetic Gene Clusters in the Human Microbiome Reveals a Common Family of Antibiotics. Cell **158**:1402–1414.

7. **Rogers TE**, **Pudlo NA**, **Koropatkin NM**, **Bell JSK**, **Moya Balasch M**, **Jasker K**, **Martens EC**. 2013. Dynamic responses of Bacteroides thetaiotaomicron during growth on glycan mixtures. Molecular Microbiology **88**:876–890.

8. **Peterson DA**, **Planer JD**, **Guruge JL**, **Xue L**, **Downey-Virgin W**, **Goodman AL**, **Seedorf H**, **Gordon JI**. 2015. Characterizing the Interactions between a Naturally Primed Immunoglobulin A and Its Conserved Bacteroides thetaiotaomicron Species-specific Epitope in Gnotobiotic Mice. Journal of Biological Chemistry **290**:12630–12649.

9. **Amor K, Heinrichs DE, Frirdich E, Ziebell K, Johnson RP, Whitfield C.** 2000. Distribution of Core Oligosaccharide Types in Lipopolysaccharides from *Escherichia coli*. Infect Immun 1116-1124.

10. **Guan S, Bastin DA, Verma NK.** 1999. Functional analysis of the O antigen glucosylation gene cluster of Shigella flexneri bacteriophage SfX. Microbiology **145**:1263-1273.

11. **Samuel G**, **Reeves P**. 2003. Biosynthesis of O-antigens: genes and pathways involved in nucleotide sugar precursor synthesis and O-antigen assembly. Carbohydrate Research **338**:2503–2519.

12. **Sturiale L**, **Garozzo D**, **Silipo A**, **Lanzetta R**, **Parrilli M**, **Molinaro A**. 2005. New conditions for matrix-assisted laser desorption/ionization mass spectrometry of native bacterial R-type lipopolysaccharides. Rapid Commun Mass Spectrom **19**:1829–1834.

13. **Phillips NJ**, **John CM**, **Jarvis GA**. 2016. Analysis of Bacterial Lipooligosaccharides by MALDI-TOF MS with Traveling Wave Ion Mobility. J Am Soc Mass Spectrom **27**:1263-1276.

14. **John CM**, **Liu M**, **Jarvis GA**. 2009. Profiles of structural heterogeneity in native lipooligosaccharides of Neisseria and cytokine induction. J Lipid Res **50**:424–438.

15. **Koropatkin NM**, **Martens EC**, **Gordon JI**, **Smith TJ**. 2008. Starch Catabolism by a Prominent Human Gut Symbiont Is Directed by the Recognition of Amylose Helices. Structure **16**:1105–1115.

16. **Marolda CL, Lahiry P, Vinés E, Saldïas S, Valvano MA.** 2006. Micromethods for the Characterization of Lipid A-Core and O-Antigen Lipopolysaccharide. In Glycobiology Protocols, **347**: 237-252.

17. **Phillips NJ**, **Schilling B**, **McLendon MK**, **Apicella MA**, **Gibson BW**. 2004. Novel Modification of Lipid A of Francisella tularensis. Infection and Immunity **72**:5340–5348.

Appendix 1

List of Bacterial Strains and Plasmids

Strain	Plasmid	Resistance	Atmosphere	Media	Source
Bacteroides thetaiotaomicron VPI-5482	n/a	n/a	Anaerobic	PYG	ATCC
Bacteroides thetaiotaomicron VPI-5482 Δ*tdk*	n/a	5-fluoro-2'-deoxyuridine	Anaerobic	PYG	Gift from Justin Sonnenburg
Bacteroides fragilis NCTC 9343	n/a	n/a	Anaerobic	PYG	ATCC
Bacteroides ovatus ATCC 8483	n/a	n/a	Anaerobic	PYG	ATCC
Bacteroides uniformis ATCC 8492	n/a	n/a	Anaerobic	PYG	ATCC
Bacteroides vulgatus ATCC 8482	n/a	n/a	Anaerobic	PYG	ATCC
Escherichia coli serotype O55:B5:H- ATCC 12014	n/a	n/a	Aerobic	LB	ATCC
Escherichia coli MG1655	n/a	n/a	Aerobic	LB	ATCC
Escherichia coli S17-1 λ pir	n/a	n/a	Aerobic	LB	Gift from Justin Sonnenburg
Escherichia coli S17-1 λ pir	pExchange-*tdk*	Ampicillin, Erythromycin	Aerobic	LB	Gift from Justin Sonnenburg
Escherichia coli S17-1 λ pir	ΔBT2152 (*lpxL*) in pExchange-*tdk*	Ampicillin, Erythromycin	Aerobic	LB	This work
Escherichia coli S17-1 λ pir	ΔBT1854 (*lpxF*) in pExchange-*tdk*	Ampicillin, Erythromycin	Aerobic	LB	This work
Escherichia coli S17-1 λ pir	BT3386 in pNBU2_ermGb_usBT1311	Ampicillin, Erythromycin	Aerobic	LB	This work
Bacteroides thetaiotaomicron VPI-5482 Δ*tdk*	n/a	5-fluoro-2'-deoxyuridine	Anaerobic	PYG	This work

ΔBT2152 (*lpxL*)					
Bacteroides thetaiotaomicron VPI-5482 Δ*tdk* ΔBT1854 (*lpxF*)	n/a	5-fluoro-2'-deoxyuridine	Anaerobic	PYG	This work
Bacteroides thetaiotaomicron VPI-5482 Δ*tdk* ΔBT2152 ΔBT1854 (*lpxL lpxF*)	n/a	5-fluoro-2'-deoxyuridine	Anaerobic	PYG	This work
Bacteroides thetaiotaomicron VPI-5482 Δ*tdk* ΔCPS	n/a	5-fluoro-2'-deoxyuridine	Anaerobic	PYG	Gift from Eric Martens
Bacteroides thetaiotaomicron VPI-5482 Δ*tdk* CPS1-only	n/a	5-fluoro-2'-deoxyuridine	Anaerobic	PYG	Gift from Eric Martens
Bacteroides thetaiotaomicron VPI-5482 Δ*tdk* CPS2-only	n/a	5-fluoro-2'-deoxyuridine	Anaerobic	PYG	Gift from Eric Martens
Bacteroides thetaiotaomicron VPI-5482 Δ*tdk* CPS3-only	n/a	5-fluoro-2'-deoxyuridine	Anaerobic	PYG	Gift from Eric Martens
Bacteroides thetaiotaomicron VPI-5482 Δ*tdk* CPS4-only	n/a	5-fluoro-2'-deoxyuridine	Anaerobic	PYG	Gift from Eric Martens
Bacteroides thetaiotaomicron VPI-5482 Δ*tdk* CPS5-only	n/a	5-fluoro-2'-deoxyuridine	Anaerobic	PYG	Gift from Eric Martens
Bacteroides thetaiotaomicron VPI-5482 Δ*tdk* CPS6-only	n/a	5-fluoro-2'-deoxyuridine	Anaerobic	PYG	Gift from Eric Martens
Bacteroides thetaiotaomicron VPI-5482 Δ*tdk* CPS7-only	n/a	5-fluoro-2'-deoxyuridine	Anaerobic	PYG	Gift from Eric Martens
Bacteroides thetaiotaomicron VPI-5482 Δ*tdk*	n/a	5-fluoro-2'-deoxyuridine	Anaerobic	PYG	Gift from Eric Martens

CPS8-only					
Bacteroides thetaiotaomicron VPI-5482 46A7 (tnBT3365)	n/a	n/a	Anaerobic	PYG	Gift from Daniel Peterson
Bacteroides thetaiotaomicron VPI-5482 2A9 (tnBT3366)	n/a	n/a	Anaerobic	PYG	Gift from Daniel Peterson
Bacteroides thetaiotaomicron VPI-5482 42_E3 (tnBT3367)	n/a	n/a	Anaerobic	PYG	Gift from Daniel Peterson
Bacteroides thetaiotaomicron VPI-5482 118E8 (tnBT3368)	n/a	n/a	Anaerobic	PYG	Gift from Daniel Peterson
Bacteroides thetaiotaomicron VPI-5482 4A12 (tnBT3370)	n/a	n/a	Anaerobic	PYG	Gift from Daniel Peterson
Bacteroides thetaiotaomicron VPI-5482 3-2-F3 (tnBT3375)	n/a	n/a	Anaerobic	PYG	Gift from Daniel Peterson
Bacteroides thetaiotaomicron VPI-5482 2.7-D11 (tnBT3376)	n/a	n/a	Anaerobic	PYG	Gift from Daniel Peterson
Bacteroides thetaiotaomicron VPI-5482 124H4 (tnBT3380)	n/a	n/a	Anaerobic	PYG	Gift from Daniel Peterson
Escherichia coli S17-1 λ pir	ΔBT3362 in pExchange-*tdk*	Ampicillin, Erythromycin	Aerobic	LB	This work
Escherichia coli S17-1 λ pir	ΔBT3363 in pExchange-*tdk*	Ampicillin, Erythromycin	Aerobic	LB	This work
Escherichia coli S17-1 λ pir	ΔBT3364 in pExchange-*tdk*	Ampicillin, Erythromycin	Aerobic	LB	This work
Escherichia coli S17-1 λ pir	ΔBT3365 in pExchange-*tdk*	Ampicillin, Erythromycin	Aerobic	LB	This work
Escherichia coli	ΔBT3366 in	Ampicillin,	Aerobic	LB	This work

S17-1 λ pir	pExchange-*tdk*	Erythromycin			
Escherichia coli S17-1 λ pir	ΔBT3367 in pExchange-*tdk*	Ampicillin, Erythromycin	Aerobic	LB	This work
Escherichia coli S17-1 λ pir	ΔBT3368 in pExchange-*tdk*	Ampicillin, Erythromycin	Aerobic	LB	This work
Escherichia coli S17-1 λ pir	ΔBT3369 in pExchange-*tdk*	Ampicillin, Erythromycin	Aerobic	LB	This work
Escherichia coli S17-1 λ pir	ΔBT3370 in pExchange-*tdk*	Ampicillin, Erythromycin	Aerobic	LB	This work
Escherichia coli S17-1 λ pir	ΔBT3371 in pExchange-*tdk*	Ampicillin, Erythromycin	Aerobic	LB	This work
Escherichia coli S17-1 λ pir	ΔBT3372 in pExchange-*tdk*	Ampicillin, Erythromycin	Aerobic	LB	This work
Escherichia coli S17-1 λ pir	ΔBT3373 in pExchange-*tdk*	Ampicillin, Erythromycin	Aerobic	LB	This work
Escherichia coli S17-1 λ pir	ΔBT3374 in pExchange-*tdk*	Ampicillin, Erythromycin	Aerobic	LB	This work
Escherichia coli S17-1 λ pir	ΔBT3375 in pExchange-*tdk*	Ampicillin, Erythromycin	Aerobic	LB	This work
Escherichia coli S17-1 λ pir	ΔBT3376 in pExchange-*tdk*	Ampicillin, Erythromycin	Aerobic	LB	This work
Escherichia coli S17-1 λ pir	ΔBT3377 in pExchange-*tdk*	Ampicillin, Erythromycin	Aerobic	LB	This work
Escherichia coli S17-1 λ pir	ΔBT3378 in pExchange-*tdk*	Ampicillin, Erythromycin	Aerobic	LB	This work
Escherichia coli S17-1 λ pir	ΔBT3379 in pExchange-*tdk*	Ampicillin, Erythromycin	Aerobic	LB	This work
Escherichia coli S17-1 λ pir	ΔBT3380 in pExchange-*tdk*	Ampicillin, Erythromycin	Aerobic	LB	This work
Bacteroides thetaiotaomicron	n/a	5-fluoro-2'-deoxyuridine	Anaerobic	PYG	This work

VPI-5482 Δ*tdk* ΔCPS ΔBT3363					
Bacteroides thetaiotaomicron VPI-5482 Δ*tdk* ΔCPS ΔBT3363	n/a	5-fluoro-2'-deoxyuridine	Anaerobic	PYG	This work
Bacteroides thetaiotaomicron VPI-5482 Δ*tdk* ΔCPS ΔBT3365	n/a	5-fluoro-2'-deoxyuridine	Anaerobic	PYG	This work
Bacteroides thetaiotaomicron VPI-5482 Δ*tdk* ΔCPS ΔBT3366	n/a	5-fluoro-2'-deoxyuridine	Anaerobic	PYG	This work
Bacteroides thetaiotaomicron VPI-5482 Δ*tdk* ΔCPS ΔBT3367	n/a	5-fluoro-2'-deoxyuridine	Anaerobic	PYG	This work
Bacteroides thetaiotaomicron VPI-5482 Δ*tdk* ΔCPS ΔBT3369	n/a	5-fluoro-2'-deoxyuridine	Anaerobic	PYG	This work
Bacteroides thetaiotaomicron VPI-5482 Δ*tdk* ΔCPS ΔBT3370	n/a	5-fluoro-2'-deoxyuridine	Anaerobic	PYG	This work
Bacteroides thetaiotaomicron VPI-5482 Δ*tdk* ΔCPS ΔBT3372	n/a	5-fluoro-2'-deoxyuridine	Anaerobic	PYG	This work
Bacteroides thetaiotaomicron VPI-5482 Δ*tdk* ΔCPS ΔBT3374	n/a	5-fluoro-2'-deoxyuridine	Anaerobic	PYG	This work
Bacteroides thetaiotaomicron VPI-5482 Δ*tdk* ΔCPS ΔBT3375	n/a	5-fluoro-2'-deoxyuridine	Anaerobic	PYG	This work
Bacteroides thetaiotaomicron VPI-5482 Δ*tdk* ΔCPS ΔBT3377	n/a	5-fluoro-2'-deoxyuridine	Anaerobic	PYG	This work
Bacteroides thetaiotaomicron VPI-5482 Δ*tdk* ΔCPS ΔBT3378	n/a	5-fluoro-2'-deoxyuridine	Anaerobic	PYG	This work

Bacteroides thetaiotaomicron VPI-5482 Δ*tdk* ΔCPS ΔBT3379	n/a	5-fluoro-2'-deoxyuridine	Anaerobic	PYG	This work
Bacteroides thetaiotaomicron VPI-5482 Δ*tdk* ΔCPS ΔBT3380	n/a	5-fluoro-2'-deoxyuridine	Anaerobic	PYG	This work
Bacteroides thetaiotaomicron VPI-5482 Δ*tdk* ΔCPS ΔBT1854	n/a	5-fluoro-2'-deoxyuridine	Anaerobic	PYG	This work
Bacteroides thetaiotaomicron VPI-5482 Δ*tdk* ΔCPS ΔBT1854 ΔBT3363	n/a	5-fluoro-2'-deoxyuridine	Anaerobic	PYG	This work
Bacteroides thetaiotaomicron VPI-5482 Δ*tdk* ΔCPS ΔBT1854 ΔBT3377	n/a	5-fluoro-2'-deoxyuridine	Anaerobic	PYG	This work
Bacteroides thetaiotaomicron VPI-5482 Δ*tdk* ΔBT3363	n/a	5-fluoro-2'-deoxyuridine	Anaerobic	PYG	This work
Bacteroides thetaiotaomicron VPI-5482 Δ*tdk* ΔBT3369	n/a	5-fluoro-2'-deoxyuridine	Anaerobic	PYG	This work
Bacteroides thetaiotaomicron VPI-5482 Δ*tdk* ΔBT3377	n/a	5-fluoro-2'-deoxyuridine	Anaerobic	PYG	This work
Bacteroides thetaiotaomicron VPI-5482 Δ*tdk* ΔCPS ΔBT3363 ΔBT3365-BT3380	n/a	5-fluoro-2'-deoxyuridine	Anaerobic	PYG	This work
Bacteroides thetaiotaomicron VPI-5482 Δ*tdk* ΔCPS ΔBT3363 ΔBT3365-BT3380	n/a	5-fluoro-2'-deoxyuridine	Anaerobic	PYG	This work

Appendix 2

List of Primers

Use	Name	Sequence
BT2152 clean deletion	BT2152_ExtUpFor	GCG GTC GAC GTA TCT CGG CGA CCT CCA TA
BT2152 clean deletion	BT2152_IntUpRev	CAT CCC GCT ATA TAC CAG CCA ATA G
BT2152 clean deletion	BT2152_IntDoFor	CTA TTG GCT GGT ATA TAG CGG GAT GTA AGG ATG AAA GTG TCA GTG G
BT2152 clean deletion	BT2152_ExtDoRev	GCG GCG GCC GCC CCG ATG CCT CTC CTT ACT T
Sequencing primer	pEx-tdk_UpForSeq	CGG TGA TCT GGC ATC TTT CT
Sequencing primer	pEx-tdk_DoRevSeq	AAC GCA CTG AGA AGC CCT TA
BT2152 clean deletion	BT2152_KOSeq	ACG CAG GCC TTG AAG ATA GA
BT2152 clean deletion	BT2152_ForXbaI	GCG TCT AGA ATG TGG CTG TT
BT2152 clean deletion	BT2152_RevSalI	CGC GTC GAC TTA CCC CCT TT
BT2152 clean deletion	BT2152_UpDiag	CAG GCT ATT CAT CGG TTG GT
BT2152 clean deletion	BT2152_DoDiag	CCC ATC AAC AGT TCC GAG TT
BT3386 overexpression	BT3386_ForNdeI	GCG CAT ATG AAG GAA TTT TTG CA
BT3386 overexpression	BT3386_RevXbaI	CGC TCT AGA CTA TAA TGC TTG CAT
Sequencing primer	pNBU2_ForSeq	CAC ACA ACT TGT CGG CAT TC
Sequencing primer	pNBU2_RevSeq	CCA ATG CAC AAA TGC TGT TC
Sequencing primer	BT3386_Seq	CCA GCT GGA AGT TAA CTC TTT TC
BT1854 clean deletion	BT1854_IntUpRev	CAT AAA ATA AAT CGT ATT ATT AAA AGG
BT1854 clean deletion	BT1854_IntDoRev	CCT TTT AAT AAT ACG ATT TAT TTT ATG TAG TTT ATA ACA TGG GCA AAA G
BT1854 clean deletion	BT1854_ExtUpFor	TGG AAA GAA AGA AGA TAA CAT TCG AGA CTC

		AAC GCC CGA ATA TCA TC
BT1854 clean deletion	BT1854_ExtDoRev	TCC ACC GCG GTG GCG GCC GCT CTA GCC AGT AGT CTT GAA CGG GCA
BT1854 clean deletion	BT1854_UpKOSeq	GCA ATA TCG GTT TAT GGA CCC G
BT1854 clean deletion	BT1854_KOSeq	ATA AGG AGA CCC CGA TGT GG
BT1854 clean deletion	BT1854_DoKOSeq	CTG AAG CAT TGT CAC GTT ATC CC
pNBU2 vector genome integration test	BTt70-CHF	TTC AAA TTG CTC GGT AAA GCT C
pNBU2 vector genome integration test	BTt70-CHR	AAA ACC TTG ATT TTA CGG GAC
pNBU2 vector genome integration test	BTt71-CHF3	TTC GAG GAA TGA AGC ATC TCC GTA
pNBU2 vector genome integration test	BTt71-CHR3	ACC GTT CCG ATT CAA TTT CGT
pNBU2 vector genome integration test	IntN2BTt71-CHF3	TTT CCG GCT CTC CAA TGC AA
BT3362 clean deletion	3362_US_F	CCT GCA GCC CGG GGG ATC CAC TAG TAT CCC GGG GCA TTT GCC C
BT3362 clean deletion	3362_US_R	CTG GCT CCT ACA TTC GTT ATT TTT TCG CAT AAA GTA CCG G
BT3362 clean deletion	3362_DS_F	ATA ACG AAT GTA GGA GCC AGG TAC TCC TG
BT3362 clean deletion	3362_DS_R	TTC CCC TCC ACC GCG GTG GCG GCC GCT TGC CCG GTC ATC TTA AAA TAT TTA TC
BT3363 clean deletion	3363_US_F	CCT GCA GCC CGG GGG ATC CAC TAG TCA TTC GCT GGC AGT ACA ATA TC
BT3363 clean deletion	3363_US_R	TCA TCT CTC ACA TTC TTG TTC CAT ATC TCA GG
BT3363 clean deletion	3363_DS_F	AAC AAG AAT GTG AGA GAT GAA GAG AAG TAT G

BT3363 clean deletion	3363_DS_R	TTC CCC TCC ACC GCG GTG GCG GCC GCG TTC TCT CGA AAT CTC CC
BT3364 clean deletion	3364_US_F	CCT GCA GCC CGG GGG ATC CAC TAG TAT AAG TTG CGT AGC GGG
BT3364 clean deletion	3364_US_R	TTA GCC ATT ACA TCT TAC GAA AAA ACA AGA ATG
BT3364 clean deletion	3364_DS_F	TCG TAA GAT GTA ATG GCT AAA GGA GGG TAA TTA ATG
BT3364 clean deletion	3364_DS_R	TTC CCC TCC ACC GCG GTG GCG GCC GCT ACC CTC TTG CAT GAT CC
BT3365 clean deletion	3365_US_F	CCT GCA GCC CGG GGG ATC CAC TAG TAT TGA AAT AAA ACC GGA TTT CTC
BT3365 clean deletion	3365_US_R	TTA CCT CTT ACA TTA ATT ACC CTC CTT TAG C
BT3365 clean deletion	3365_DS_F	GTA ATT AAT GTA AGA GGT AAT TGT TTG ATT TGA G
BT3365 clean deletion	3365_DS_R	TTC CCC TCC ACC GCG GTG GCG GCC GCT ATC CTC AAA AGC CGG TG
BT3366 clean deletion	3366_US_F	CCT GCA GCC CGG GGG ATC CAC TAG TAG CAA AGT ATC ATG ATA AAG TG
BT3366 clean deletion	3366_US_R	AGT CAT TCT ACA TAT TAT TCT ACT TGT CAA CTT TTT ATT TTT AC
BT3366 clean deletion	3366_DS_F	GAA TAA TAT GTA GAA TGA CTA AGG AAA AGA TAG C
BT3366 clean deletion	3366_DS_R	TTC CCC TCC ACC GCG GTG GCG GCC GCA TCG TTT CAA GTA AAA TAA GTG
BT3367 clean deletion	3367_US_F	CCT GCA GCC CGG GGG ATC CAC TAG TGA

		GCA GAC CTA TAA GAA CC
BT3367 clean deletion	3367_US_R	ATT CTA CTT ACA TAC GAC AAT GAT ATT CAG C
BT3367 clean deletion	3367_DS_F	TTG TCG TAT GTA AGT AGA ATG TTG TAT TAA GGG AAG
BT3367 clean deletion	3367_DS_R	TTC CCC TCC ACC GCG GTG GCG GCC GCT TTC ATA ACG AGA AGG ATT C
BT3368 clean deletion	3368_US_F	CCT GCA GCC CGG GGG ATC CAC TAG TGA ACA AGA AGA AAT AAA GGC C
BT3368 clean deletion	3368_US_R	ATA AAG ATT TAC ATC TGA CAA TGA TAT TCA GC
BT3368 clean deletion	3368_DS_F	TTG TCA GAT GTA AAT CTT TAT ATA TTT TCG ATA ACA TGC
BT3368 clean deletion	3368_DS_R	TTC CCC TCC ACC GCG GTG GCG GCC GCA AAA AGA AAG CTA AAC CGG
BT3369 clean deletion	3369_US_F	CCT GCA GCC CGG GGG ATC CAC TAG TAT TTC TTC AAA TTA TTC TTC ATA TCA AC
BT3369 clean deletion	3369_US_R	CTA AAT CTT TAC ATA TTA ATA TAA TAA GCT TTC CGG C
BT3369 clean deletion	3369_DS_F	ATA TTA ATA TGT AAA GAT TTA GAT ACT CTT GAT AGC TTG
BT3369 clean deletion	3369_DS_R	TTC CCC TCC ACC GCG GTG GCG GCC GCA AAG AAG GCT AAA CCA G
BT3370 clean deletion	3370_US_F	CCT GCA GCC CGG GGG ATC CAC TAG TGA TCA CTA TAT TGT TTG CCT AC
BT3370 clean deletion	3370_US_R	CAA ATA CTT ACA TGC

		ATG CTC TCC ATT AAT AAA C
BT3370 clean deletion	3370_DS_F	AGC ATG CAT GTA AGT ATT TGG TTA GTA TAA TAG TGC
BT3370 clean deletion	3370_DS_R	TTC CCC TCC ACC GCG GTG GCG GCC GCA AAT ATC CCT TTT TCT ATT CAC G
BT3371 clean deletion	3371_US_F	CCT GCA GCC CGG GGG ATC CAC TAG TAT TAA TGG AGA GCA TGC ATG
BT3371 clean deletion	3371_US_R	TTT CTA TTC ACA CTA TTT ATC TTT TTA AGT TTA AAA TGT AC
BT3371 clean deletion	3371_DS_F	ATA AAT AGT GTG AAT AGA AAA AGG GAT ATT TAC TTA ATA TC
BT3371 clean deletion	3371_DS_R	TTC CCC TCC ACC GCG GTG GCG GCC GCA TTT GTA GCA CAT ATA ATC ATG G
BT3372 clean deletion	3372_US_F	CCT GCA GCC CGG GGG ATC CAC TAG TTT CGC CCC ACT TGG TGA
BT3372 clean deletion	3372_US_R	TCC CTT TTT ACA TTC AAT ATT AAC TTT TGT GTA CCT CTT TC
BT3372 clean deletion	3372_DS_F	ATA TTG AAT GTA AAA AGG GAA AAA AAC TAT CTA GTG
BT3372 clean deletion	3372_DS_R	TTC CCC TCC ACC GCG GTG GCG GCC GCA CCG CTG ATT ATT TGC ATA AAT G
BT3373 clean deletion	3373_US_F	CCT GCA GCC CGG GGG ATC CAC TAG TGC ATA TGC TTC AGA TCC
BT3373 clean deletion	3373_US_R	ATT CAA TAT TAC ATA TTT TAA TCA ATA ATA ATA TGT ACA AAC TG
BT3373 clean deletion	3373_DS_F	ATT AAA ATA TGT AAT ATT GAA TGA AAG ATA

		TAG CAA ATA C
BT3373 clean deletion	3373_DS_R	TTC CCC TCC ACC GCG GTG GCG GCC GCT TTT CCC TTT TTA CTT CCT TTC
BT3374 clean deletion	3374_US_F	CCT GCA GCC CGG GGG ATC CAC TAG TCC CCT AAT GCC GGA TTA TTA G
BT3374 clean deletion	3374_US_R	CTC ATA TTT TAC ATT AAA ACT TTT TTC ATC TTA TAA ACT TTC G
BT3374 clean deletion	3374_DS_F	AGT TTT AAT GTA AAA TAT GAG CAT AAC AAT CCA TAC
BT3374 clean deletion	3374_DS_R	TTC CCC TCC ACC GCG GTG GCG GCC GCT TCT TTC AAG TAC TCC ATT AC
BT3375 clean deletion	3375_US_F	CCT GCA GCC CGG GGG ATC CAC TAG TCA CCA AAA GCT AGA AGA GG
BT3375 clean deletion	3375_US_R	TTT CAT CTT ACA TAC TAT TTC TTT ATA ATT TGG AGG ATA TAC
BT3375 clean deletion	3375_DS_F	AAA TAG TAT GTA AGA TGA AAA AAG TTT TAA TGC TAG GAG G
BT3375 clean deletion	3375_DS_R	TTC CCC TCC ACC GCG GTG GCG GCC GCC GTC CGG TCT GTT TGC T
BT3376 clean deletion	3376_US_F	CCT GCA GCC CGG GGG ATC CAC TAG TCC GTT CCC AAT CAA TTG C
BT3376 clean deletion	3376_US_R	TAT CAT ACT ACA TTG TAA TTA TGG ATA TTA TTG GTC
BT3376 clean deletion	3376_DS_F	AAT TAC AAT GTA GTA TGA TAC AAT TAT CAG AAA TAA CAA AC
BT3376 clean deletion	3376_DS_R	TTC CCC TCC ACC GCG

		GTG GCG GCC GCA GAT TTT AAT CCG GTA GAT TTT ATA TTT AAC
BT3377 clean deletion	3377_US_F	CCT GCA GCC CGG GGG ATC CAC TAG TAT AAT TGT GGC GTA CTC C
BT3377 clean deletion	3377_US_R	TAT ACA TTC ACA TAT ATT TTG ATA AGT ATT GGA ATC TAT C
BT3377 clean deletion	3377_DS_F	CAA AAT ATA TGT GAA TGT ATA AAG TGA TGT GTG
BT3377 clean deletion	3377_DS_R	TTC CCC TCC ACC GCG GTG GCG GCC GCT ATT TAC GCA TCA AAC TCT CC
BT3378 clean deletion	3378_US_F	CCT GCA GCC CGG GGG ATC CAC TAG TGA TAA GAA AGT CGT GCT C
BT3378 clean deletion	3378_US_R	ACT TTA CTC ACA TCA TCC AAT ACT CTT TTA TTG ATT TTG
BT3378 clean deletion	3378_DS_F	TTG GAT GAT GTG AGT AAA GTT AGT GTT TTA ATA CC
BT3378 clean deletion	3378_DS_R	TTC CCC TCC ACC GCG GTG GCG GCC GCA CTT CCT ATT ATC AAC AGA AAT G
BT3379 clean deletion	3379_US_F	CCT GCA GCC CGG GGG ATC CAC TAG TTC GAA TAA GCT TTT TAA AGT TGC
BT3379 clean deletion	3379_US_R	ATC TTA GCT ACA TAT TTT TTT AGA TTT TAG AAC AAA ACG
BT3379 clean deletion	3379_DS_F	AAA AAA ATA TGT AGC TAA GAT TAT GAG TAA AAA AAC G
BT3379 clean deletion	3379_DS_R	TTC CCC TCC ACC GCG GTG GCG GCC GCA TTC CAA ACA ATT GCC GG

BT3380 clean deletion	3380_US_F	CCT GCA GCC CGG GGG ATC CAC TAG TAG TGC CGG TTA ATT TTC
BT3380 clean deletion	3380_US_R	ATG AAT ACT ACA TAA TCT TAG CTA TTG TTT CAC AC
BT3380 clean deletion	3380_DS_F	TAA GAT TAT GTA GTA TTC ATT TGT GAT AAT AGA TGA TTG
BT3380 clean deletion	3380_DS_R	TTC CCC TCC ACC GCG GTG GCG GCC GCG GAT GTT GCA ACA ATG CC
Sequencing primer	pEx_SeqF	CGG TGA TCT GGC ATC TTT CT
Sequencing primer	pEx_SeqR	AAC GCA CTG AGA AGC CCT TA
Sequencing primer	3362KO_SeqF	ATA TTG ATC CGG TGG CAG CC
Sequencing primer	3363KO_SeqF	GCC GAT CCG AAG GTG AAG G
Sequencing primer	3364KO_SeqF	GCA AAA ATA CGA CTG ATC CGG C
Sequencing primer	3365KO_SeqF	CAT ATT TTA TGA GCA TAC AAT CTC CCT ATC G
Sequencing primer	3366KO_SeqF	CTC CCC ATT GGT ATG GAG AGG
Sequencing primer	3367KO_SeqF	GAA TGA AAG CAT TAC TCG TGG TGG
Sequencing primer	3368KO_SeqF	TGA TGA TGC GGA GAA AGT AGC G
Sequencing primer	3369KO_SeqF	GCA AGC AAT TCC TCA TAC ATA TTG ACG
Sequencing primer	3370KO_SeqF	TAA GAA GCA ATA GCT AGA AAG TGA CAT TTG
Sequencing primer	3371KO_SeqF	TAC ATA ATA TGT ATG AGG ATC GTC TTA TCT TGC
Sequencing primer	3372KO_SeqF	TGA GCA TAA CAA TCC ATA CAG AAC C
Sequencing primer	3373KO_SeqF	CAA CCG CAT ATA ATG TCG AGG C
Sequencing primer	3374KO_SeqF	CGT TTG GGT TAT ATA

		GCT GCA CC
Sequencing primer	3375KO_SeqF	CCC CGG TAT TAA TAG TAA AGT AGA TGA GG
Sequencing primer	3376KO_SeqF	ACC CCA TCT TAC GTC AAG ACG
Sequencing primer	3377KO_SeqF	AAA CAG GTT TGA TTC CAT TCC ACC
Sequencing primer	3378KO_SeqF	GGT GAC GAA ATA TTT CTT CAA TCT ATA TTG TGG
Sequencing primer	3379KO_SeqF	TGC TGG TCT TAT GTA TTA TTT ATA ATA TTG TAC CG
Sequencing primer	3380KO_SeqF	TGT AAA CGC TTT GAA ACA GAT GCG
Sequencing primer	BT3362KO_SeqR	CAC TTT TTG TTT GCT CAT CTT GTG C
Sequencing primer	BT3363KO_SeqR	CTT TCT CCA ACA GTT TCT CCG G
Sequencing primer	BT3364KO_SeqR	ACG ACC GAC ATC TGC AAA GAA G
Sequencing primer	BT3365KO_SeqR	GAA GAG CCG TCG TCA GAA CC
Sequencing primer	BT3366KO_SeqR	ACA TCT GTA CAA GAA GTG CCT CC
Sequencing primer	BT3367KO_SeqR	GCT GGT TTA GCC TTC TTT GCG
Sequencing primer	BT3368KO_SeqR	CAA CCC ATC ACT GTA TGA AAG CC
Sequencing primer	BT3369KO_SeqR	GTG AAT CCT TCT CGT TAT GAA AGC C
Sequencing primer	BT3370KO_SeqR	CAT CTA ACA TTT TCT CAA ACA TTG CAG G
Sequencing primer	BT3371KO_SeqR	ACT GCA TTT TAT ATC CAC AAA TTT AAT ACT CC
Sequencing primer	BT3372KO_SeqR	CTT TTT AAA ATT AGG ACT AGG TTG ATT GGG
Sequencing primer	BT3373KO_SeqR	ATT GCA ATA TAC TTT CCT CTG ACT CG
Sequencing primer	BT3374KO_SeqR	AAT TAA TTG TTT TTT TAG AGA TCC CAT GAC C
Sequencing primer	BT3375KO_SeqR	TTC TAC AGA AGT ATA

		GGG GCT GG
Sequencing primer	BT3376KO_SeqR	TCC ATT CCC CCA ACT GTA ACC
Sequencing primer	BT3377KO_SeqR	AAT ACC ATA ATG AGT AGC AGT TGC C
Sequencing primer	BT3378KO_SeqR	GGA TGT TGC AAG TCA GCA TCC
Sequencing primer	BT3379KO_SeqR	ACG ACT GCT CCA GAA TAT GAG G
Sequencing primer	BT3380KO_SeqR	GTC AAA AGG AGA TTC AGG TAT CTC C
Sequencing primer	80_SeqR_new	TCT TGT TCG TGT TGA ATA TCT TCT TCG
BT2152 clean deletion	BT2152KO_ForSeq	ACG CAG GCC TTG AAG ATA GA
BT2152 clean deletion	BT2152KO_RevSeq	CCC ATC AAC AGT TCC GAG TT
BT1854 clean deletion	BT1854KO_ForSeq	ATA AGG AGA CCC CGA TGT GG
BT1854 clean deletion	BT1854KO_RevSeq	CTG AAG CAT TGT CAC GTT ATC CC
BT2152 clean deletion	BT2152_KORevSeq	GCC ATC AAG ATA GGA GAT CAT CGG
BT1854 clean deletion	BT1854_KORevSeq	TCG AAC ATT TCA TCG GTA TAA GGC
BT3365-BT3380 clean deletion	pEx_us65_For	CCT GCA GCC CGG GGG ATC CAC TAG TGA GAT GAA GAG AAG TAT GAC
BT3365-BT3380 clean deletion	pEx_us65_Rev	ATG AAT ACT ACA TTA ATT ACC CTC CTT TAG C
BT3365-BT3380 clean deletion	pEx_ds80_For	GTA ATT AAT GTA GTA TTC ATT TGT GAT AAT AGA TGA TTG
BT3365-BT3380 clean deletion	pEx_ds80_Rev	TTC CCC TCC ACC GCG GTG GCG GCC GCG GAT GTT GCA ACA ATG CC

Appendix 3

Full lipid A MALDI-TOF MS and MS/MS spectra for all strains discussed

Bacteroides thetaiotaomicron VPI-5482 Δ*tdk*
Waters Synapt G2 HDMS 32k
MALDI-TOF MS (450-5000 m/z)

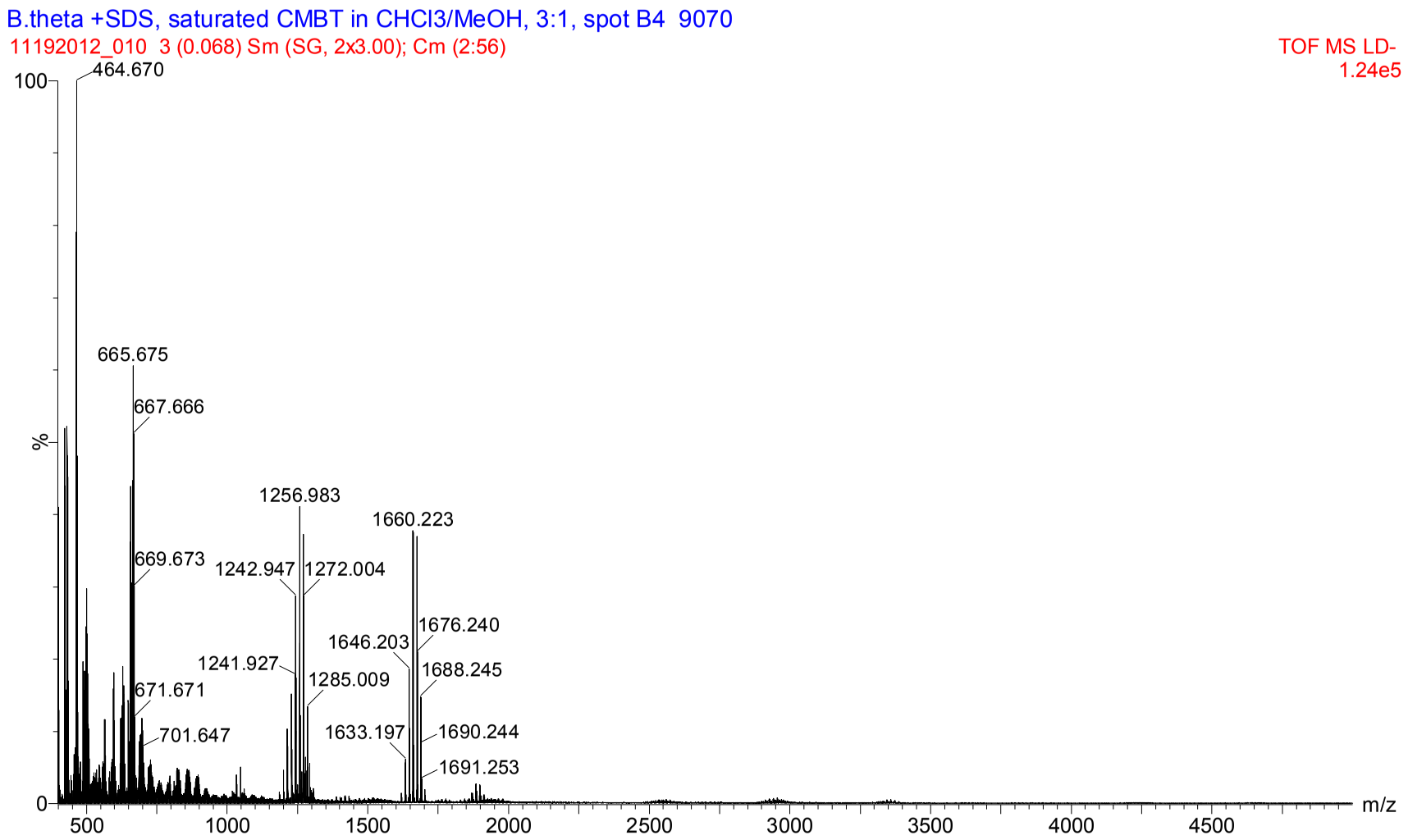

Bacteroides thetaiotaomicron VPI-5482 Δ*tdk*
Waters Synapt G2 HDMS 32k
MALDI-TOF MS (1500-1850 m/z)

B.theta +SDS, saturated CMBT in CHCl3/MeOH, 3:1, spot B4 9070

11192012_010 3 (0.068) Sm (SG, 2x3.00); Cm (3:56)

TOF MS LD-
4.68e4

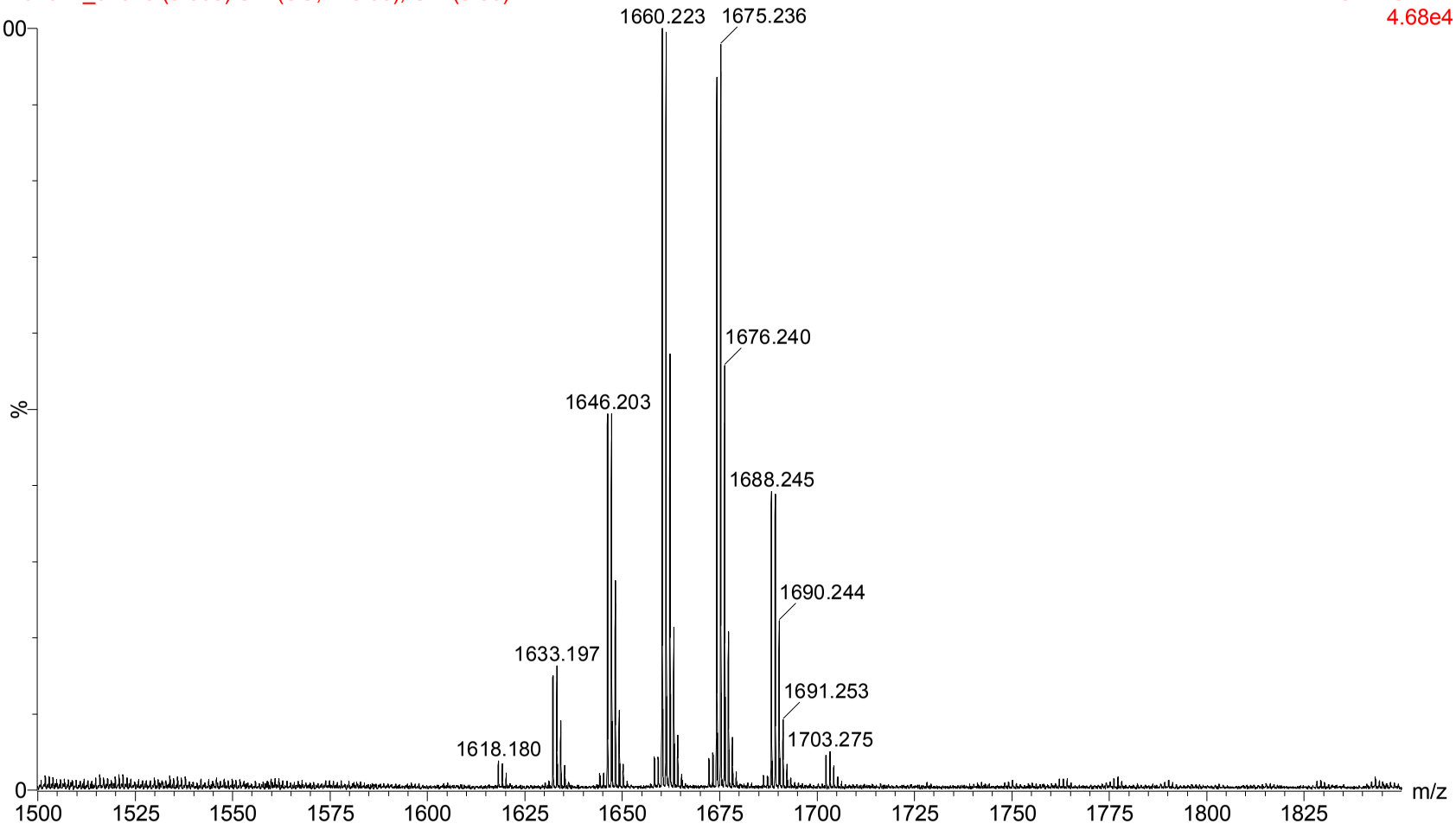

Bacteroides thetaiotaomicron VPI-5482 Δ*tdk*
Waters Synapt G2 HDMS 32k
MALDI-TOF MS/MS 1688.25 m/z

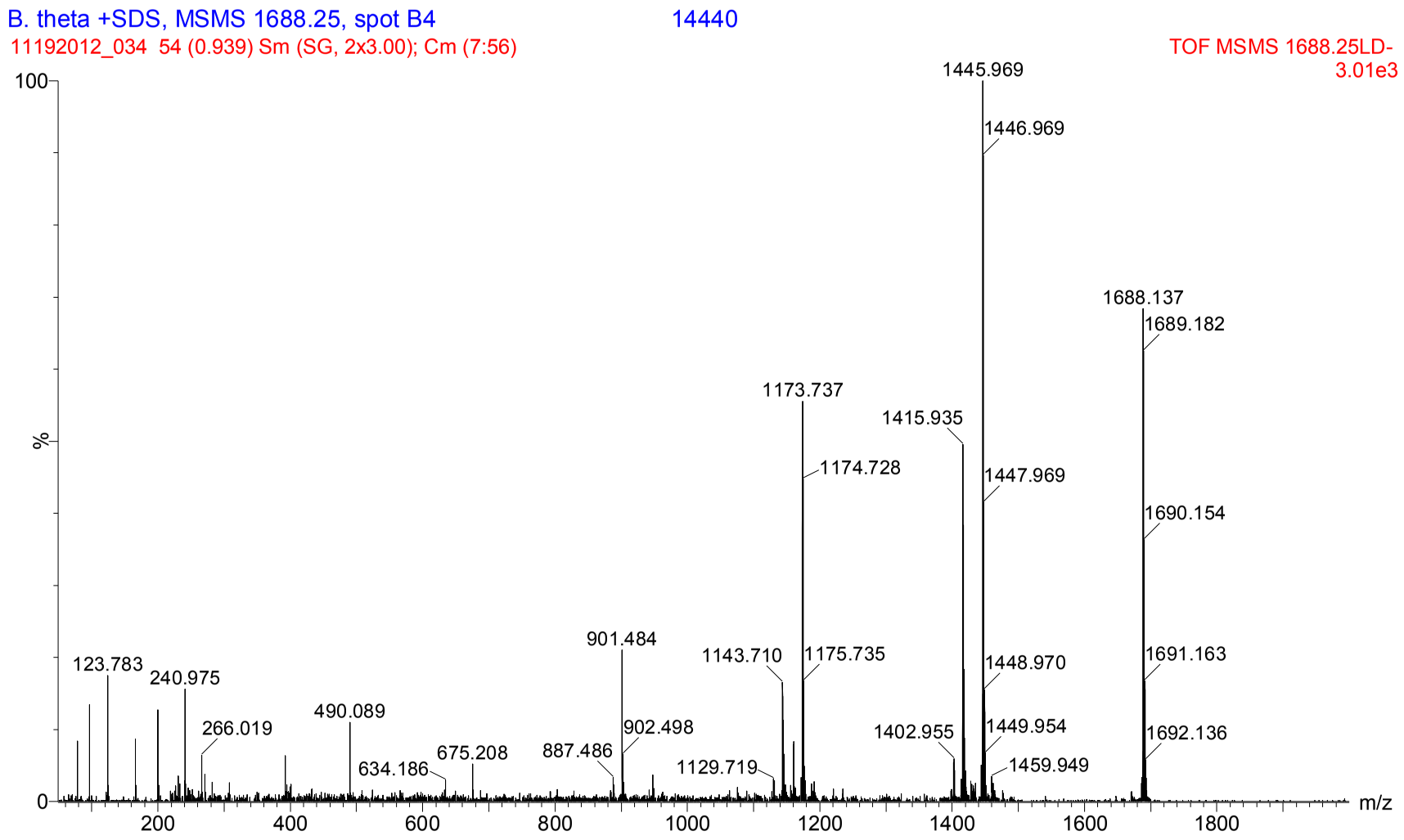

Bacteroides fragilis NCTC 9343
Waters Synapt G2 HDMS 32k
MALDI-TOF MS (450-5000 m/z)

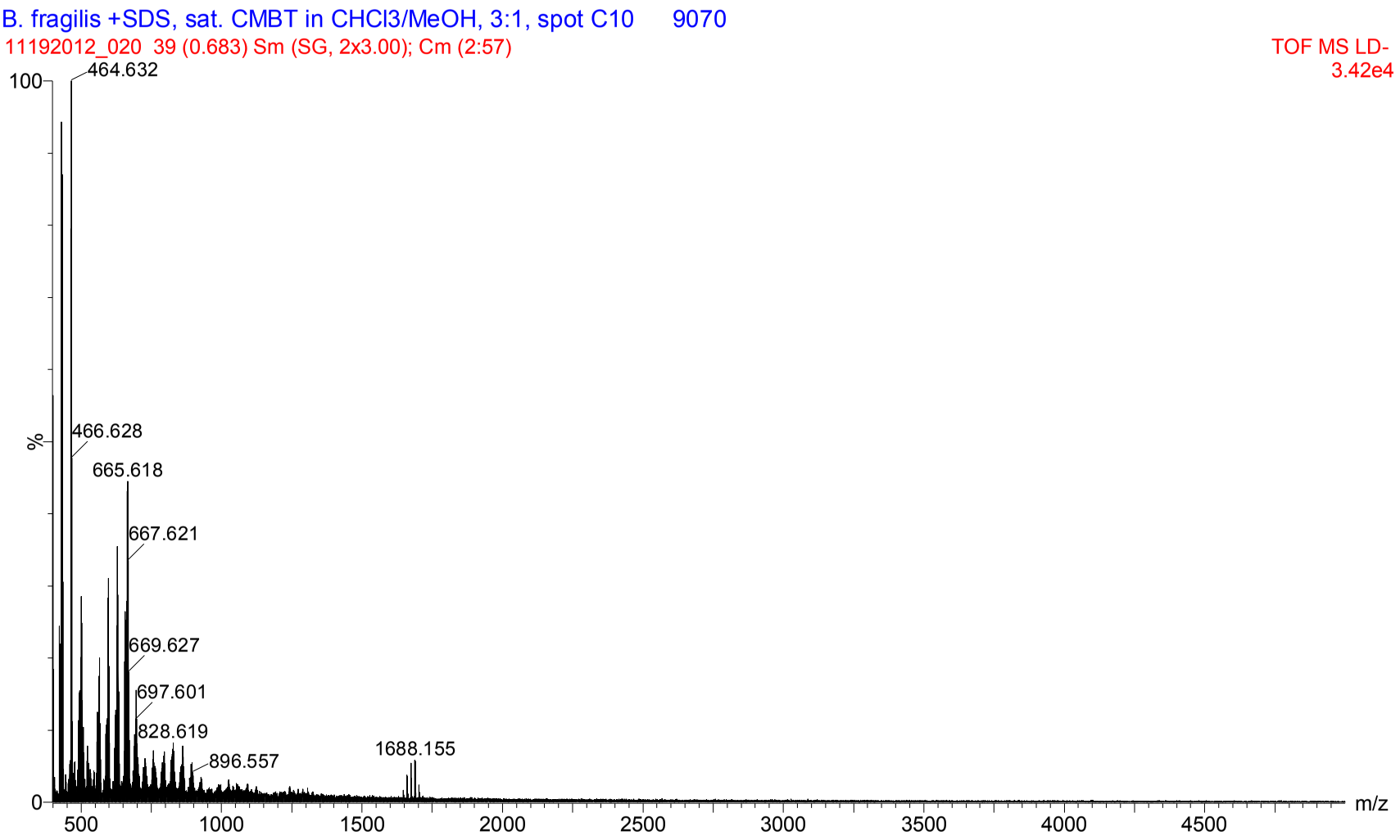

Bacteroides fragilis NCTC 9343
Waters Synapt G2 HDMS 32k
MALDI-TOF MS (1500-1850 m/z)

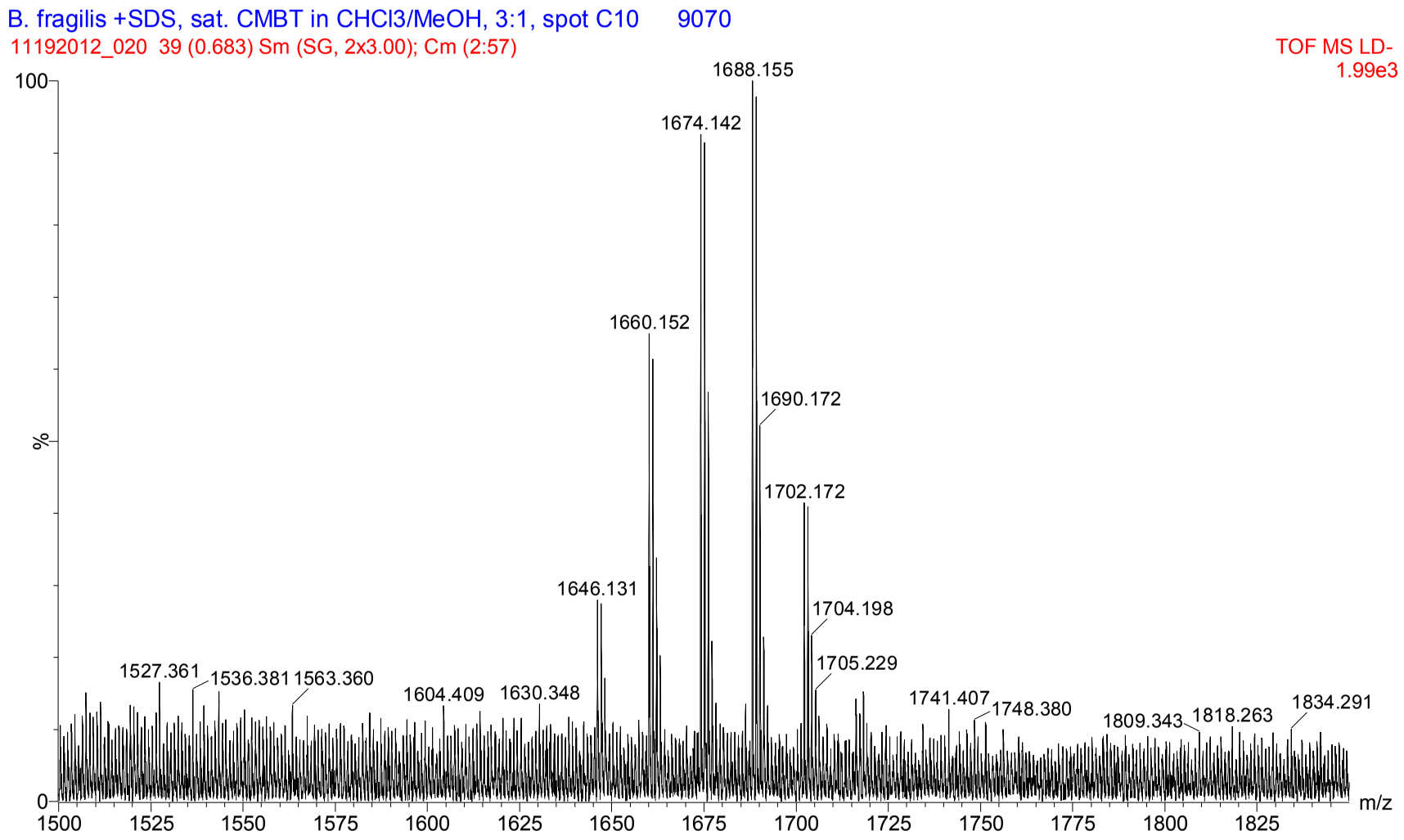

Bacteroides ovatus ATCC 8483
Waters Synapt G2 HDMS 32k
MALDI-TOF MS (450-5000 m/z)

B. ovatus +SDS, sat. CMBT in CHCl3/MeOH, 3:1, spot D5 9070

11192012_024 39 (0.683) Sm (SG, 2x3.00); Cm (3:57)

TOF MS LD-
2.24e5

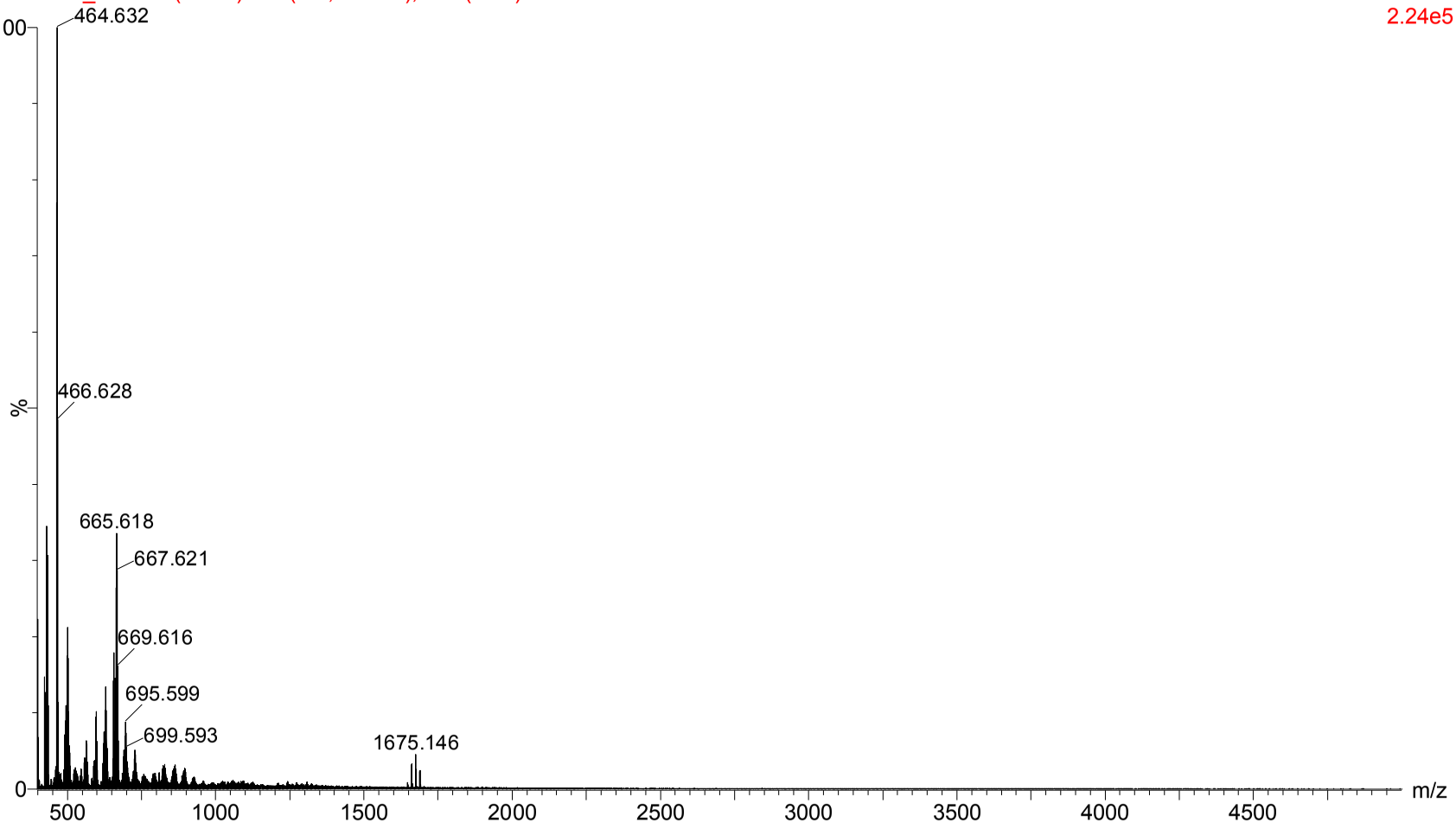

Bacteroides ovatus ATCC 8483
Waters Synapt G2 HDMS 32k
MALDI-TOF MS (1500-1850 m/z)

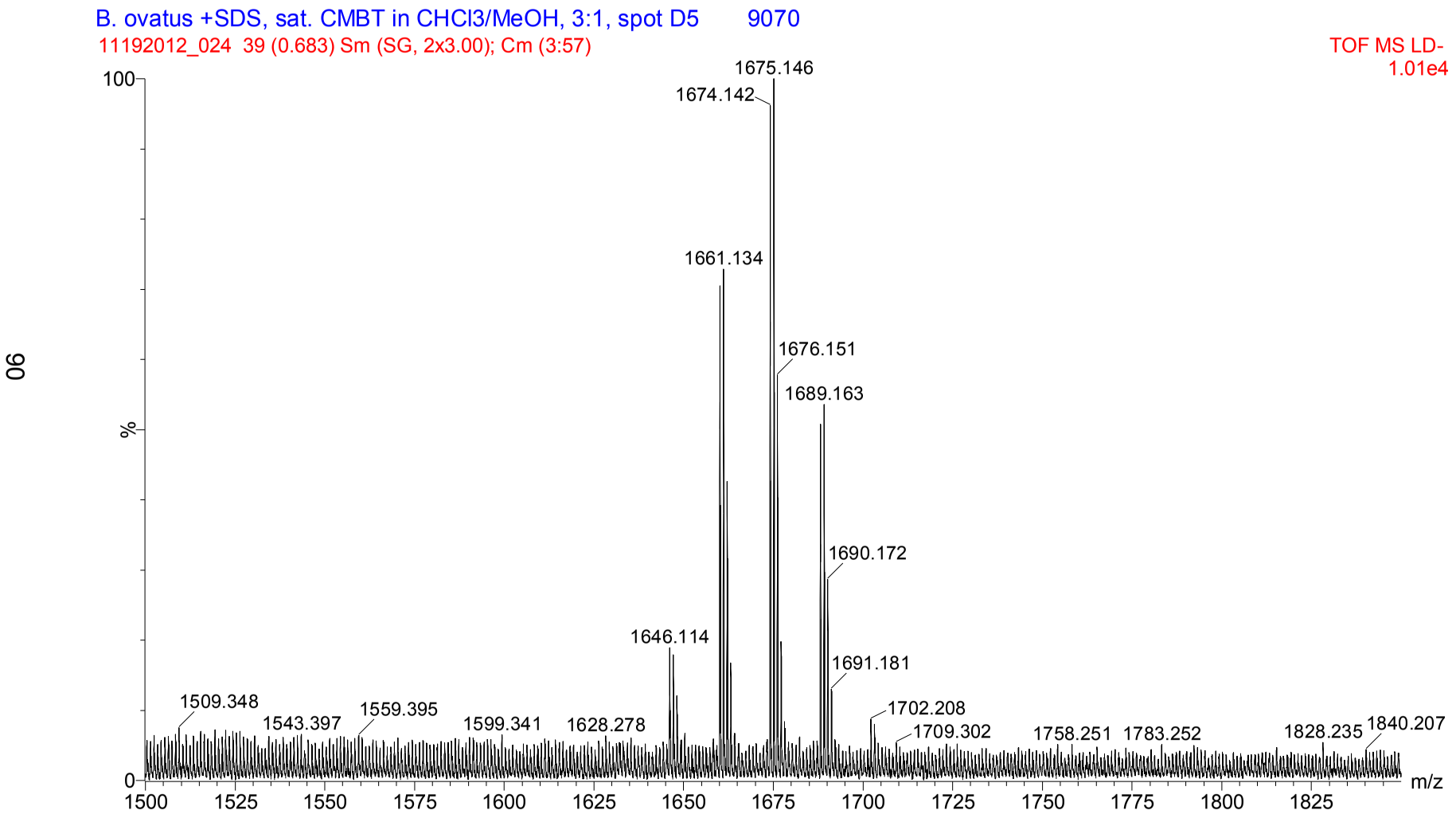

Bacteroides uniformis ATCC 9492
Waters Synapt G2 HDMS 32k
MALDI-TOF MS (450-5000 m/z)

B. uniformis +SDS, sat. CMBT in CHCl3/MeOH, 3:1, spot D10

11192012_026 15 (0.273) Sm (SG, 2x3.00); Cm (3:56)

TOF MS LD-
7.24e4

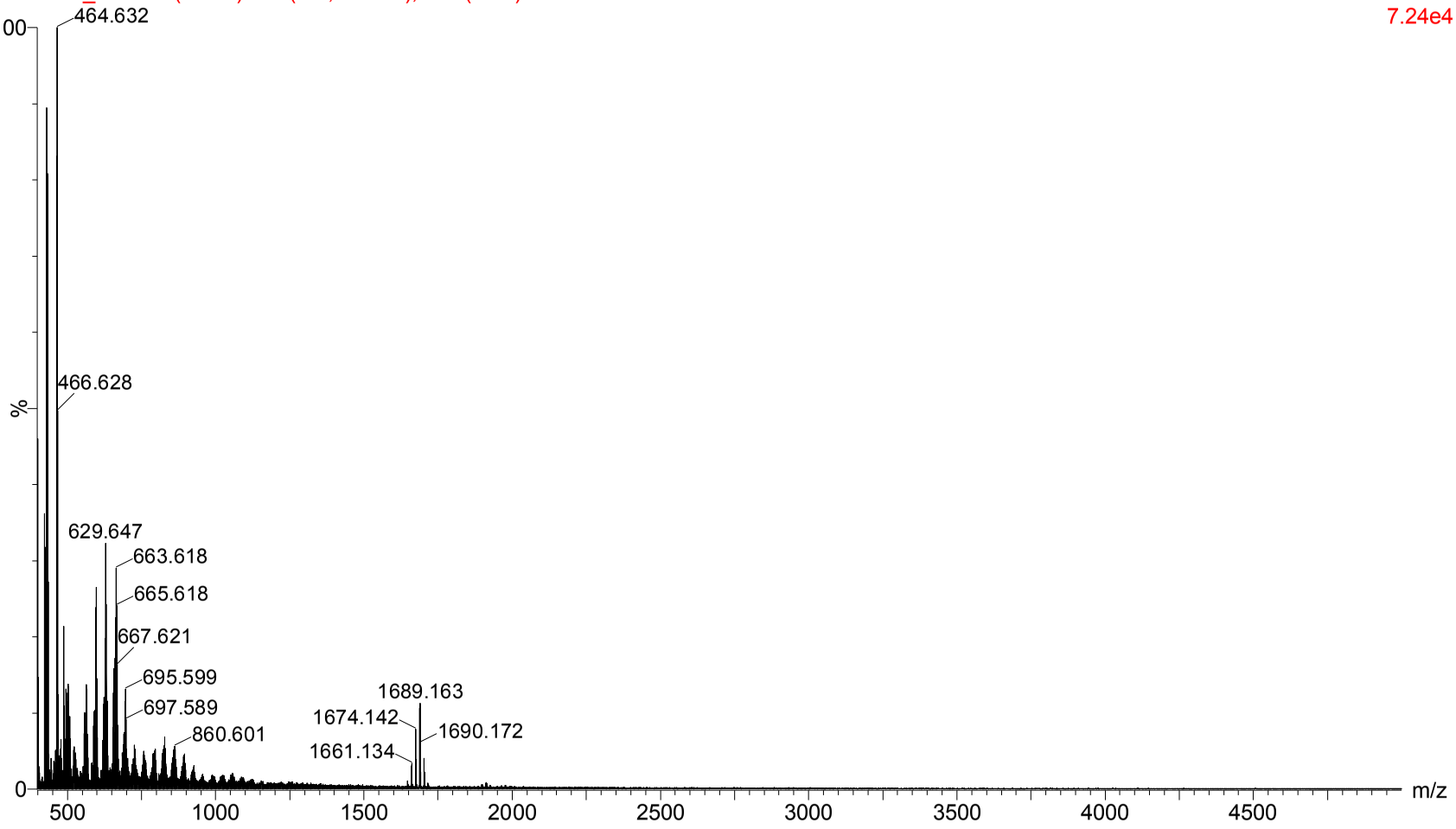

Bacteroides uniformis ATCC 9492
Waters Synapt G2 HDMS 32k
MALDI-TOF MS (1500-1850 m/z)

B. uniformis +SDS, sat. CMBT in CHCl3/MeOH, 3:1, spot D10

11192012_026 15 (0.273) Sm (SG, 2x3.00); Cm (3:56)

TOF MS LD-
8.13e3

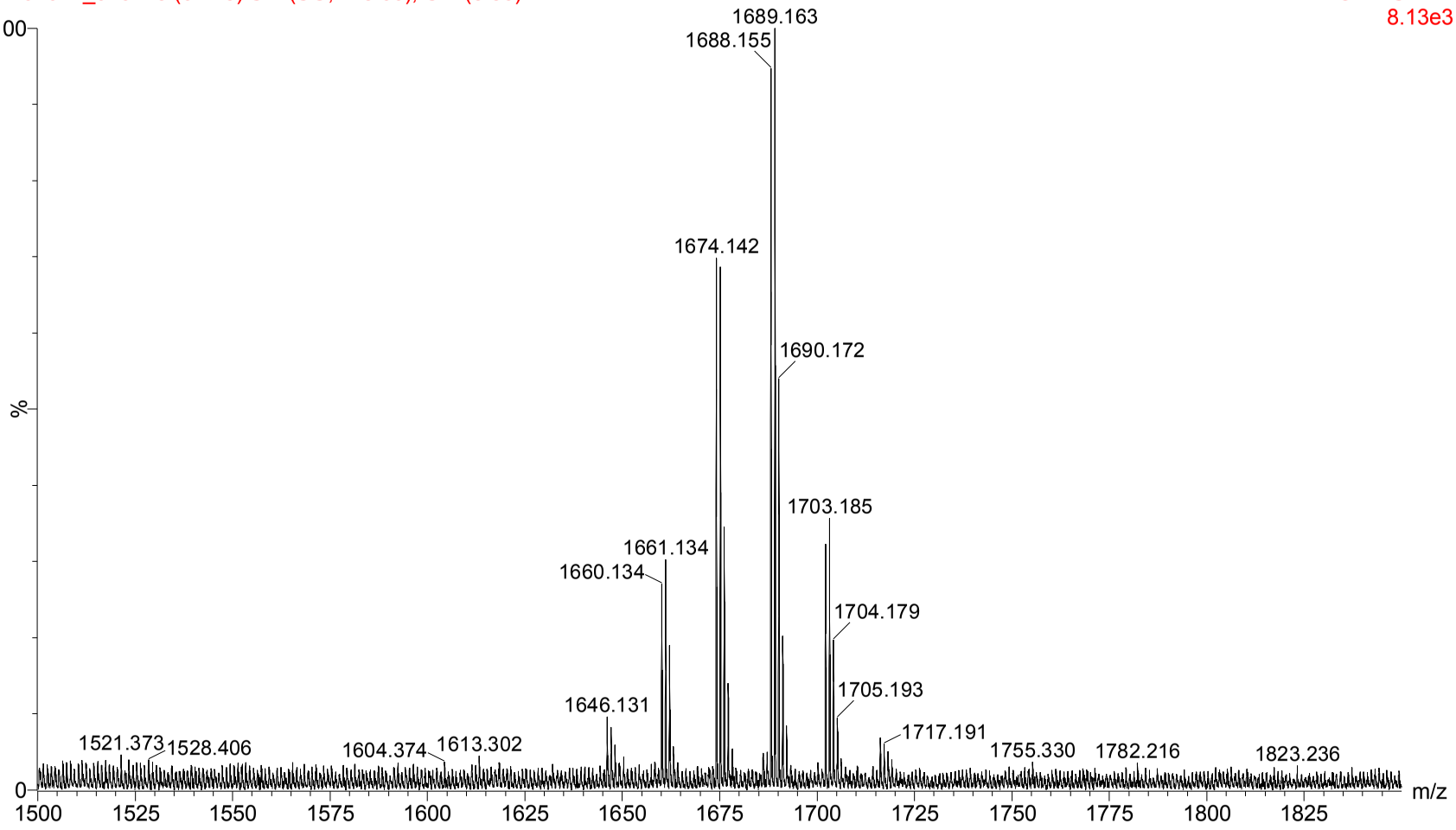

Bacteroides vulgatus ATCC 8482
Waters Synapt G2 HDMS 32k
MALDI-TOF MS (450-5000 m/z)

B. vulgatus +SDS, sat. CMBT in CHCl3/MeOH, 3:1, spot E5 9070

11192012_030 50 (0.871) Sm (SG, 2x3.00); Cm (3:56)

TOF MS LD-
1.26e5

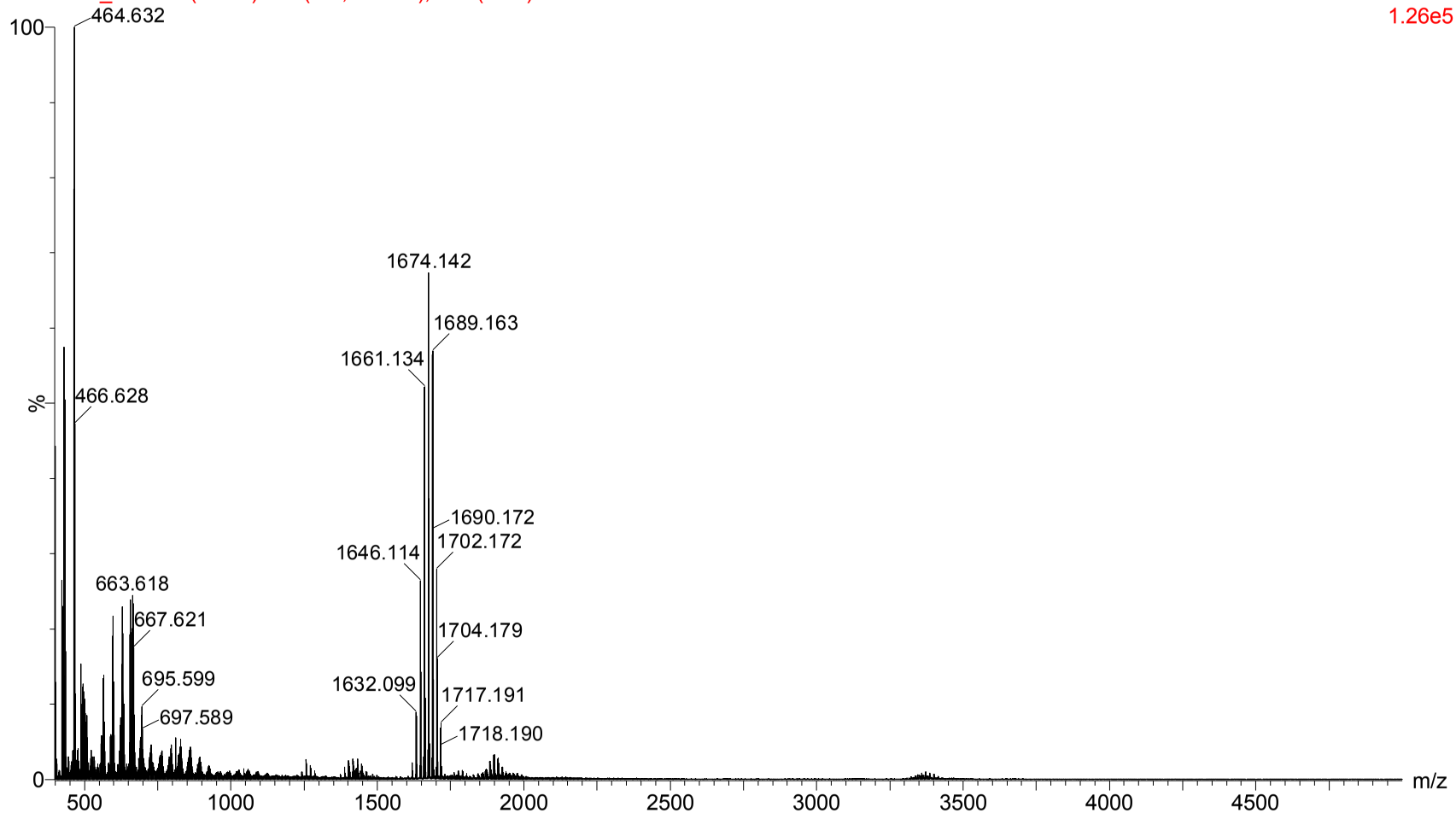

Bacteroides vulgatus ATCC 8482
Waters Synapt G2 HDMS 32k
MALDI-TOF MS (1500-1850 m/z)

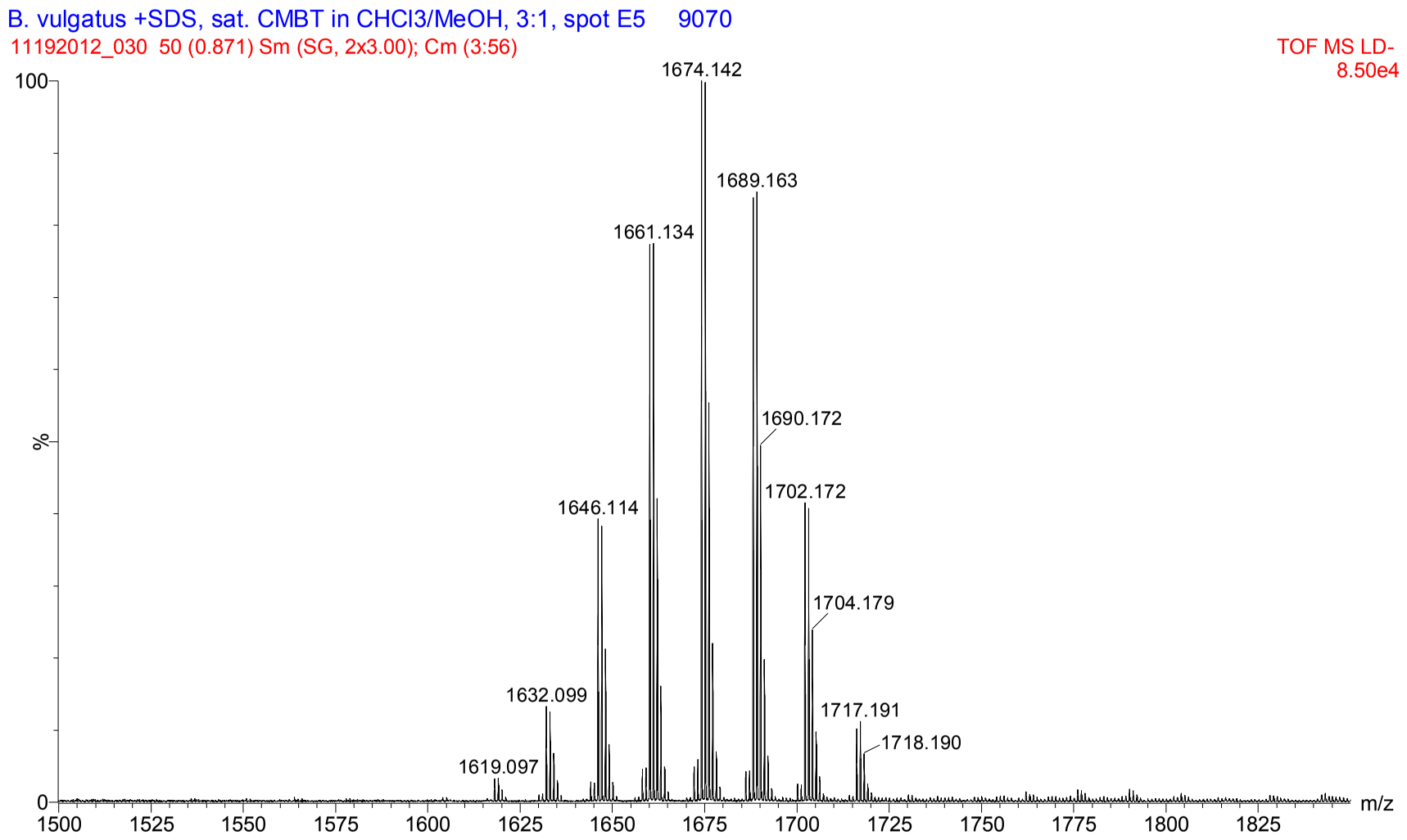

Bacteroides thetaiotaomicron VPI-5482 Δ*tdk* ΔBT2152 (*lpxL*)
Waters Synapt G2 HDMS 32k
MALDI-TOF MS (450-5000 m/z)

B.theta d2152 +SDS, sat. CMBT in CHCl3/MeOH, 3:1, spot B10

11192012_014 3 (0.068) Sm (SG, 2x3.00); Cm (2:55)

TOF MS LD-
8.96e4

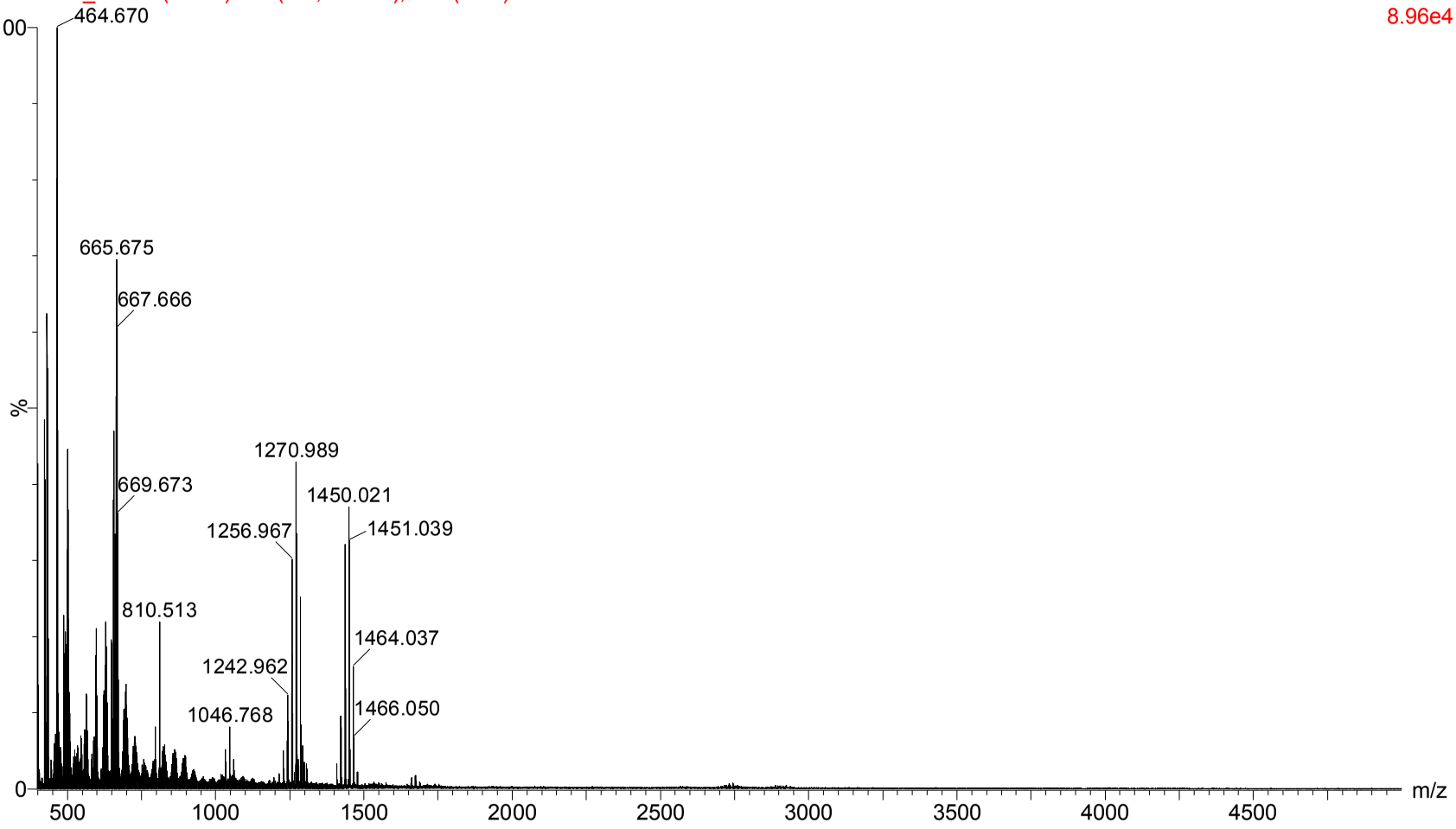

Bacteroides thetaiotaomicron VPI-5482 Δ*tdk* ΔBT2152 (*lpxL*)
Waters Synapt G2 HDMS 32k
MALDI-TOF MS (450-5000 m/z)

B.theta d2152 +SDS, sat. CMBT in CHCl3/MeOH, 3:1, spot B10

11192012_014 3 (0.068) Sm (SG, 2x3.00); Cm (2:55)

TOF MS LD-
8.96e4

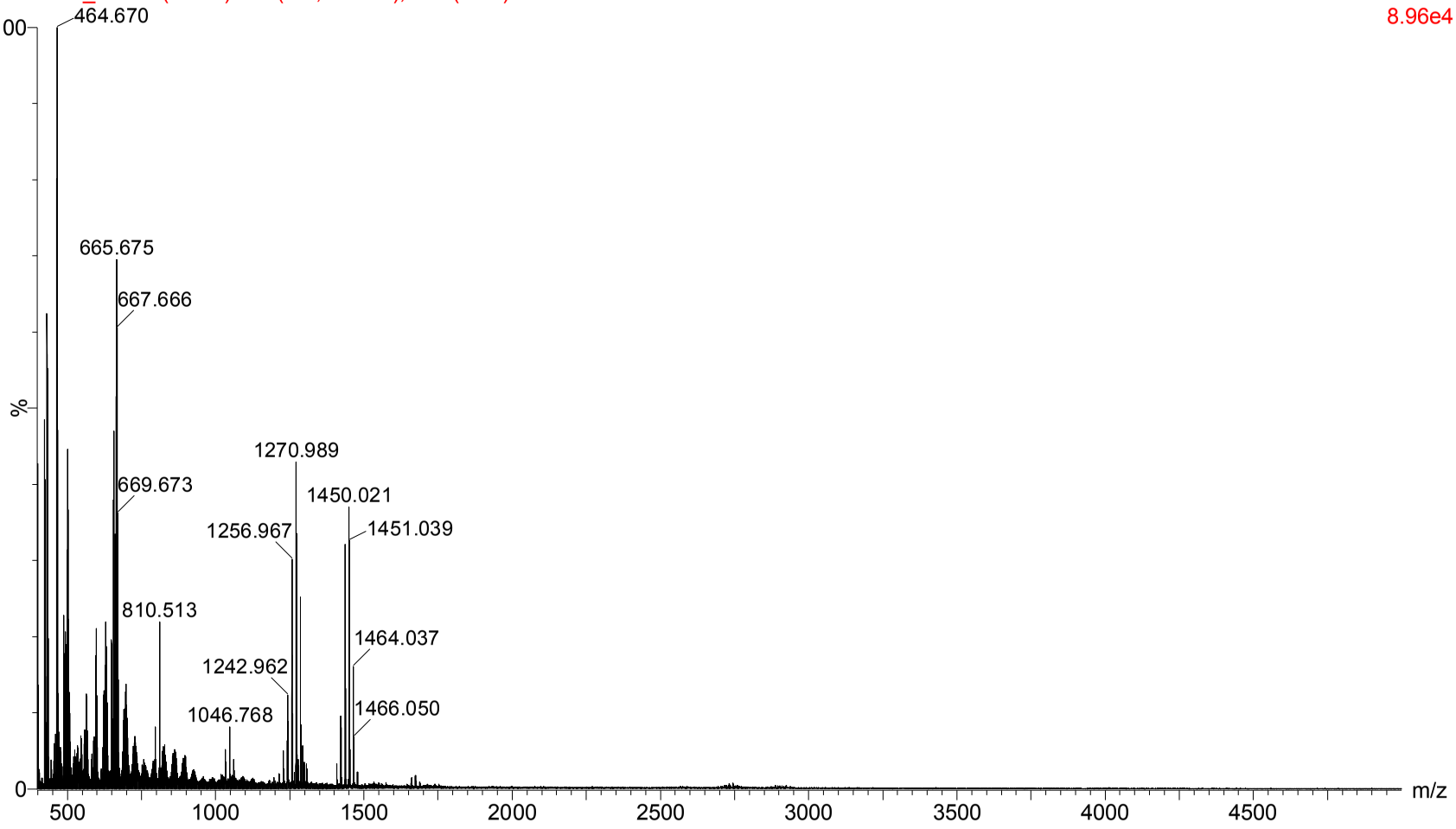

Bacteroides thetaiotaomicron VPI-5482 Δ*tdk* ΔBT2152 (*lpxL*)
Waters Synapt G2 HDMS 32k
MALDI-TOF MS/MS 1464.04 m/z

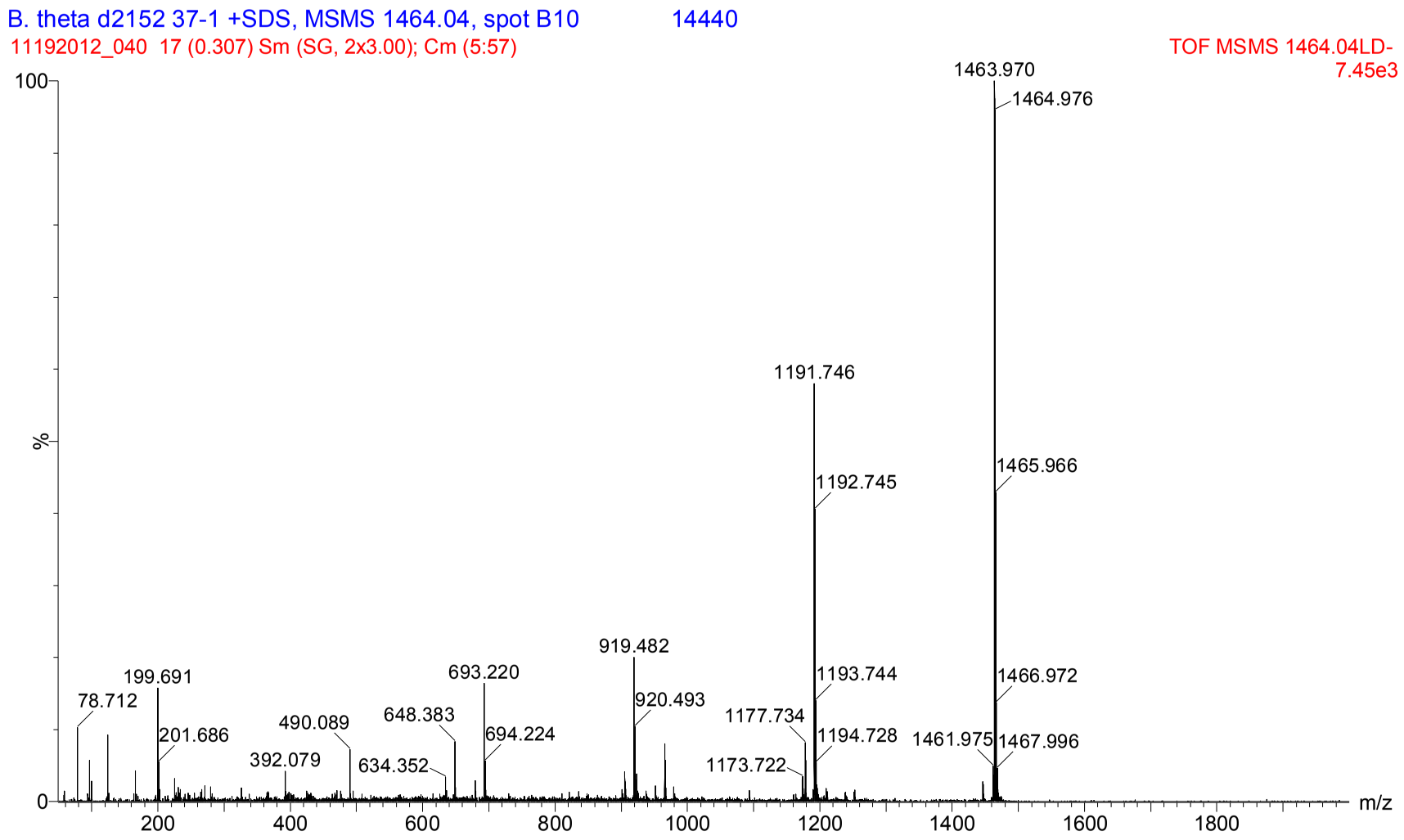

Bacteroides thetaiotaomicron VPI-5482 Δ*tdk* ΔBT1854 (*lpxF*)
Waters Synapt G2 HDMS 32k
MALDI-TOF MS (450-5000 m/z)

Bt T+KO1#6, CMBT 3:1 CHCl3/MeOH, spot A10 9070
20140107_007 27 (0.478) Cm (4:57)
TOF MS LD-
1.39e4

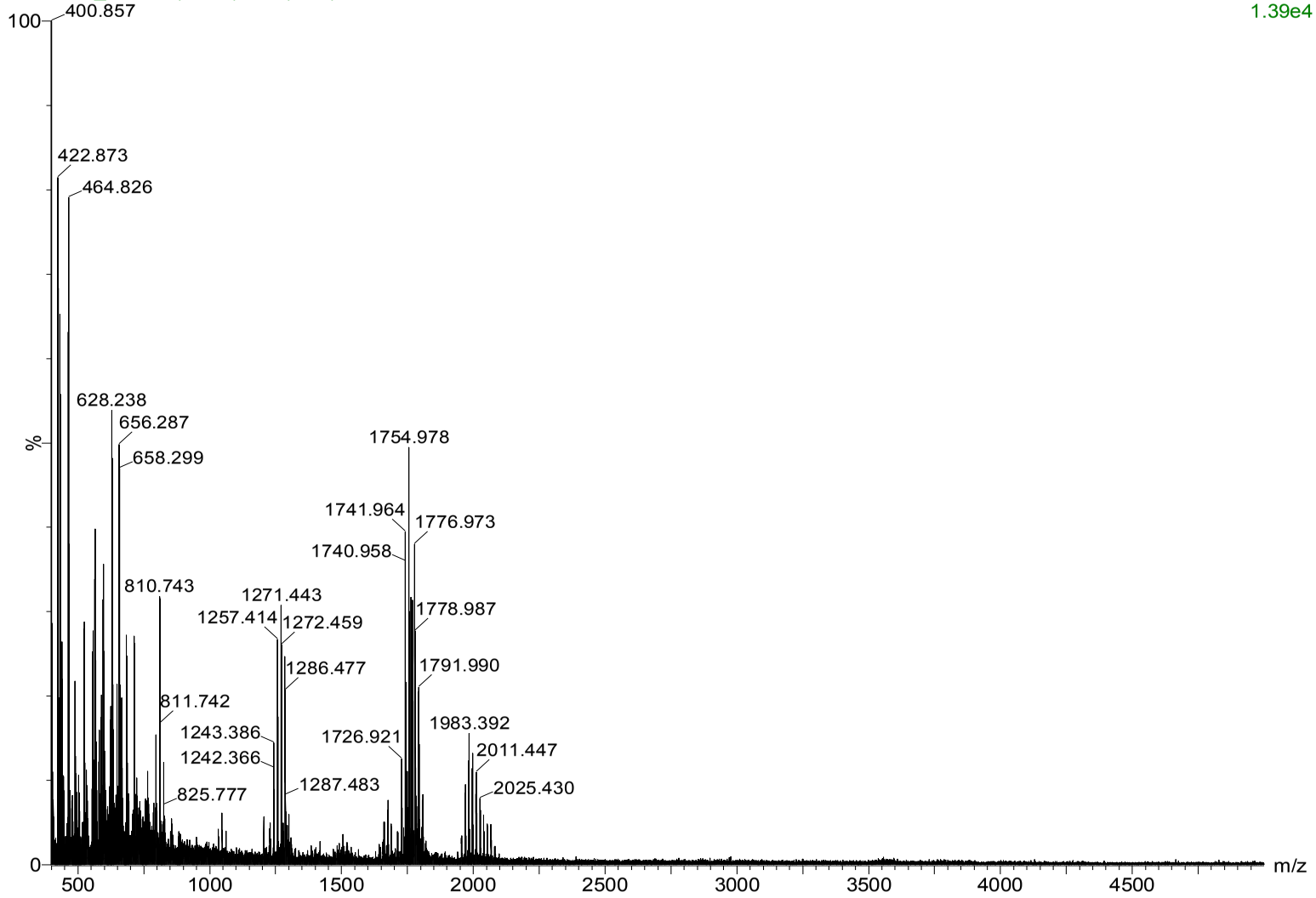

Bacteroides thetaiotaomicron VPI-5482 Δ*tdk* ΔBT1854 (*lpxF*)
Waters Synapt G2 HDMS 32k
MALDI-TOF MS (1100-2200 m/z)

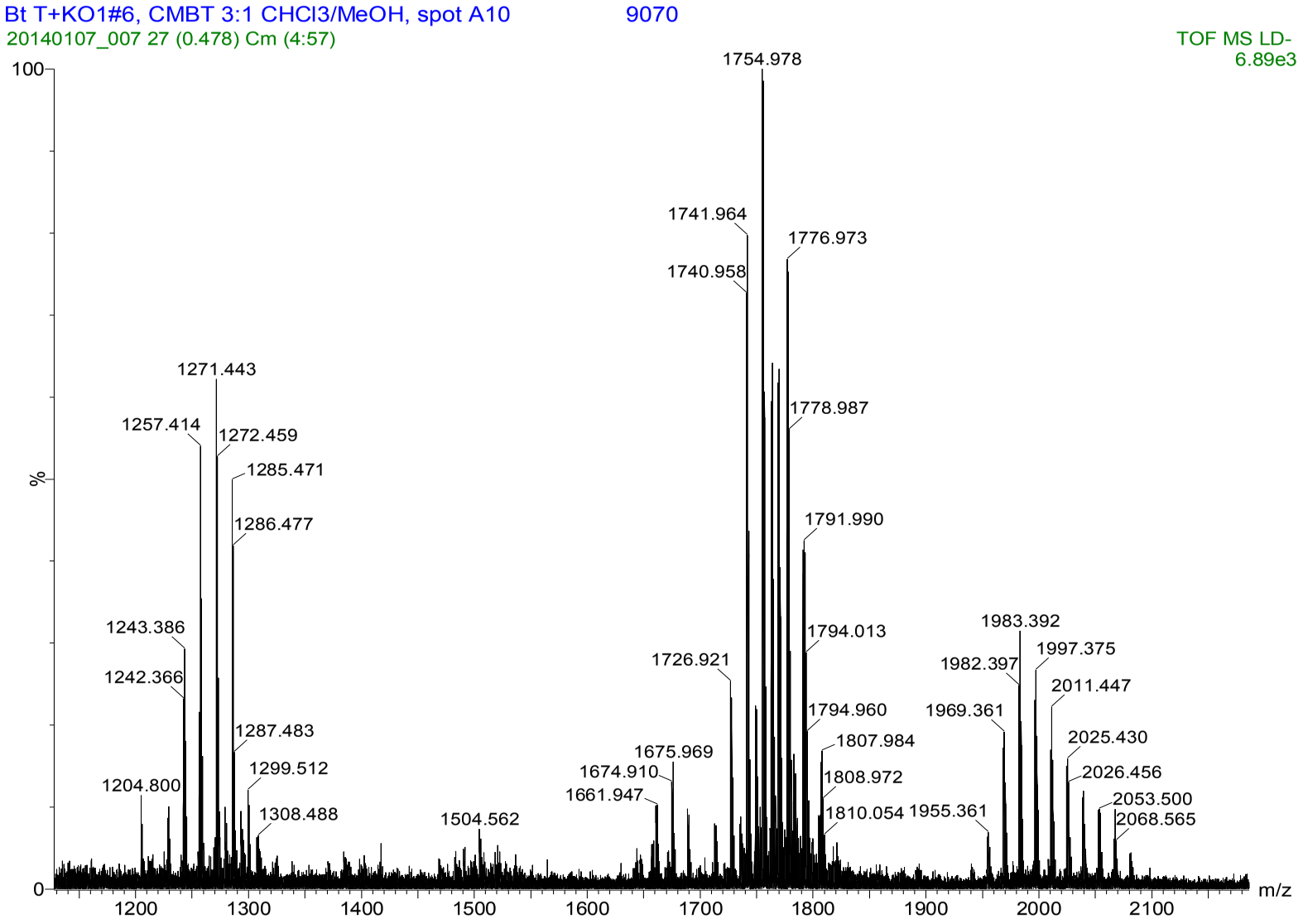

Bacteroides thetaiotaomicron VPI-5482 Δ*tdk* ΔBT1854 (*lpxF*)
Waters Synapt G2 HDMS 32k
MALDI-TOF MS (1580-1880 m/z)

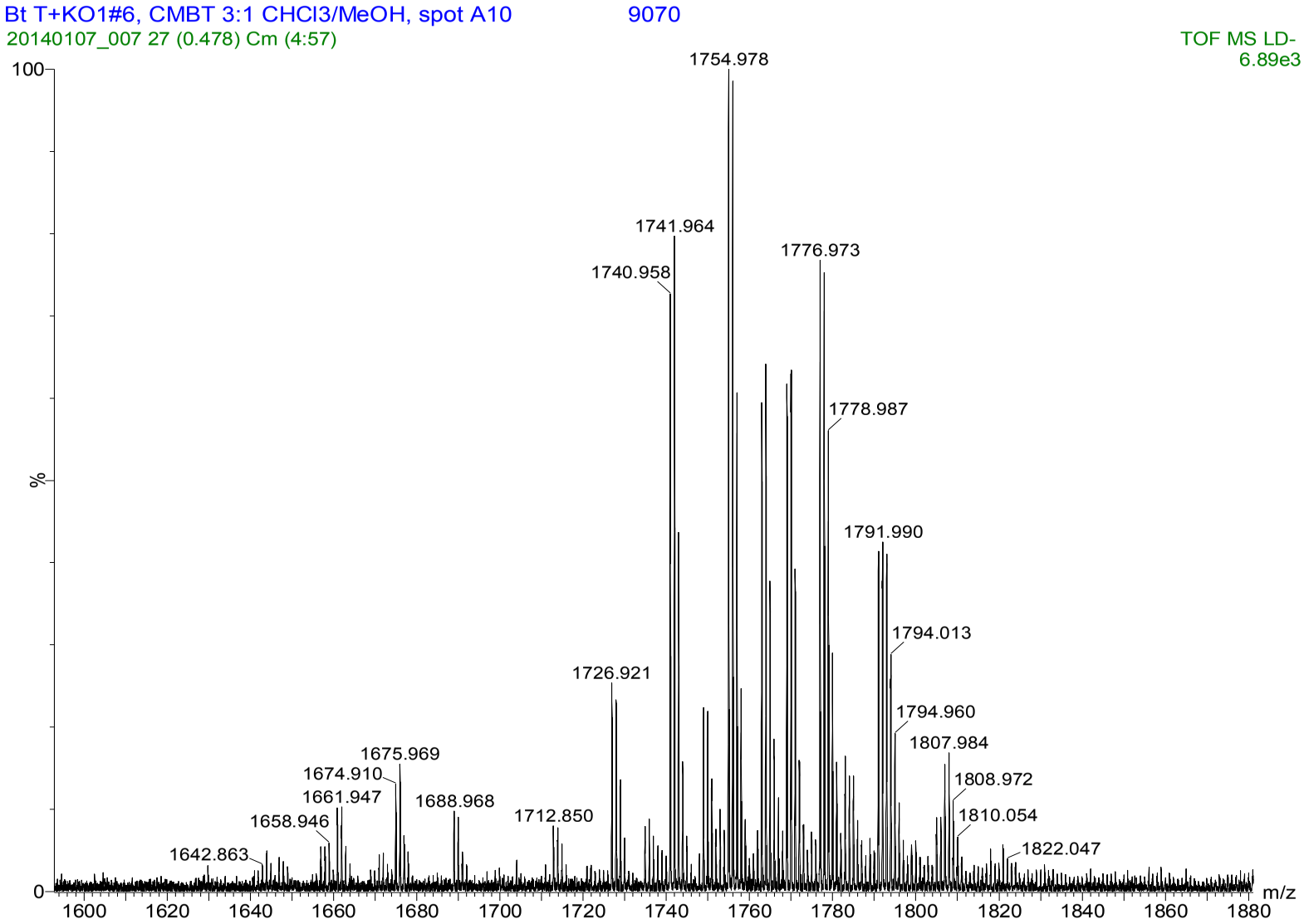

100

Bacteroides thetaiotaomicron VPI-5482 Δ*tdk* ΔBT 2152 ΔBT1854 (*lpxL lpxF*)
Waters Synapt G2 HDMS 32k
MALDI-TOF MS (450-5000 m/z)

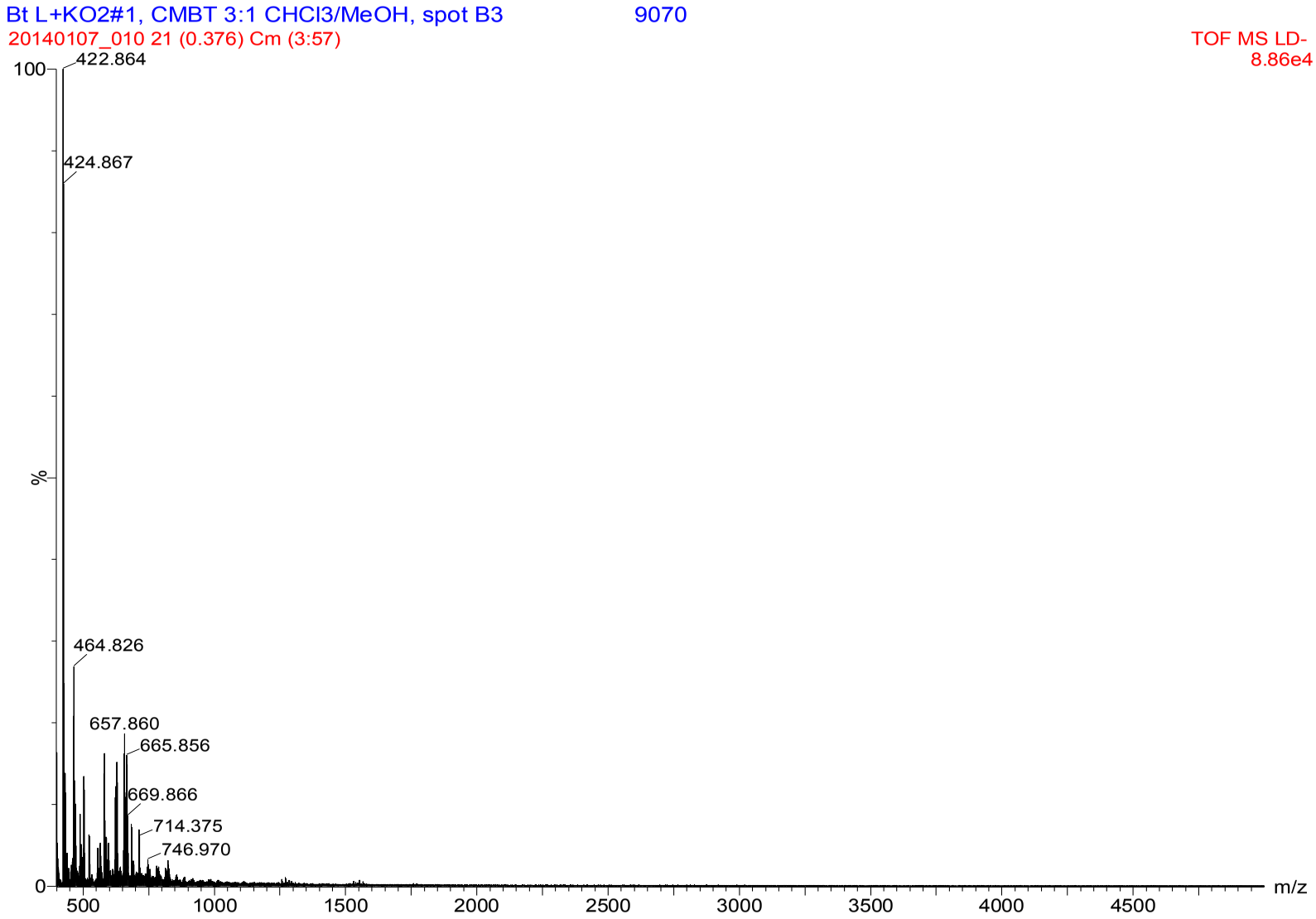

Bacteroides thetaiotaomicron VPI-5482 Δ*tdk* ΔBT 2152 ΔBT1854 (*lpxL lpxF*)
Waters Synapt G2 HDMS 32k
MALDI-TOF MS (1425-1775 m/z)

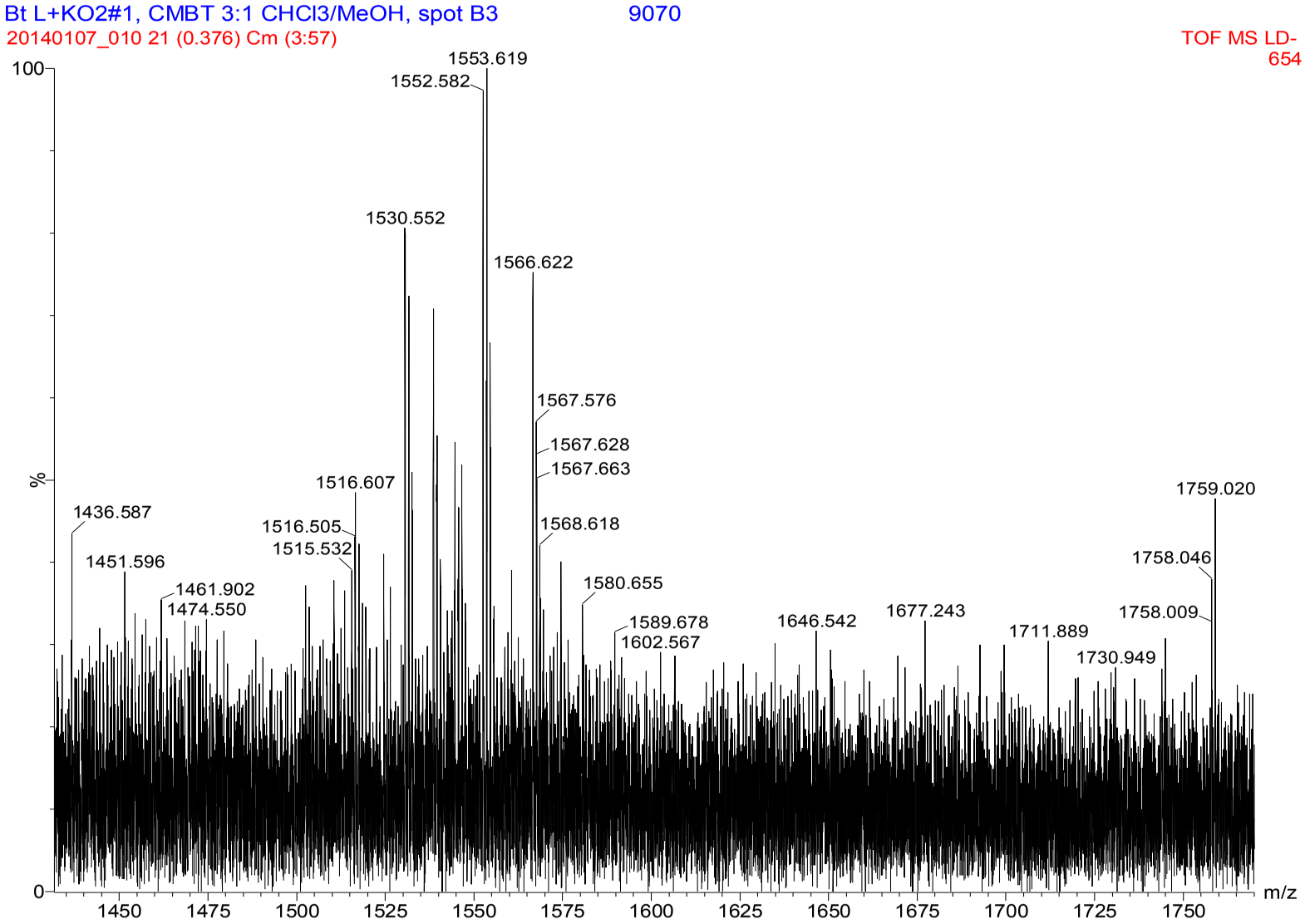

Appendix 4

Full intact LOS MALDI-TOF MS spectra for all strains discussed

Bacteroides thetaiotaomicron VPI-5482 Δ*tdk* ΔCPS
Shimadzu AXIMA Performance, intact LOS
MALDI-TOF MS (800-6500 m/z)

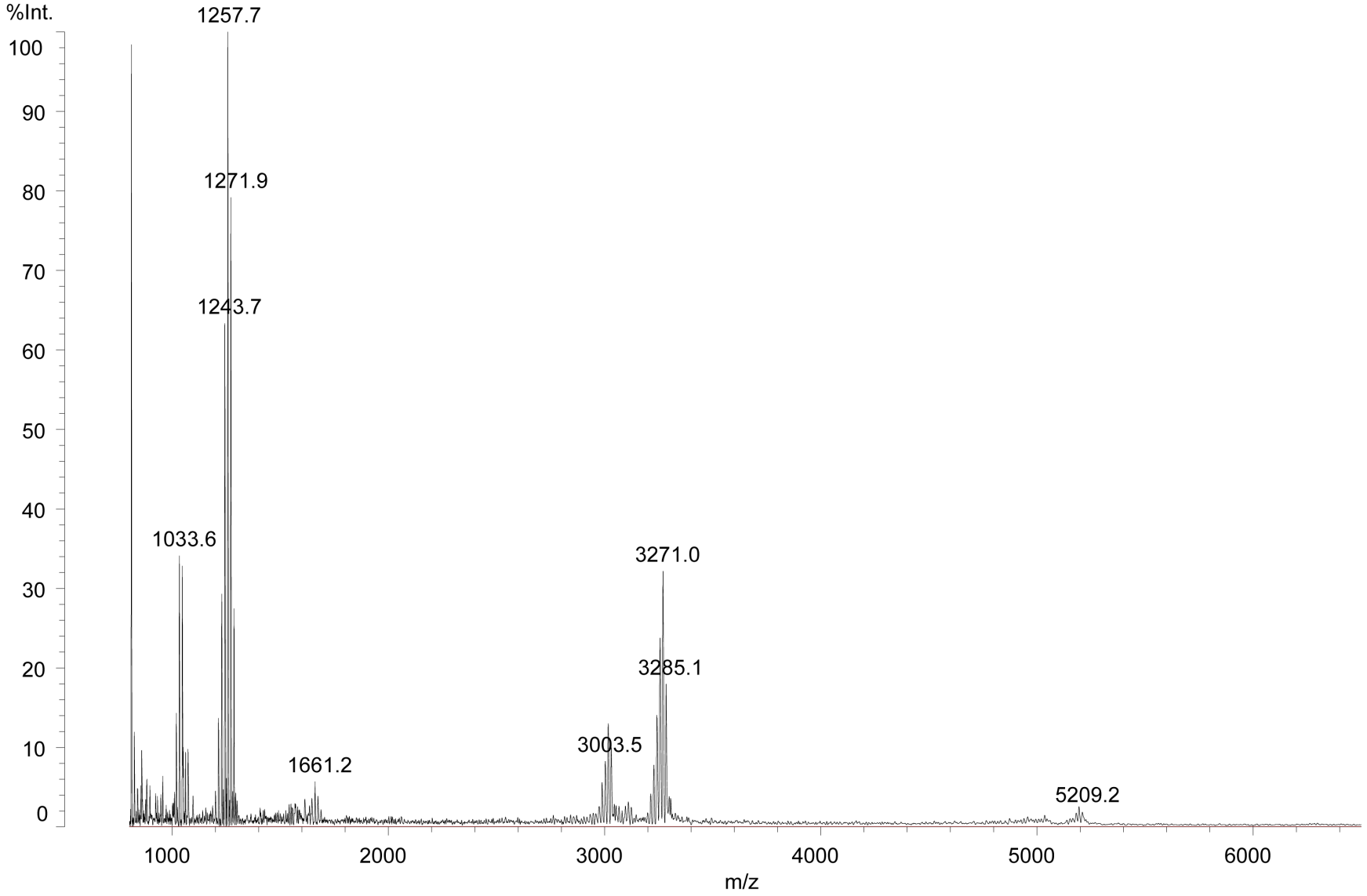

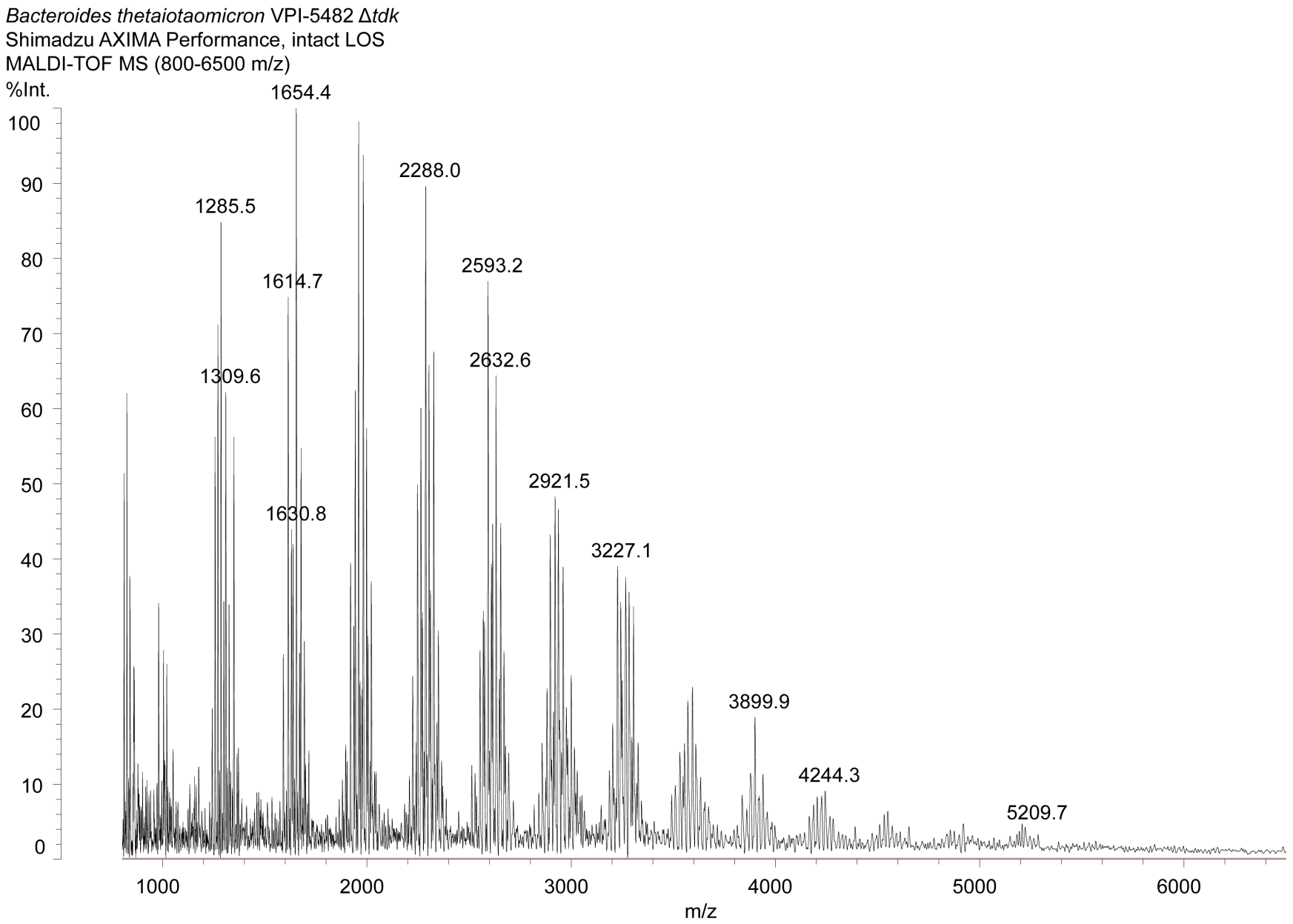
Bacteroides thetaiotaomicron VPI-5482 Δ*tdk*
Shimadzu AXIMA Performance, intact LOS
MALDI-TOF MS (800-6500 m/z)
%Int.
1654.4
2288.0
1285.5
2593.2
1614.7
2632.6
1309.6
2921.5
1630.8
3227.1
3899.9
4244.3
5209.7
100
90
80
70
60
50
40
30
20
10
0
1000
2000
3000
4000
5000
6000
m/z

Bacteroides thetaiotaomicron VPI-5482 46A7 (tnBT3365)
Shimadzu AXIMA Performance, intact LOS
MALDI-TOF MS (800-6500 m/z)

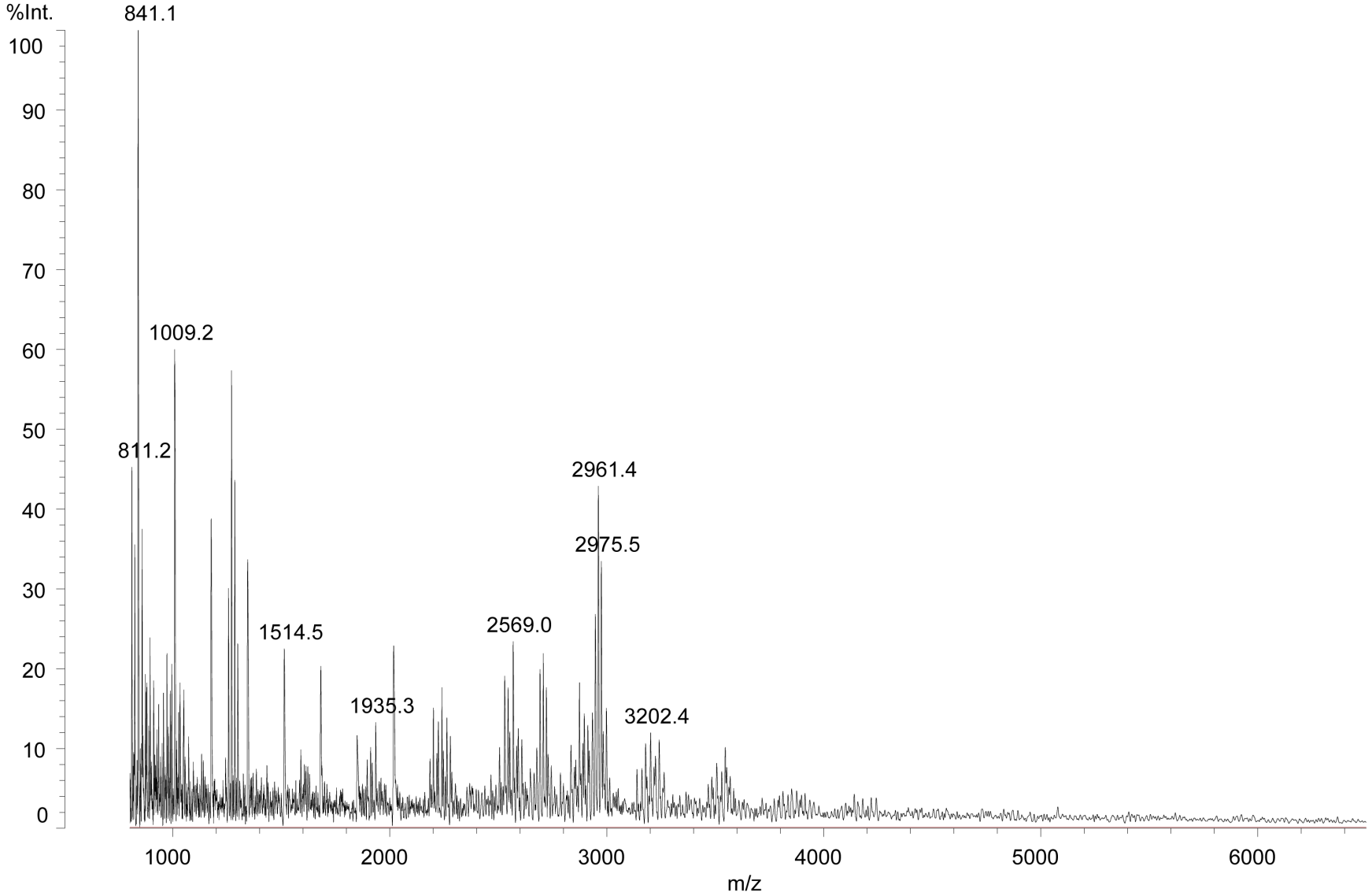

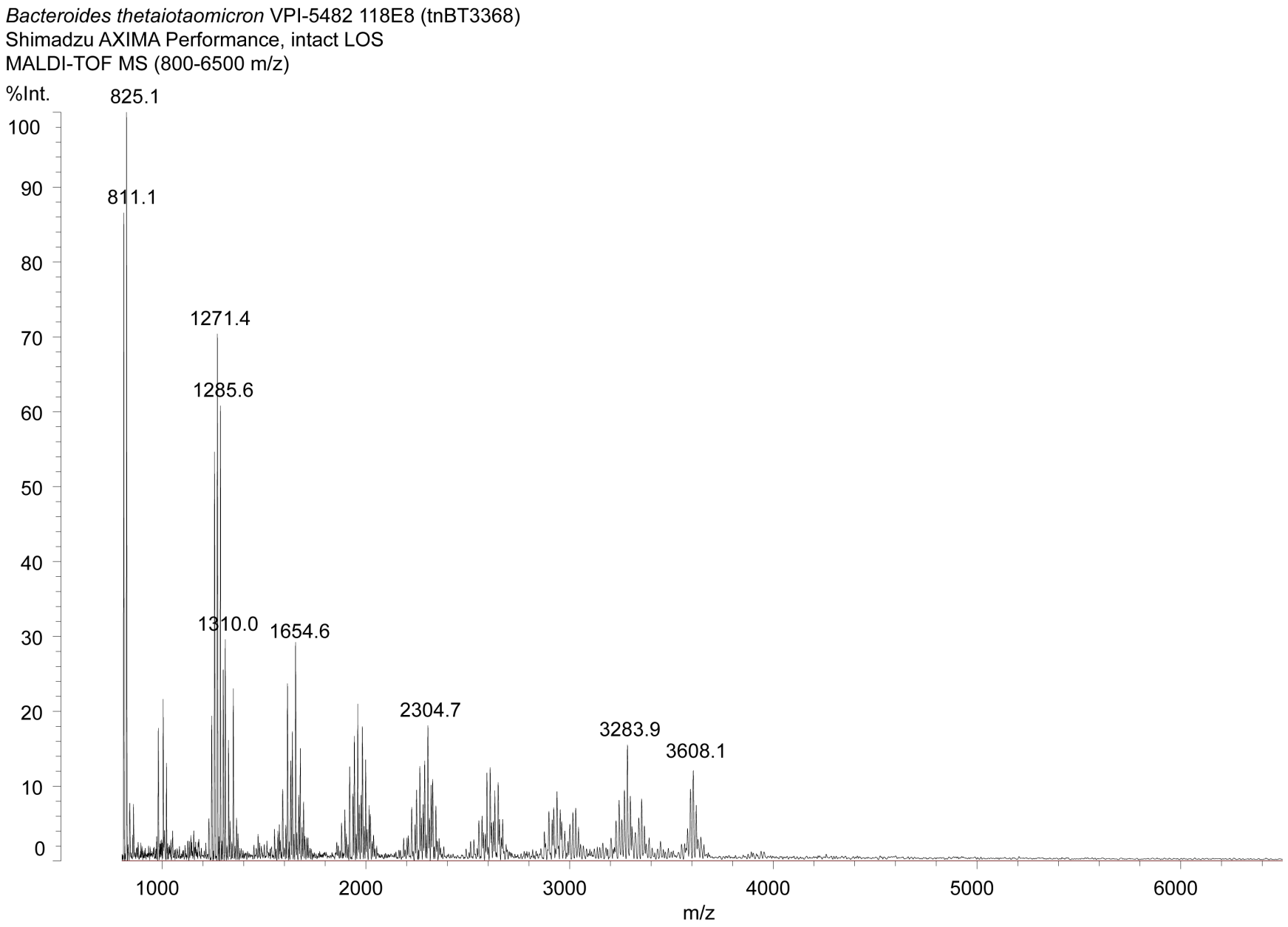
Bacteroides thetaiotaomicron VPI-5482 118E8 (tnBT3368)
Shimadzu AXIMA Performance, intact LOS
MALDI-TOF MS (800-6500 m/z)
%Int.
825.1
811.1
1271.4
1285.6
1310.0
1654.6
2304.7
3283.9
3608.1
100
90
80
70
60
50
40
30
20
10
0
1000
2000
3000
4000
5000
6000
m/z

Bacteroides thetaiotaomicron VPI-5482 2.7-D11 (tnBT3376)
Shimadzu AXIMA Performance, intact LOS
MALDI-TOF MS (800-6500 m/z)

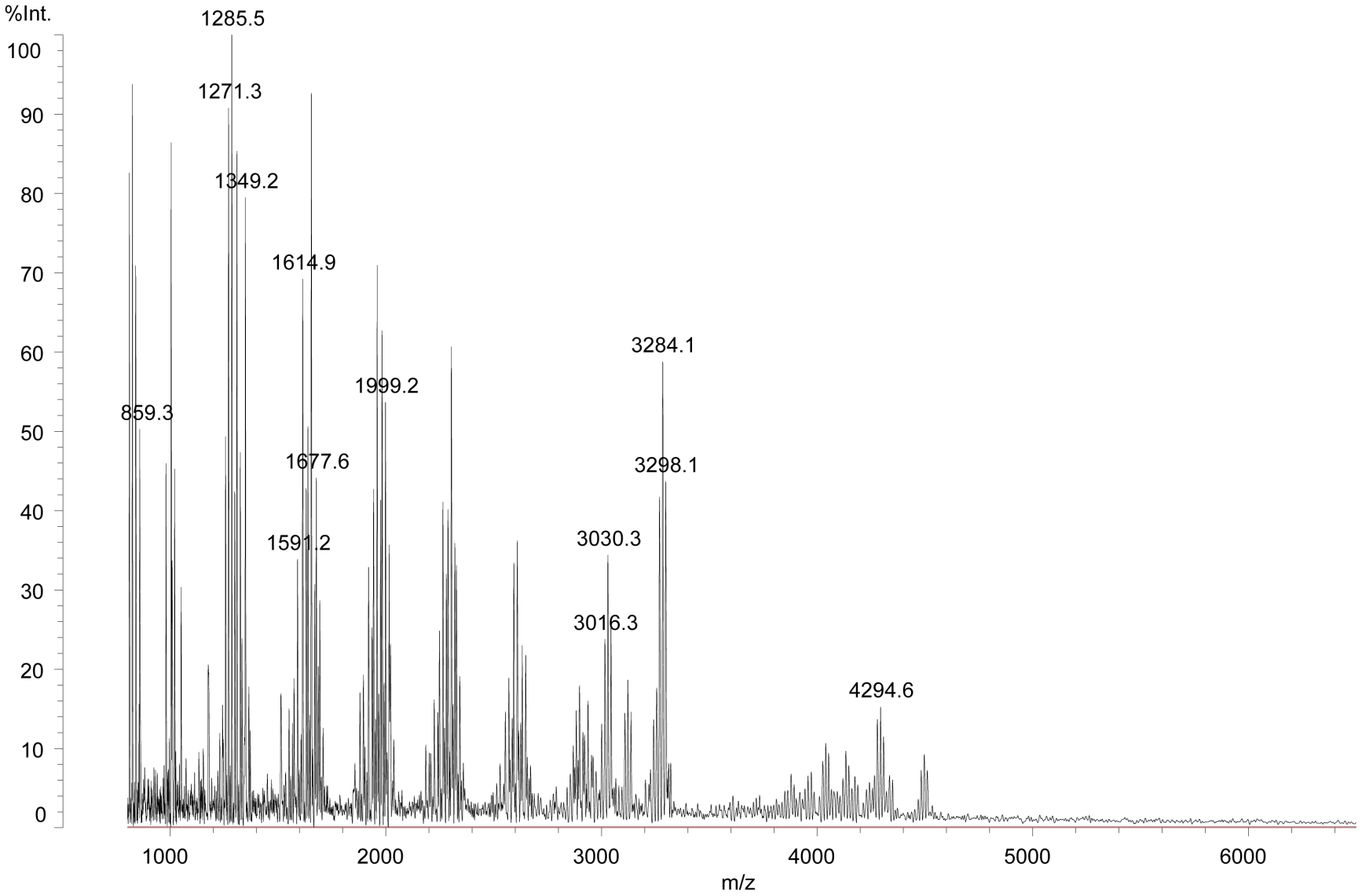

Bacteroides thetaiotaomicron VPI-5482 Δ*tdk* ΔCPS ΔBT3363 ΔBT3365-BT3380
Shimadzu AXIMA Performance, intact LOS
MALDI-TOF MS (800-6500 m/z)

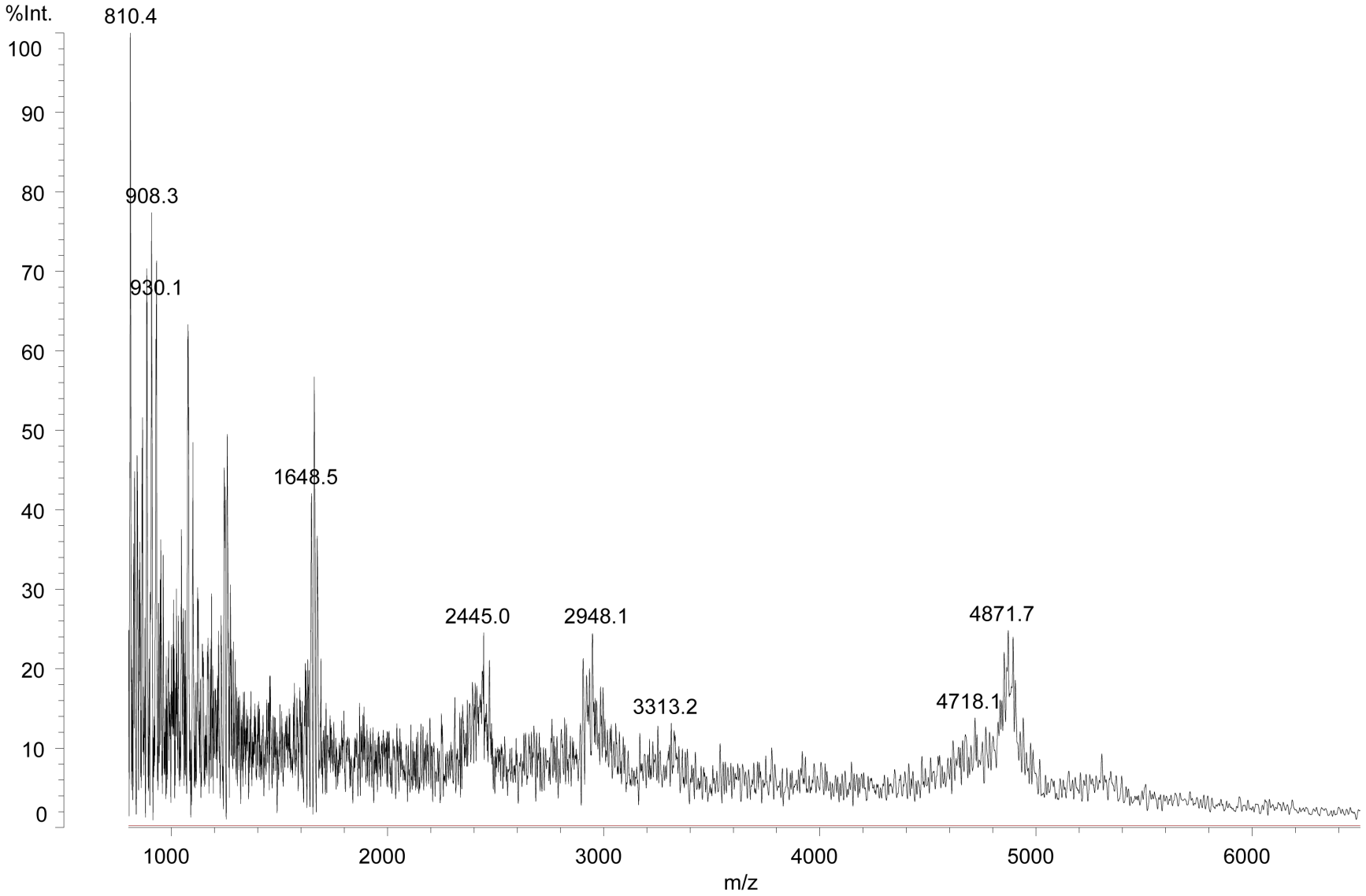

Bacteroides thetaiotaomicron VPI-5482 Δ*tdk* ΔBT3363 ΔBT3365-BT3380
Shimadzu AXIMA Performance, intact LOS
MALDI-TOF MS (800-6500 m/z)

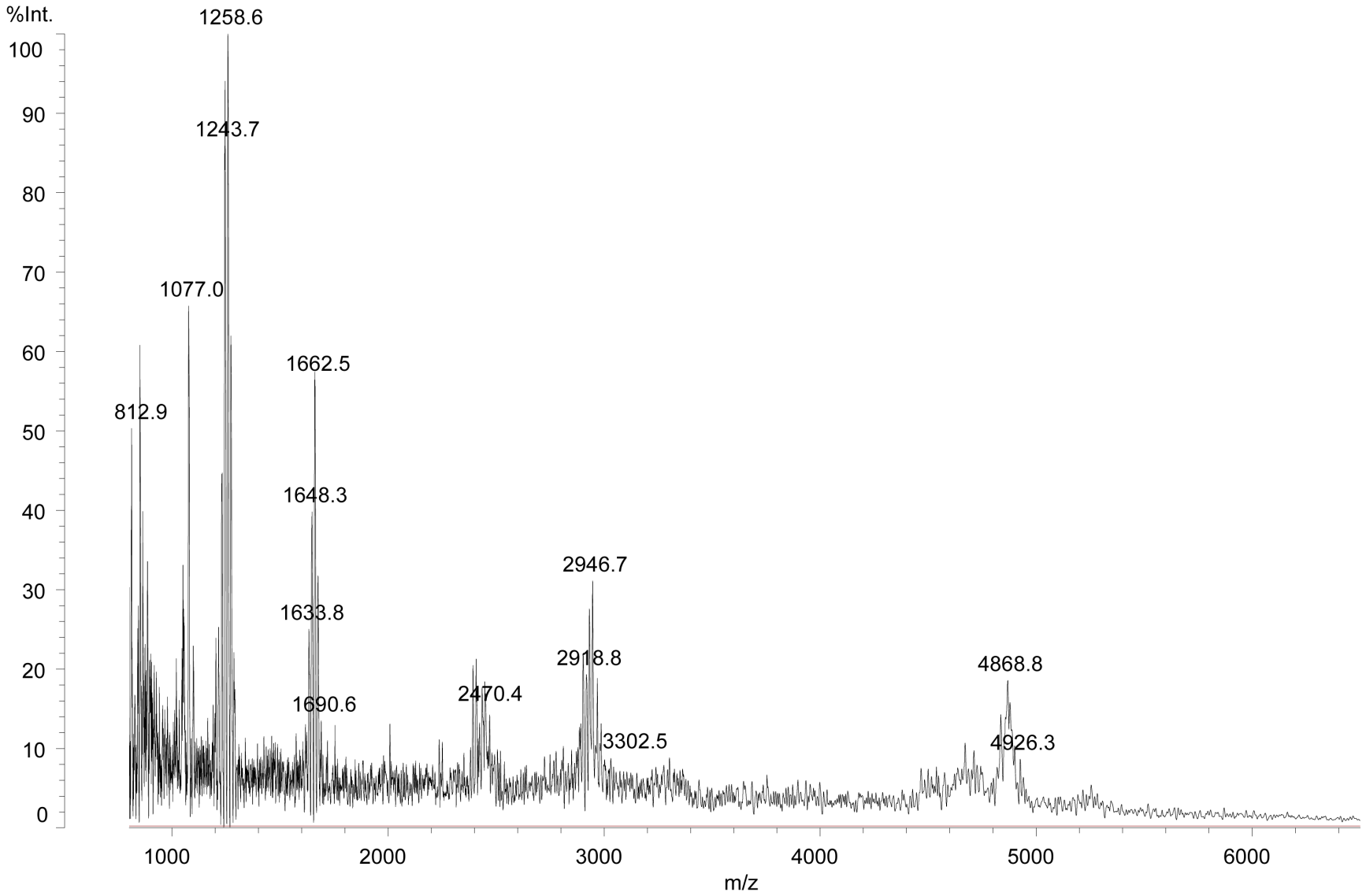

Publishing Agreement

It is the policy of the University to encourage the distribution of all theses, dissertations, and manuscripts. Copies of all UCSF theses, dissertations, and manuscripts will be routed to the library via the Graduate Division. The library will make all theses, dissertations, and manuscripts accessible to the public and will preserve these to the best of their abilities, in perpetuity.

I hereby grant permission to the Graduate Division of the University of California, San Francisco to release copies of my thesis, dissertation, or manuscript to the Campus Library to provide access and preservation, in whole or in part, in perpetuity.

Amy Jacobson
Author Signature

8/28/17
Date